RESEARCH AND DEVELOPMENT TECHNICAL REPORT
ECOM-0101-F

RELIABILITY OF HIGH FIELD SEMICONDUCTOR DEVICES

FINAL REPORT

By
J.L. HEATON and T.B. RAMACHANDRAN

MAY 1974

APPROVED FOR PUBLIC RELEASE;
DISTRIBUTION UNLIMITED

ECOM

UNITED STATES ARMY ELECTRONICS COMMAND · FORT MONMOUTH, N.J. 07703
CONTRACT DAAB07-72-C-0101

MICROWAVE ASSOCIATES, INC.
Burlington, Massachusetts

NOTICES

Disclaimers

Disposition

TR-ECOM-0101-3
February 1974

REPORTS CONTROL SYMBOL
OSD-____

AD781572

RELIABILITY OF HIGH FIELD SEMICONDUCTOR DEVICES

FINAL REPORT

1 April 1973 to 31 January 1974

Contract No. DAAB07-72-C-0101

Distribution Statement

Approved for public release; distribution unlimited

Prepared For

U.S. Army Electronics Command
Fort Monmouth, N.J. 07703

Prepared By

T.B. Ramachandran and J.L. Heaton

MICROWAVE ASSOCIATES, INC.
BURLINGTON, MASSACHUSETTS 01803

TABLE OF CONTENTS

		Page
ABSTRACT		xiii
PURPOSE		ix
I.	INTRODUCTION	1
II.	ESTABLISHMENT OF THE REQUIRED DC BURN-IN TIME FOR GUNN DIODES	4
III.	CHANGE OF PARAMETERS OF GALLIUM ARSENIDE IMPATT DIODES DURING DC BURN-IN	15
IV.	LONG-TERM LIFE TEST RESULTS	19
V.	GUNN DIODE ACTIVE REGION TEMPERATURE DETERMINATION	28
VI.	GUNN DIODE STEP STRESS TESTING	41
VII.	GUNN DIODE CONSTANT STRESS TESTING	71
VIII.	ANALYSIS OF FAILURE MECHANISMS	74
IX.	CONCLUSIONS AND SUMMARY	88
REFERENCES		91

LIST OF ILLUSTRATIONS

Figure		Page
1	Apparatus used to Determine Gunn Diode DC and RF Parameters	5
2	Percentage chnage in Gunn Diode Power Output Caused by 168 Hours of High Temperature Burn-In. The Horizontal Scale is Diode Identification Number	10
3	Change in Gunn Diode CW-Threshold Voltage Caused by Sequential High Temperature Burn-In. The Horizontal Scale is Diode Identification Number	11
4	Change in Gunn Diode CW-Threshold Current Caused by Sequential High Temperature Burn-In. The Horizontal Scale is Diode Identification Number	12
5	Schematic for GaAs IMPATT Life Test Control Panel	16
6	Apparatus Used in Cycling Gunn Diode Oscillators On and Off	20
7	Apparatus Used to Monitor the Current and RF Output Power of One Gunn Diode	23
8	Gunn Diode Thermal Resistance Test Set	32
9	Block Diagram of Improved Electrical Method for Gunn Diode Thermal Resistance Measurement	35
10	Gunn Diode Thermal Resistance Measured Using the Improved Electrical Method Versus Average Thermal Resistance from IR Measurements	36
11	Infrared Microscope and Record Apparatus	38
12	Temperature versus Position GaAs IMPATT 5028-2 - Scan #1	39
13	Generalized Failure Rate versus Time	42
14	Accelerated Failure Curve Showing Step-Stress Test and Constant Stress Test	45

List of Illustrations (Cont.)

Figure		Page
15	Circuit Used in Step-Stress to Failure Testing of Gunn Diodes	46
16	Reciprocal Absolute Active Region Failure Temperature versus Cumulative Percent of Diodes Failing for Gunn Diode Step-Stress Test Numbers 1 and 2	50
17	Reciprocal Absolute Active Region Failure Temperature versus Cumulative Percent of Diodes Failing for Gunn Diode Step-Stress Test Number 3	53
18	Reciprocal Absolute Active Region Failure Temperature versus Cumulative Percent of Diodes Failing for Gunn Diode Step-Stress Test Number 5	54
19	Operating Current versus Active Region Temperature for Gunn Diode Number 14. The Data was Recorded During Step-Stress Test Number 5	55
20a	Microscope Photograph of a Cross-Sectioned Gunn Diode Following 1200 Hours of High Temperature Storage. Penetration at the Contact Metallization into the Active Region is Evident at 340°C. Each Scale Division is 0.2 mil	59
20b	Microscope Photograph of a Cross-Sectioned Gunn Diode From the Same Wafer as the Diode Shown in Figure 20a. This Diode was not Subjected to High Temperature Storage. Each Scale Division is 0.1 mil	59
21	Microscope Photograph of a Cross-Sectioned Gunn Diode Which Exhibited Current Drop Failure During Step-Stress Testing. Penetration of the Contact Metallization into the Active Region is Evident. The Diode is From Step-Stress Run 5, Wafer 6024-1A, Identification Number 7. Each Scale Division is 0.2 mil	60
22	Two Microscope Photographs of a Cross-Sectioned Gunn Diode which Exhibited Current Drop During Step-Stress Testing. Each Scale Division is 0.4 mil in the Upper Photograph, 0.2 mil in the Lower. The Diode is From Step-Stress Run 5, Wafer 6024-1A, Identification Number 16	61

List of Illustrations (Cont.)

Figure		Page
23	Micrograph of Inverted Gunn Diode Obtained Using Electron Microprobe Analysis. The Diode Exhibited Current Drop Following 1,200 Hours of Storage at 340°C . .	62
24	X-Ray Images of (a) Gold; (b) Gallium; (c) Germanium; and (d) Nickel Obtained for the Diode of Figure 23	63
25	Reciprocal Absolute Active Region Failure Temperature versus Cumulative Percent of Diodes Failing for Gunn Diode Step-Stress Test Number 4	65
26	Reciprocal Absolute Active Region Failure Temperature versus Cumulative Percent of Diodes Failing for Gunn Diode Step-Stress Test Number 6	66
27	Microscope Photographs of Two Gunn Diodes which Failed during Step-Stress Testing. Extreme Heat Damage is Evident. These Diodes are from Step-Stress Run 4, Wafer 1016-2B.	70
28	Circuit Diagram of One Section of 40-Section Gunn Diode Constant Stress Test Kit	72
29	Outline of Mesa Process for TCB Diodes	75
30	Cross-Section of a Plated Heat Sink Gunn Diode	76
31	Gunn Diode 211-1D #2 Before Failure. 15 x 15 mil Chip TCB Bond	77
32	Gunn Diode 2111-1D #1 Following Failure. 15 x 15 mil Chip TCB Bonded	78
33	Gunn Diode 2139-2B After Failure - Plated Heat Sink Construction - 16 mil Diameter Mesa. The Only Visual Evidence of Failure is a Small Hole Through the Center of the Contact Straps	79
34	GaAs IMPATT Diode 5028-2. Following Failure	80
35	Scanning Electron Microscope Photographs of a PHS Construction Gunn Diode Following Failure. The Top Straps Have Been Removed, Revealing the Failure Region. Cracking at the Edges Possibly Due to Stress from the Plated Gold Heat Sink is Shown	82

List of Illustrations (Cont.)

Figure		Page
36	Enlargement of the Failure Region of the PHS Construction Gunn Diode Shown in Figure 27. The Depth of the Failure Region and Effect of Extreme Heat Damage are Visible . . .	83
37	Scanning Electron Microscope Photograph of a PHS Construction Gunn Diode. A Crack Possibly Caused by Excessive Pressure During Top Bonding is Visible. A Slight Overhang of the Upper Electrode is also Shown . . .	84
38	Scanning Electron Microscope Photograph of the Back of a TCB Construction Gunn Diode Chip. The Connecting Straps have been Pulled Off, Fracturing the Gallium Arsenide. This Fracturing is an Indication that Top Bonding may have Damaged the Gallium Arsenide Substrate. 500X	85
39	Scanning Electron Microscope Photographs of a TCB Construction Gunn Diode Showing the Squeeze-Out of the Metallization During Bonding. 4000X	87

LIST OF TABLES

Table		Page
I	Distribution of Gunn Diode Failures in Time During Burn-In for 24-Hour Burn-In Intervals	6
II	Distribution of Gunn Diode Failures in Time During Burn-In During the First 24 Hours of Operation . . .	6
III	Gunn Diode Parameters Monitored Before and After Burn-In	7
IV	Summary of Observed Direction of Changes of Gunn Diode Parameters Due to Burn-In	9
V	Characterization of Gallium Arsenide IMPATT Diodes Before and After DC Burn-In at 50^{o}C	17
VI	Change in RF and DC Parameters During Gunn Diode Switching Transient Test	21
VII	Variation in Parameters of a Gunn Diode Oscillator During Long-Term Operation	25
VIII	DC Parameters of Gallium Arsenide IMPATT Diodes Before and After 1728 Hours of DC Burn-In at 80^{o}C Case Temperature	27
IX	A Comparison of Values of α for Diodes From Three Gallium Arsenide Wafers	30
X	A Comparison of Thermal Resistance Measuring Using the IR Radiometer with Thermal Resistance Measuring Using the Pulse Method	33
XI	Summary of Gunn Diode Step-Stress Testing Results .	49
XII	Summary of Step-Stress Data Used In Preparing Figure 16	52
XIII	Degradation of Gunn Diode RF Performance During Elevated Storage Temperature Test at 340^{o}C	57
XIV	Summary of Gunn Diode Step-Stress Testing Results Using a Low Temperature Asymptote to Establish a 25% Failure Active Region Temperature	69

ABSTRACT

This report describes the results of a program of investigation concerning the reliability and failure modes of gallium arsenide Gunn and IMPATT diodes.

Data is presented concerning the burn-out distribution in time of Gunn diodes. Also, the changes in dc and RF parameters of 700 Gunn and 100 gallium arsenide IMPATT diodes resulting from 24 to 168 hours of dc high temperature burn-in are present.

The results of long-term RF burn-in experiments on Gunn and gallium arsenide IMPATT diodes are reported, including calculation of the MTBF for a class of Gunn diodes. An improved thermal resistance measurement technique is described for Gunn diodes and results are compared with data obtained using an IR radiometer.

The results of three Gunn diode step stress experiments are presented. An abrupt failure mode occurring above approximately 325°C and not at all at lower temperatures has masked the long-term mode of failure and precluded determination of an activation energy using step stress techniques.

Constant stress testing of Gunn diodes at a lower stress level was initiated in order to avoid this catastrophic failure mode. At present, these tests have not been completed.

Optical and electron microscope photographs are presented which are used in the analysis of the manufacturing defects leading to early failure in Gunn diodes. Correction of these defects has lead to an increased 24-hour burn-in yield.

PURPOSE

The purpose of this program was to identify the prime failure modes of solid-state microwave power generators, so that through improved device design and technology, these failure modes could be eliminated.

Procedures have been developed for the rapid assessment of device characteristics insuring elimination of detected modes of failure. An estimate of the long-term reliability of these devices was also made.

I. INTRODUCTION

The popularity of Gunn and IMPATT diode solid-state microwave signal sources has grown dramatically as the demonstrated reliability of these devices has increased. At present, Gunn and IMPATT devices are being used in many critical applications, particularly in military systems, where failure cannot be tolerated. Therefore, the determination of the necessary processing steps and required modification of fabrication techniques to ensure reliability has become of extreme importance. Because these devices involve use of gallium arsenide rather than the more familiar silicon, new guidelines are required to ensure reliable operation. Those limitations previously placed on operating device parameters, such as maximum active region temperature, may no longer be applicable.

Gunn and IMPATT diodes are generally used in the direct conversion of DC to microwave energy, or in low level microwave signal amplification. Commercially available power outputs range from 5 to 500 mW at conversion efficiencies of up to 7% for Gunn diodes and up to 1.5 W at 13% for IMPATTs. In Gunn diode construction, an n+-n-n+ sandwich structure is employed where a typically 10^{15} electron/cc n layer of 2 to 20 microns thickness is grown on a 10^{18}/cc substrate. A second 10^{18}/cc contact layer is grown 1 to 2 microns thick on top of the n layer to facilitate ohmic contact. Ohmic contact metalization is then alloyed into the contact and substrate layers. Round mesas of 6 to 12 mils diameter are etched through the active layer using a photolithographic technique, and the chips separated by scribing and cleaving. In the majority of cases, these chips are thermo-compression bonded, contact layer down into microwave diode packages. These packages incorporate either a 3-48 threaded stud or a 62 mil diameter prong for diode heat sinking.

The gallium arsenide IMPATT diodes used in this study were platinum Schottky barrier units involving sputtered platinum barriers applied to n-type

epitaxial gallium arsenide layers over n^+ substrates. Mesas are formed as in the case of Gunn diodes, and the chips thermo compression bonded into microwave diode packages. The diodes are then etched to the required capacitance specification.

It was the purpose of this study to arrive at manufacturing processes which would lead to the production of reliable Gunn and IMPATT devices, and to determine just how reliable these devices were. The program was divided into two parts. First, a dc burn-in schedule was established which would reduce device early failures to a tolerable level (3 percent), and minimize device parameter change with time. Early failures are the result of occasional unavoidable device damage during manufacture, or variations in starting materials.

Second, accelerated aging tests were carried out on Gunn diodes in order to determine the mechanisms responsible for long-term diode failure. The assumption was made that the long-term failure mechanism would be accelerated by an increase in device active region temperature according to the Eyring-Arrhenius rate law. Initially, step stress testing was employed, whereby groups of diodes were operated for fixed periods of time at successively higher active region temperatures, until all units failed. Because of a catastrophic failure occurring at about 325°C and never at lower temperatures, problems were encountered in Gunn diode step stress testing. For this reason, Gunn diode constant stress testing was initiated, but has not been completed.

In connection with the step stress testing of Gunn diodes, two electrical methods for determining Gunn diode thermal resistance were perfected. These methods were demonstrated to be reasonably accurate by measuring the dice temperature of operating diodes using a Barnes Engineering Infrared Radiometer. One method was shown to be superior because of increased speed and accuracy of measurements.

Several other long-term reliability tests have been instituted during this program. Six Gunn diode cavity oscillators have been switched on and off every two minutes for 9,288 hours (139,320 cycles) without degradation in performance. A single cavity oscillator has operated 15,620 hours with no change in output or current.

In an experiment started before the inception of the contract, 15 Gunn diodes, on long-term dc burn-in at 10 volts bias and $75^{\circ}C$ case temperature, have accumulated 325,000 unit hours without a failure.

Long-term reliability studies of gallium arsenide IMPATT diodes include long-term RF burn-in (49,000 unit hours accumulated). Three failures have occurred.

High Temperature Reverse Bias tests were also carried out for gallium arsenide IMPATTs, but proved to be a poor reliability assurance measure for IMPATTs, as diodes surviving HTRB sometimes failed during subsequent RF testing.

The reliability assurance program described here has increased our confidence in the reliability of Gunn and gallium arsenide IMPATT diodes. Some problem areas in the manufacturing process have been isolated and corrected through observation of the diode dc burn-in yield. Long-term reliability testing has established minimum values for the expected Gunn diode useful life, and has demonstrated the Gunn diode's resistance to damage from turn-on/turn-of transients.

II. ESTABLISHMENT OF THE REQUIRED DC BURN-IN TIME FOR GUNN DIODES

DC burn-in has often been used in the semiconductor field as a means of weeding out inferior devices from a production lot which can be characterized as infant mortality failures, and also to stabilize parameter drift. In order to establish the appropriate dc burn-in schedule for Gunn diodes, over 700 units in the prong package (ODS-30) were characterized as to dc RF parameters before and after burn-in. Burn-in was conducted at full rated operating voltage and a case temperature of 100°C. In some cases, groups of diodes were tested for parameter change or complete failure, (open or shorted condition), following sequential 24-hour burn-in periods. Other diodes were tested only after 168 hours of burn-in. Table III enumerates the parameters measured before and after burn-in, while Figure 1 depicts the testing apparatus used.

The dc burn-in testing produced two useful pieces of information. First, the necessary dc burn-in time required to eliminate early diode failures was determined. This screening was necessary to eliminate diodes which were inadvertently damaged during processing, perhaps cracked during bonding, or not securely contacted during top strapping. Second, the type and amount of diode parameter change occurring during aging and the length of operating time needed to affect parameter stabilization were investigated.

Tables I and II present the distribution of diode dc high temperature burn-in failures (opens and shorts) in time for 386 units. As shown, the majority of diode failures occurred during the first 10 minutes of operation. The observed freak failure rate dropped to 3.5% following 24 hours of burn-in, to 1/2% following 48 hours, and to 0% for the 87 diode lot examined again after 72 hours of burn-in. This data indicates that high temperature dc burn-in is effective in eliminating freak failures. Accordingly, all units are not routinely burned-in a minimum of 24 hours at high temperature. For high reliability products, longer burn-in times may be specified.

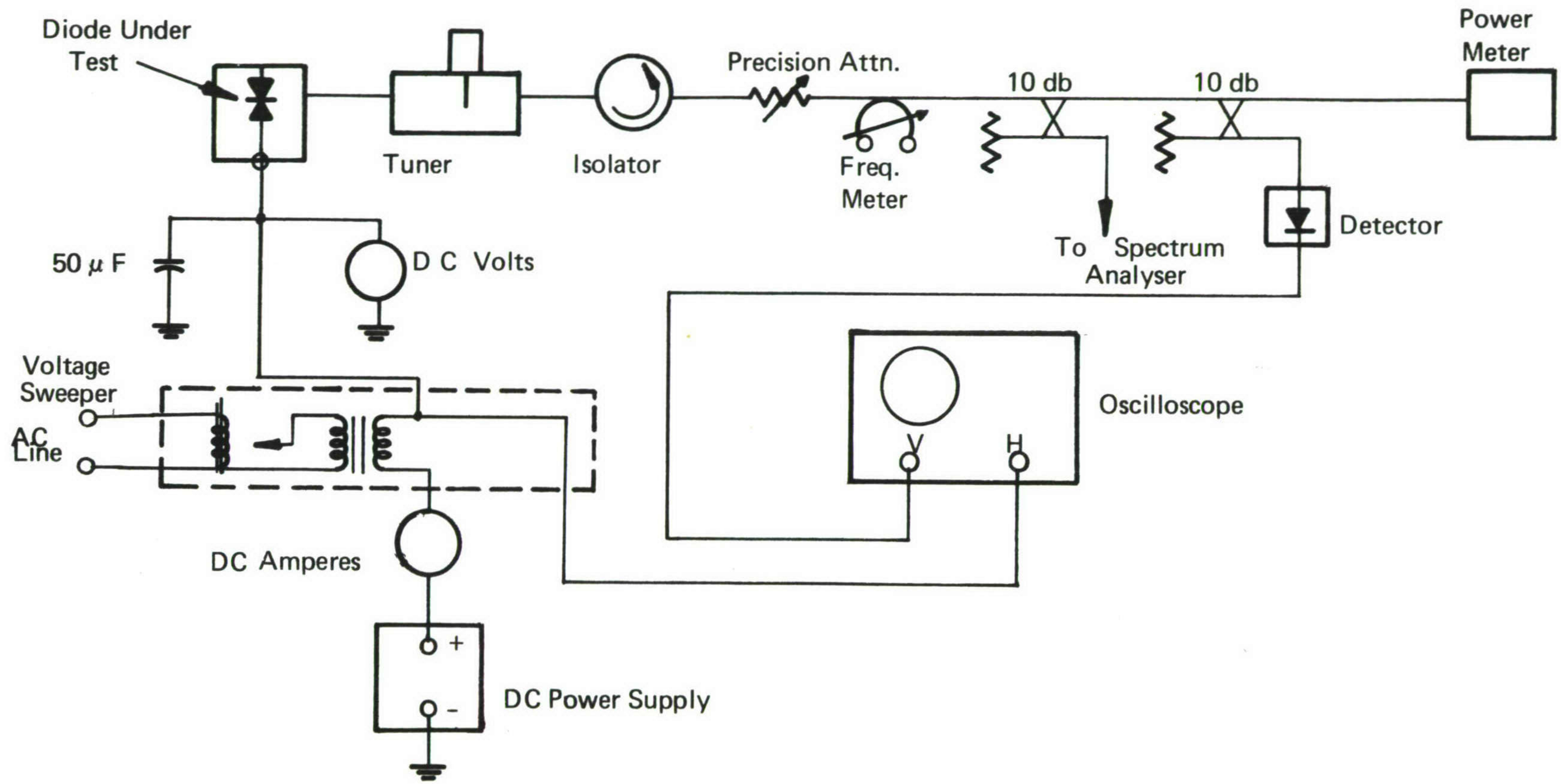

FIGURE 1 APPARATUS USED TO DETERMINE GUNN DIODE DC AND rf PARAMETERS

D-11163

TABLE I

DISTRIBUTION OF GUNN DIODE FAILURES IN TIME
DURING BURN-IN FOR 24-HOUR BURN-IN INTERVALS

Total Hours on Burn-In	Number of Diodes Tested	Number of Failures	Percent Failures
24	386	108	28
48	229	7	3
72	202	1	1/2
100 to 168	87	0	0

TABLE II

DISTRIBUTION OF GUNN DIODE FAILURES IN TIME
DURING BURN-IN DURING THE FIRST 24 HOURS OF OPERATION

Total Minutes On Burn-In	Number of Diodes Tested	Number of Failures
10	95	19
20	76	2
30	74	0
24 Hours	55	4

TABLE III

GUNN DIODE PARAMETERS MONITORED BEFORE AND AFTER BURN-IN

Symbol	Parameter
V_{Tcw}	DC Threshold Voltage
V_{TP}	Pulse Threshold Voltage
I_{Tcw}	DC Threshold Current
I_{Tp}	Pulse Threshold Current
V_B	Pulse Breakdown Voltage
I_{op}	Operating Current
V_{op}	Operating Voltage
P_o	Output Power
f	Oscillation Frequency
η	Efficiency
V_N	Prethreshold Noise Voltage
V_{pp}	Power Peak Voltage

DC burn-in was expected to not only eliminate substandard units, but would also result in stabilization of device parameters, eliminating further change which could cause malfunctions in the field. In order to determine how burn-in affected diode parameters, the quantities listed in Table III were measured before and after 24-hour sequential high temperature burn-in periods for over 700 Gunn diodes. The majority of the diodes tested were ODS-30, TCB construction, (thermo-compression bonded) units of 50 to 250 mW power output in X-band. DC burn-in was conducted at 12 volts bias and 100^{o}C case temperature with from 5 to 12 watts of dc input power. About 20% of the units were C or Ku-band diodes and were burned-in at 14 or 10 volts, respectively. Also, 20 ODS-118 minipack package X-band diodes were processed.

Table IV summarizes the trends observed for diodes from various wafers after a minimum of 50 hours of high temperature burn-in. As shown, no clear-cut trends were established, since on the average, diodes from different wafers did not exhibit the same parameter change. For diodes from a particular processing run, trends such as shown in Figure 2 were often seen. In general, it was determined that the following parameters may be expected to be increased by burn-in: V_{TP}, V_B, I_{op}, V_{pp}. A decrease would be expected in the following: I_{TP} and V_N. Other parameters would not be expected to change on the average. However, as shown by Table IV, these trends are not clear-cut. Diodes from any particular wafer chosen at random could behave differently.

The parameter stabilization observed during sequential dc burn-in is exemplified by the data presented in Figures 3 and 4. In general, extreme changes in a particular parameter observed during the first 24 hours of burn-in were reversed during the latter burn-in intervals, yielding a smaller net change than occurred during the first interval. In the third 24-hour interval,

TABLE IV

SUMMARY OF OBSERVED DIRECTION OF CHANGE OF GUNN DIODE PARAMETERS DUE TO BURN-IN

Parameter	Number of Wafers Exhibiting Change on the Average		
	Increase	Decrease	No Change
V_{Tcw}	7	7	14
V_{TP}	14	4	10
I_{Tcw}	7	8	13
I_{Tp}	7	10	10
V_B	11	4	5
I_{op}	9	7	12
P_o	10	15	3
η	11	13	4
V_N	9	12	7
V_{pp}	3	1	5

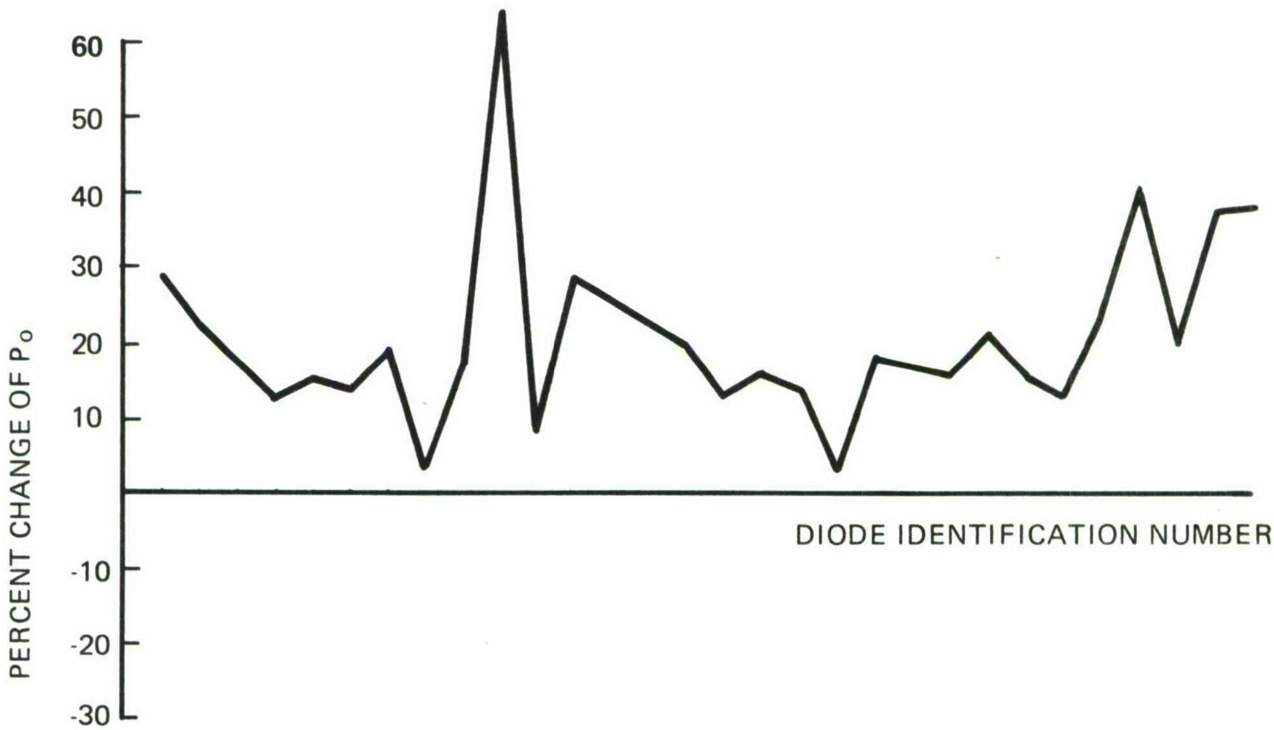

PROCESSING RUN NO. 2077-2D

FIGURE 2 PERCENTAGE CHANGE IN GUNN DIODE POWER OUTPUT CAUSED BY 168 HOURS OF HIGH TEMPERATURE BURN-IN. THE HORIZONTAL SCALE IS DIODE IDENTIFICATION NUMBER.

D-11134

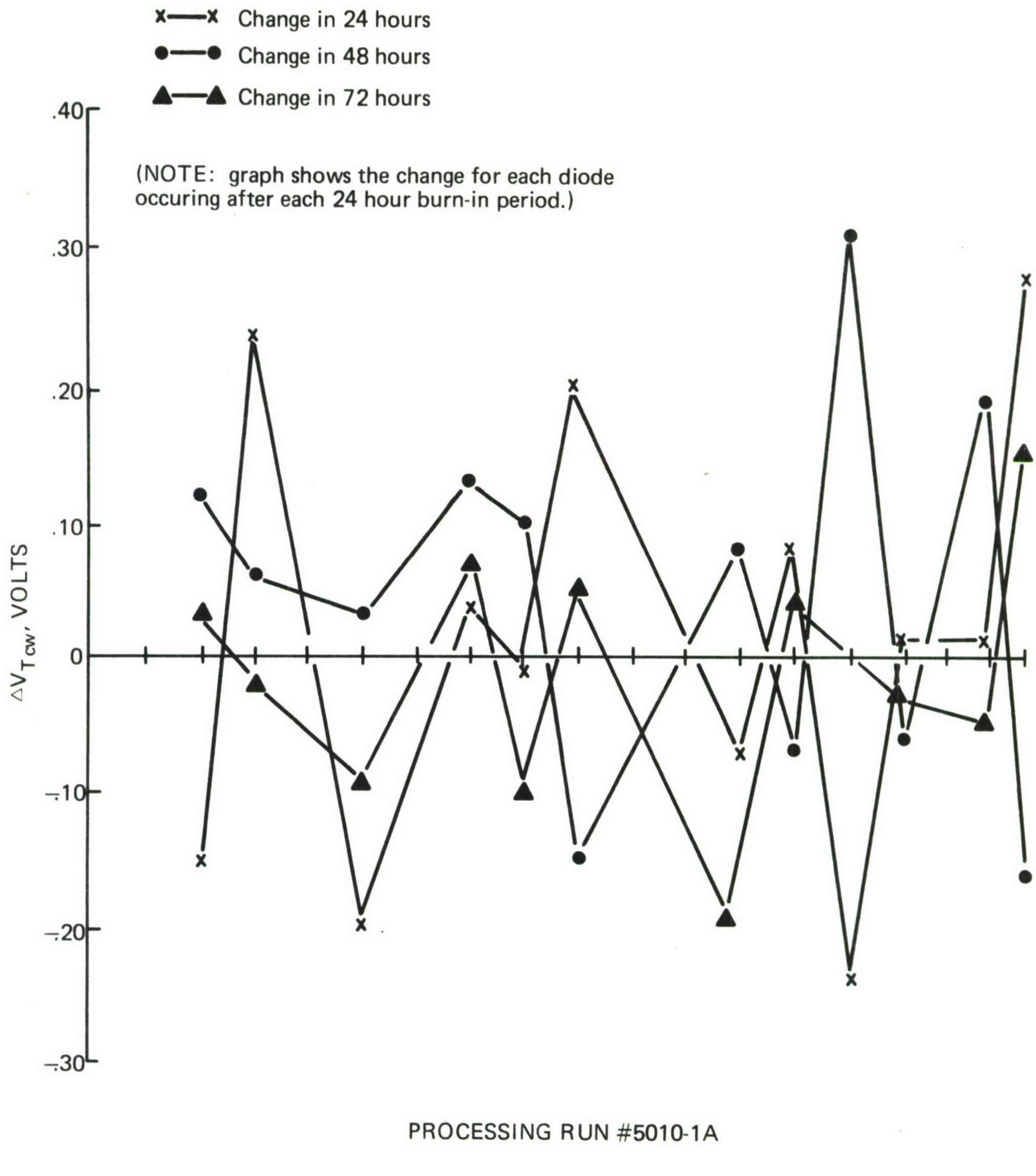

FIGURE 3 CHANGE IN GUNN DIODE CW-THRESHOLD VOLTAGE CAUSED BY SEQUENTIAL HIGH TEMPERATURE BURN-IN. THE HORIZONTAL SCALE IS DIODE IDENTIFICATION NUMBER.

D-11136

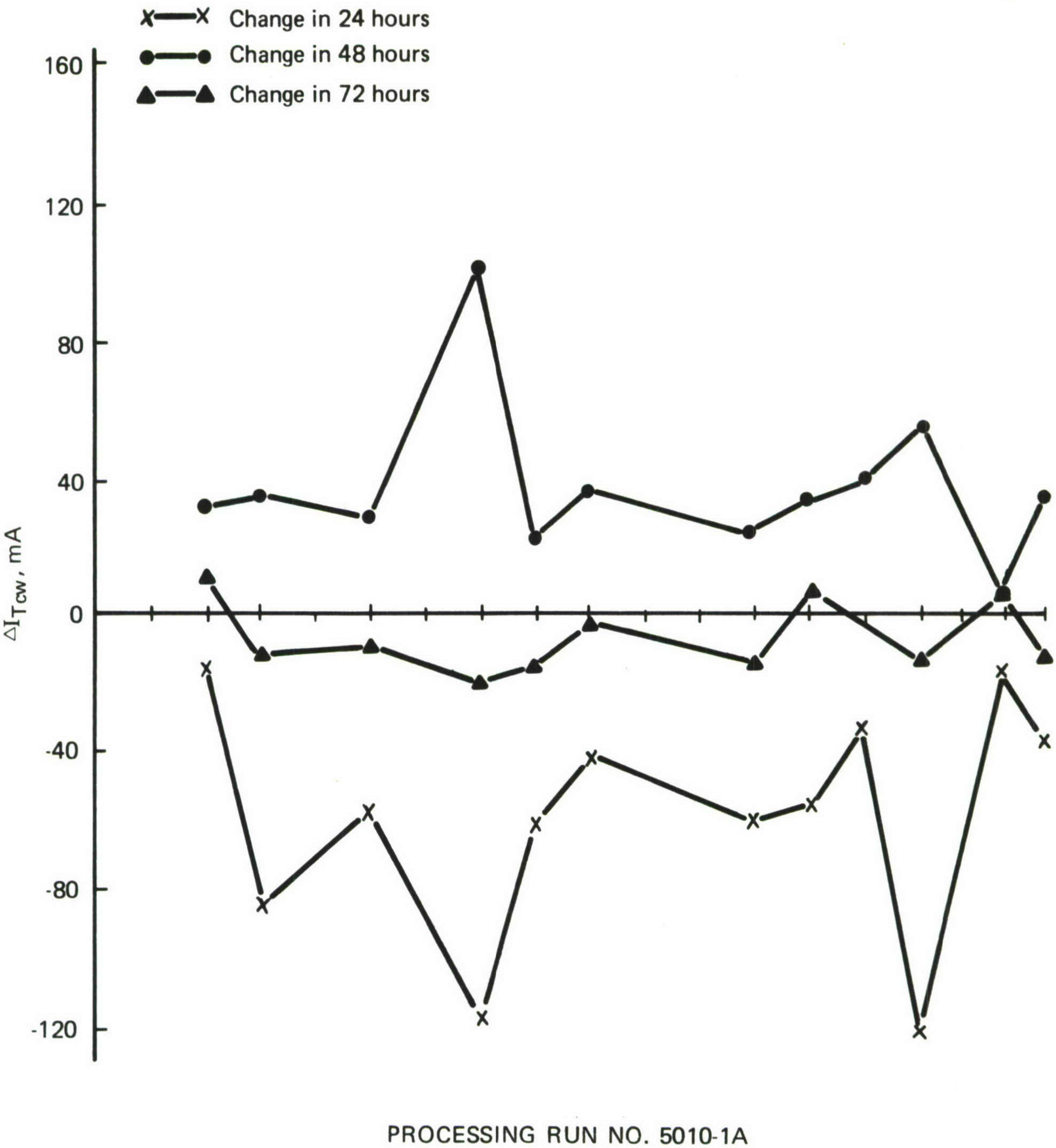

FIGURE 4 CHANGE IN GUNN DIODE CW–THRESHOLD CURRENT CAUSED BY SEQUENTIAL HIGH TEMPERATURE BURN-IN. THE HORIZONTAL SCALE IS DIODE IDENTIFICATION NUMBER.

D-11137

only small (compared with the first interval) changes were observed. Hence, following 48 hours of high temperature burn-in, diode parameters could be considered to have stabilized.

The 20 Gunn diodes in the ODS-118 minipack package were tested following successive periods of high temperature 12-volt burn-in at from 3.6 to 5 watts of dc input power. The ODS-118 package incorporates a 52 mil outside diameter, 32 mil inside diameter, 15 mil high ceramic and threaded heat sink, while the ODS-30 package previously used has an 81 mil diameter, 60 mil high ceramic and prong heat sink. After the first 18 hours of $25^{\circ}C$ burn-in, no diodes failed and very little parameter change was observed. Diodes were retested at the frequency where they had exhibited maximum power before burn-in. After an additional 93 hours at $100^{\circ}C$, two diodes failed and significant parameter change was observed. In particular, the RF output power had decreased about 20% and the power peak voltage had dropped by about 10%. Other parameters on the average had not changed. During an additional 24 hours of burn-in, the diodes, on the average, exhibited little change. It was discovered that the frequency of maximum power output was somewhat reduced. The thermal resistance of these diodes was measured and on the average, was $42^{\circ}C/W$ or about 170% of theoretical. (The thermal resistance data was obtained with the improved measurement technique developed during this study.) Hence, the parameter change could have been the result of excessive chip temperature. In the worst case, these diodes could have reached an active region temperature of $310^{\circ}C$. As discussed in a subsequent section, such a temperature, if exceeded for prolonged periods, could result in permanent diode damage.

Gunn Diode Reliability Assessment with Respect to Early Failures

Use of 24 hours of high temperature burn-in has been shown to reduce the rate of Gunn diode early failure from 28% to 3.5%. In the field,

these units should exhibit a failure rate of less than 3.5%, because in all probability, diodes would be operated at much lower case temperatures than those used during burn-in. If required, the early failure rate could be reduced to a negligible level by 168 hours of high temperature burn-in.

Additional reduction in the early failure rate has been achieved by monitoring the burn-in yield of all units during the first 24-hour burn-in. Abnormally high failure rates have been related to correctable bonding variables such as bonding weight and amount of ultrasonic agitation. Also, a close monitoring of diode thermal resistance using an improved electrical method, to be discussed in a later section, has resulted in an increase in 24-hour burn-in yield, particularly in the case of high output power Gunn devices ($P_o \geq 250$ mW). Slight errors in bonder settings are now corrected before many inferior units are constructed, preventing large number of high thermal resistance units from reaching burn-in.

During the course of this contract, the 24-hour burn-in yield has been increased from 72%, as determined in September 1972, to 84.6% for calendar 1973 and January 1974. A total of 8,622 diodes were burned-in with a yield of 7,297 units, representing the entire product line.

In general, the high temperature burn-in serves to induce premature failure in marginal units, thus reducing the probability of failure in the field. Those defects leading to burn-in failure include cracked or damaged chips due to excessive die or strap bonding pressure, surface contamination, loose top strap connection, metallization squeeze-out due to excessive bonding pressure, failure to completely rinse etchants from the package before capping, and undercut of top metallization due to excessive etching.

Units surviving the high temperature burn-in should be reasonably free of these defects.

III. CHANGE OF PARAMETERS OF GALLIUM ARSENIDE IMPATT DIODES DURING DC BURN-IN

Gallium Arsenide IMPATT diodes were also subjected to dc burn-in testing in order to establish a burn-in schedule for removal of inferior units, and to investigate parameter stabilization.

One-hundred IMPATT diodes in ODS-30 and ODS-111 packages were characterized before and after from 24 to 112 hours of dc burn-in at rated operating voltage and 50°C case temperature. Those parameters monitored included junction capacitance, breakdown voltage, power output, frequency of operation, operating voltage and operating current. Diodes used for this test were selected for efficient RF performance prior to burn-in. Hence, these diodes had been partially screened prior to burn-in, in that diodes failing during initial RF testing were not included. In general, X-band units in the 500 to 1000 mW range were employed.

The apparatus used in the dc burn-in of IMPATT diodes is shown schematically in Figure 5. Each diode was protected against power supply voltage changes by an adjustable series resistance, allowing individual adjustment of the burn-in voltage. A relay in the power supply line leads prevented sudden reapplication of power following possible power failure. Diode temperature was controlled by water flow through the copper diode mount.

Of 100 selected IMPATT diodes placed on 50°C burn-in, only six failed. In each case, failures were detected following the initial 24-hour burn-in period. One failure occurred during RF testing following 24 hours of burn-in, while another unit showed power degradation of from 1 watt to 800 mW. In general, less than 5% changes in diode parameters were observed due to burn-in and are considered insignificant in light of the repeatability error of the apparatus used. Table V presents a partial tabulation of the data accumulated.

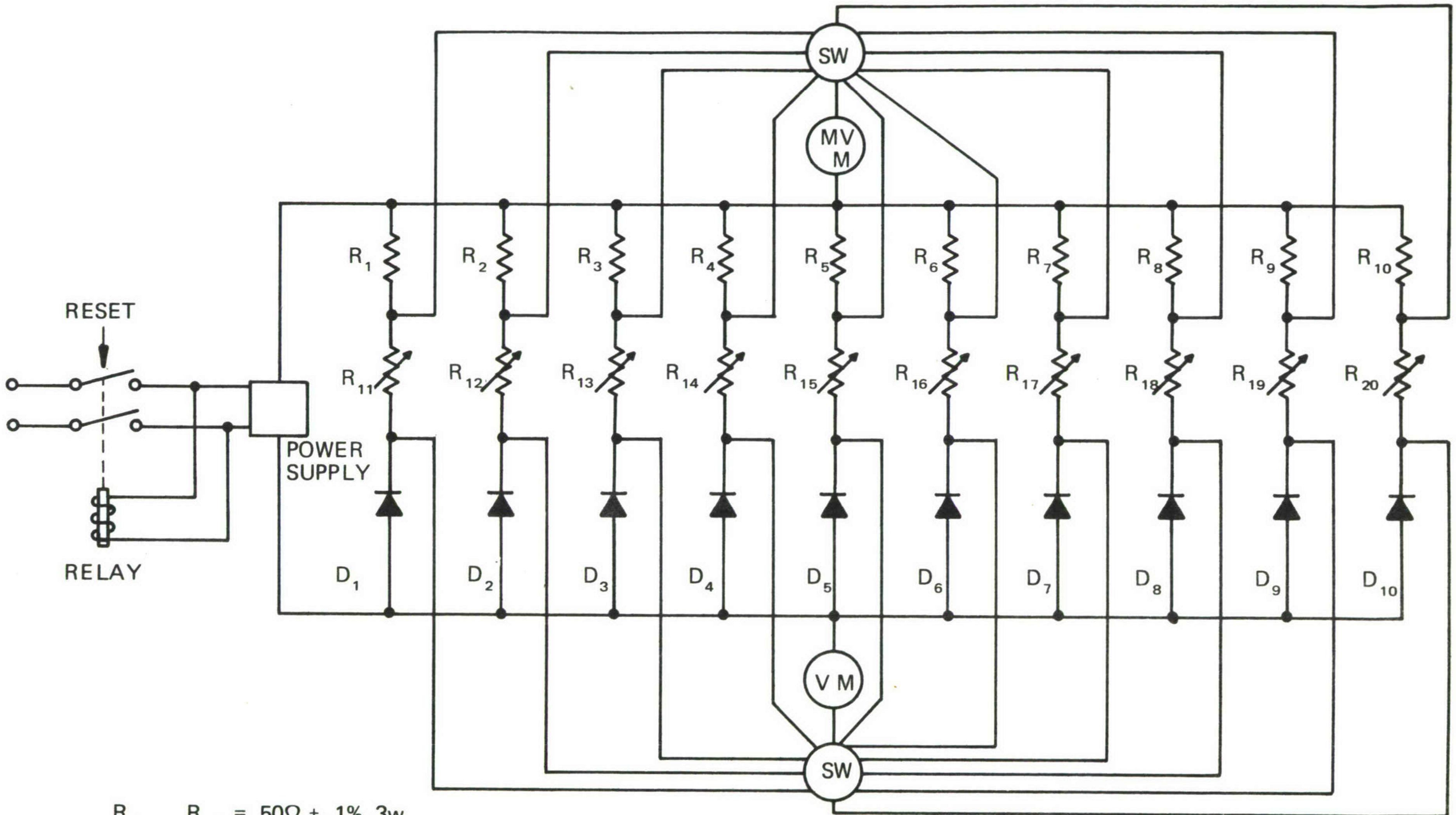

R_1 R_{10} = 50Ω ± .1%, 3w
R_{11} R_{20} = 1KΩ POTENTIOMETER, 10w
D_1 D_{10} = GaAs IMPATTS ON TEST

FIGURE 5 SCHEMATIC FOR GaAs IMPATT LIFE TEST CONTROL PANEL

D-11693

TABLE V

CHARACTERIZATION OF GALLIUM ARSENIDE IMPATT DIODES BEFORE AND AFTER DC BURN-IN AT 50°C

Diode		C_{TO}	V_B	P_o	F_o	V_{op}	I_{op}	Package Style	Burn-In Volts	Run #	Hours
1	Before	3.30	46.5	600	11.55	59.1	80	ODS-30	60.0	5060-1A	24
	After	3.30	46.3	600	11.59	58.9	80	ODS-30	60.0	5060-1A	24
2	Before	3.30	45.5	600	11.50	57.7	83	ODS-30	58.0	5060-1A	24
	After	3.30	45.2	600	11.53	57.8	85	ODS-30	58.0	5060-1A	24
3	Before	4.70	45.3	1W	10.36	61.5	136	ODS-30	62.0	5031-2A	24
	After	4.70	45.1	1W	10.40	61.2	135	ODS-30	62.0	5031-2A	24
4	Before	4.90	43.9	1W	10.43	60.1	140	ODS-30	61.0	5031-2A	24
	After	4.90	44.0	1W	10.44	59.9	140	ODS-30	61.0	5031-2A	24
5	Before	5.10	45.5	1W	10.42	61.2	141	ODS-30	62.0	5060-1A	24
	After	5.10	45.6	1W	10.43	61.2	142	ODS-30	62.0	5060-1A	24
6	Before	4.50	44.5	1W	10.53	61.3	136	ODS-30	62.0	5031-2A	24
	After	4.50	44.1	1W	10.52	61.4	137	ODS-30	62.0	5031-2A	24
7	Before	5.40	44.0	1W	10.20	60.9	151	ODS-30	61.0	5031-2A	24
	After	5.40	43.9	1W	10.23	60.6	148	ODS-30	61.0	5031-2A	24
8	Before	3.80	40.5	1W	11.22	56.3	143	ODS-30	57.0	5079-1B	24
	After	3.80	40.2	1W	11.28	56.4	146	ODS-30	57.0	5079-1B	24
9	Before	4.60	41.8	1W	10.80	56.6	137	ODS-30	57.0	5079-1B	24
	After	4.60	42.1	1W	10.75	56.8	146	ODS-30	57.0	5079-1B	24
10	Before	3.80	45.6	750	10.95	60.1	99	ODS-30	61.0	5060-1A	24
	After	3.80	45.4	750	10.94	59.9	99	ODS-30	61.0	5060-1A	24

C_{TO} = Zero Bias Junction Capacitance

V_B = Breakdown Voltage

In 24-hour production burn-in at 35°C, a yield of 91% was observed for 142 unselected units. This yield is higher than that achieved for Gunn diodes because all IMPATTs were necessarily preselected for RF, capacitance, and breakdown characteristics in order to determine the proper burn-in voltage.

HTRB (high temperature reverse bias) testing of gallium arsenide IMPATT diodes has also been carried out. The diodes were biased below breakdown (40 volts) and subjected to a 150°C heat sink temperature. These diodes were RF characterized following 168, 500 and 1000 hours. Parameter changes of less than 10% were seen. Of thirty one-watt units tested, only one diode failed (electrically open). However, two diodes burned out during RF testing following HTRB. Hence, HTRB testing was judged to be insufficient as a reliability assurance test for gallium arsenide IMPATT diodes.

Although high 24-hour burn-in yields have been achieved for gallium arsenide IMPATTs at 50°C case temperature, diode reliability has not been assured. Even diodes surviving extended burn-in have been damaged by RF mismatch during testing. Hence, although 24-hour, 50°C burn-in appears to be sufficient to weed out thermally poor units and affect parameter stabilization, additional screening is required to insure reliable RF performance in the case of a mismatch condition.

IV. LONG-TERM LIFE TEST RESULTS

DC burn-in has established the short-term reliability of Gunn and gallium arsenide IMPATT devices with respect to high temperature operation. Additional experiments have been conducted to determine long-term reliability with respect to switching transients, as well as degradation of RF performance.

The switching transient study involved six Gunn diode oscillators operated at 10 volts bias and a case temperature of 40°C. Each oscillator was connected to a matched RF load. An automatic switch was used to turn the bias voltage on and off for alternate two-minute periods. A total operating time of 9,288 hours has been accumulated by each oscillator without failure. Figure 6 depicts the experimental situation, while Table VI presents the RF and dc parameters of these units at approximately monthly intervals. Although some changes in parameters are presented, it is felt that these are due to operator error and do not represent real changes in the diodes involved. In testing, each oscillator is critically matched for maximum power output using an external slide screen tuner, the power output and, hence, operating current and frequency are, to some degree, a function of the patience of the operator.

The diodes now being cycled in the switching transient apparatus were loaded into the six oscillators on 1 January 1973. Previously, the experiment had been run an additional 5,312 hours, but severe performance degradation was observed. A 3 dB or greater power loss was recorded in all but two surviving units, and one unit failed entirely after 2,204 hours. Those degradations in performance are believed to be due to two factors. First, the thermal resistance of the original set of diodes was not measured because at the time the experiment was started, a reliable thermal resistance measurement method was not available. When the first run was terminated on November 18, 1972, the thermal resistance of the surviving diodes was

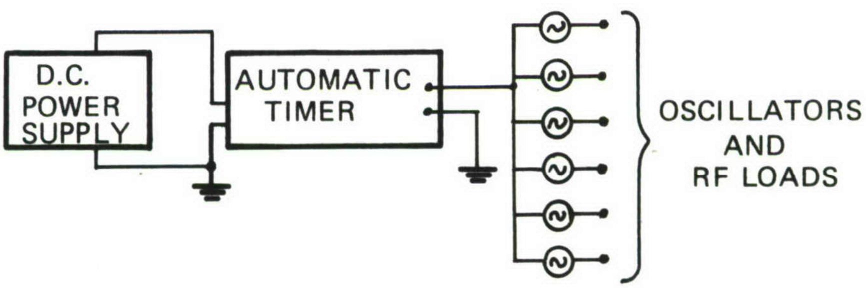

FIGURE 6 APPARATUS USED IN CYCLING GUNN DIODE OSCILLATORS ON AND OFF

D-11170

TABLE VI

CHANGE IN RF AND DC PARAMETERS DURING
GUNN DIODE SWITCHING TRANSIENT TEST

Oscillator Number	Time (Hours)	V_T (Volts)	I_T (mA)	P_o (mW)	f (GHz)	I_{op} (mA)
1	0	3.57	443	84	10.72	409
	2,832	3.44	447	89	10.71	408
	5,376	3.31	442	70	10.72	400
	8,016	3.28	446	85	10.715	408
	9,288	3.30	452	84	10.71	410
2	0	4.25	757	155	10.56	524
	2,832	3.79	762	150	10.60	524
	5,376	3.47	749	145	10.58	523
	8,016	3.55	764	150	10.55	539
	9,288	3.39	765	155	10.60	527
3	0	3.34	553	123	10.05	432
	2,832	2.11	557	106	10.04	428
	5,376	2.84	545	106	10.04	421
	8,016	2.90	555	113	10.05	429
	9,288	2.85	557	105	10.07	430
4	0	3.07	425	95	10.83	367
	2,832	2.92	431	102	10.84	373
	5,376	2.82	422	94	10.84	349
	8,016	2.78	428	105	10.83	363
	9,288	2.78	435	110	10.84	361
5	0	4.56	550	59	10.22	414
	2,832	4.30	555	54	10.22	408
	5,376	4.12	553	45	10.21	407
	8,016	4.11	555	52	10.218	407
	9,288	4.00	555	58	10.237	417
6	0	3.69	953	248	10.78	722
	2,832	3.21	959	250	10.78	717
	5,376	2.83	956	185	10.76	689
	8,016	2.92	967	238	10.76	715
	9,288	2.86	963	230	10.75	712

measured using the improved method to be described in a later section. In the case of three of the diodes, the measured thermal resistance was over twice the theoretical value. An additional diode failed during the thermal resistance measurement. Hence, the performance degradation is believed to have been due, in part, to excessive diode thermal resistance. These diodes were burned-in 24 hours at 35°C case temperature prior to installation in the switching transient apparatus.

A second cause of changes in output power during the Gunn diode switching transient test became evident when the six oscillators were reloaded with fresh diodes of nearly theoretical thermal resistance. After 1104 hours of operation, one of the reloaded units produced no power output. Before starting the second run (and also the first run) each oscillator had been critically coupled for maximum power using an iris coupling screw. A slight adjustment of this screw restored full power to the unit, described above, which had no power output upon initial testing. Evidently, a slight change in diode impedance or cavity characteristics with age caused the diode to stop oscillating, since in the critically coupled condition, the diode operation was extremely sensitive to impedance change.

Accordingly, the experiment was restarted using the same diodes but without iris coupling. Critical coupling was achieved during RF power measurement using an external slide screen tuner. As the data of Table VI shows, no performance degradations have been observed in this set of diodes.

In a separate experiment, the RF output power and bias current of one Gunn diode in a cavity resonator has been continuously monitored for 15,620 hours. As shown in Figure 7, the diode was connected in one arm of a wheatstone bridge circuit with a Rustrack recorder in the adjacent arm. In this way, a full scale deflection on the recorder was made to correspond to

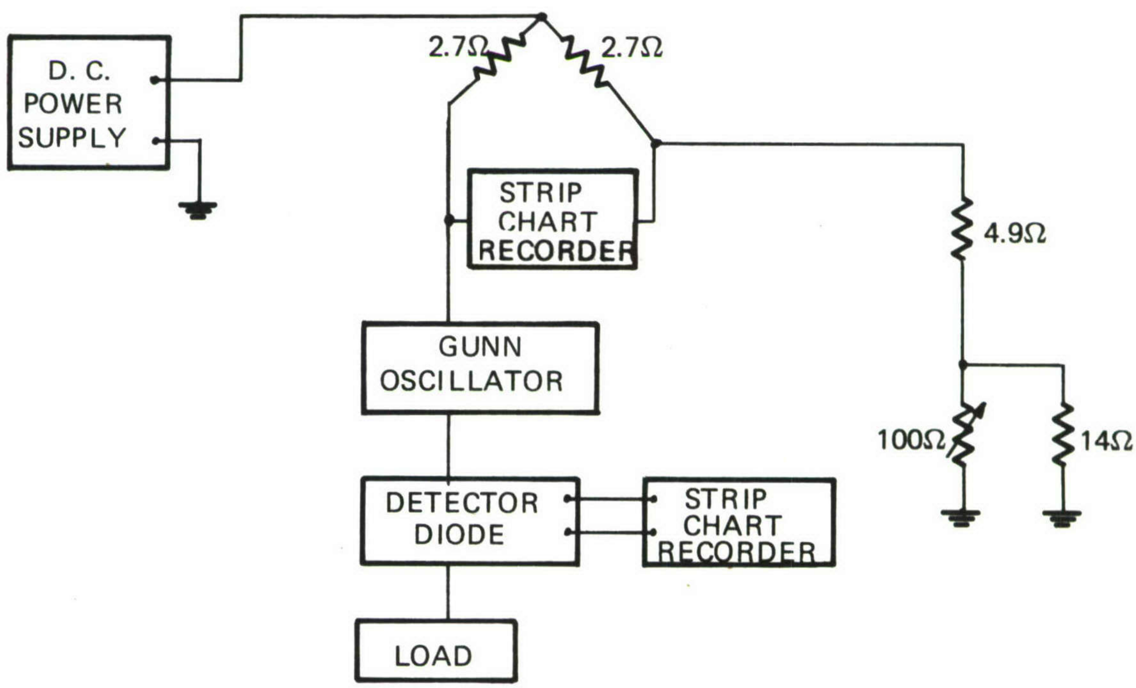

FIGURE 7 APPARATUS USED TO MONITOR THE CURRENT AND RF OUTPUT POWER OF ONE GUNN DIODE

D-11139

a change in diode current of only 10 mA. A 579 mA, 10 volt, 170 mW X-band diode was used and operated at a 40°C case temperature. A second recorder driven by a diode detector monitored RF power output.

During the first 2500 hours of operation, a 2.5 mA drop in current and 14% increase in output power were observed. No other significant changes were seen. Some fluctuations in output power has occurred but was traced to a poor RF connection at the detector diode. Table VII presents measured diode parameters following 0, 10,248 and 14,628 hours of operation. As shown, no change has occurred following almost two years of operation.

Before inception of this program, fifteen TCB construction Gunn diodes were placed on long-term dc burn-in at 10 volts bias, 75°C heat sink temperature, and an average operating current of 500 mA. These diodes have accumulated 325,000 unit hours of operation without a failure. If this figure is combined with previous long-term life test data obtained in the same test kit, a total of 461,000 unit hours without failure is obtained. If a failure is assumed to occur now, a minimum MTBF for Gunn diodes of this type may be calculated from the chi square distribution. If a 90% confidence level is chosen, the true MTBF for these units would lie between 153,900 and 8.9×10^{6} hours.

The exact level of stress applied to these diodes during this test is not known because diode thermal resistance was not measured prior to initiation of the test. Indeed, at the time the test was initiated, a reliable thermal resistance measurement technique did not exist. As described in a following section, additional long-term life tests have been initiated using diodes of known thermal resistance. However, only a few thousand unit hours of operation have been accumulated to date.

Long-term reliability testing of gallium arsenide IMPATT diodes was initiated in September 1972. All diodes used were burned-in in a minimum

TABLE VII

VARIATION IN PARAMETERS OF A GUNN DIODE OSCILLATOR DURING LONG-TERM OPERATION

V_T (Volts)	I_T (mA)	P_o (mW)	f (GHz)	I_{op} (mA)	Hours
3.86	805	168	10.674	579	0
3.50	795	167	10.694	573	10,248
3.62	801	170	10.69	573	14,648

of 24 hours at 35°C case temperature. Seven X-band 0.5 watt output level units have accumulated 26,572 unit hours of RF burn-in operation at 5.5 watts of dc input power and a case temperature of 55°C. Three failures have occurred following 400, 450 and 1,400 hours of operation. These failures were apparently related to turn-on/turn-off transients in the life test apparatus, as they occurred upon restarting following power line failure. Such failures emphasize the problem of extreme sensitivity to bias line transients shown by gallium arsenide IMPATT diodes.

Two 100 mW output level diodes biased at 2.2 watts of dc input power have operated for a total of 22,736 unit hours in a long-term RF test. A case temperature of 50°C was maintained. No failures have occurred.

In a dc burn-in experiment, 25 Ku-band, 1/2 watt output gallium arsenide IMPATTs on permanent dc burn-in have accumulated 40,944 unit hours of operation at 80°C case temperatures and rated dc input power (5 to 7.5 watts). These diodes had been previously burned-in 24 hours at 35°C and rated operating voltage. One diode failed (short) after 100 hours

of operation, while a second failed due to a power supply malfunction after 400 hours. This unit was replaced with a fresh diode and the test continued. At 1100 hours of operation, a third diode failed (breakdown shifted from 41.1 to 12 volts).

Upon completion of the test (after 1728 hours), the dc parameters of surviving diodes were remeasured. Table VIII presents the data obtained. In addition to the three diodes mentioned above, three additional diodes had degraded slightly in that the breakdown was no longer sharp. These units were not considered to have failed for the purpose of computing unit hours of operation.

Because of the limited amount of data available concerning gallium arsenide IMPATT diode long-term reliability, no prediction of expected field reliability can be made at this time. Obviously, severe reliability problems remain to be solved, since only 80% of the diodes surviving standard 24-hour burn-in passed the 1700 hour dc burn-in without degradation.

TABLE VIII

DC PARAMETERS OF GALLIUM ARSENIDE
IMPATT DIODES BEFORE AND AFTER 1728 HOURS OF DC BURN-IN
AT 80^{o}C CASE TEMPERATURE

Diode	Initial C_{TO}, (pF)	Final C_{TO}, (pF)	Initial V_B, Volts at 1 mA	Final V_B, Volts at 1 mA	Comments
1	2.90	3.23	41.2	43.0	
2	3.00	3.17	43.1	44.0	
3	2.10	2.41	42.3	44.0	Soft breakdown
4	3.90	3.85	44.3	45.0	
5	3.95	3.86	44.6	46.0	
6	3.45	3.50	47.0	48.0	
7	3.70	3.55	44.7	47.0	
8	4.30	4.18	45.2	46.5	
9	4.10	3.94	45.0	46.0	
10	3.00	-	41.5	-	Short after 100 hours
11	3.10	2.30	44.7	50.0	Soft breakdown
12	4.60	4.75	41.8	44.0	
13	4.65	4.79	41.1	42.0	Slightly soft breakdown
14	3.90	3.78	41.8	44.0	
15	4.30	4.19	44.0	47.6	
16	4.70	4.66	44.0	45.5	
17	3.50	3.48	42.0	44.0	
18	2.80	2.87	39.9	42.0	
19	3.60	3.75	38.3	40.0	
20	3.30	3.25	38.7	41.0	
21	3.70	3.72	41.3	43.0	
22	4.00	4.08	40.0	41.6	Accidentally damaged after
23	3.90	3.97	42.0	43.5	400 hrs, replaced with
24	3.40	3.44	39.8	41.5	fresh diode
25	3.40	3.93	41.1	12	Soft breakdown following 1100 hours

V. GUNN DIODE ACTIVE REGION TEMPERATURE DETERMINATION

Knowledge of the operating temperature of the active region of a Gunn diode is of importance from the standpoint of reliable long-term operation. Much research involving various semiconductor devices has shown that the mean-time to wearout failure is accelerated exponentially with absolute active region temperature. An accurate determination of active region temperature allows prediction of the useful diode lifetime if accelerated life testing has established the activation energy.

The active region operation temperature is commonly expressed in terms of the device thermal resistance, defined as follows:

$$\theta = \frac{T_{AR} - T_c}{P_{in} - P_{out}} \tag{1}$$

where

T_{AR} = the temperature of the diode active region, ^oC

T_c = the case temperature, ^oC

P_{in} = the dc power input to the device

P_{out} = the RF power output

In most cases, P_{out} in the denominator of (1) may be ignored in comparison to P_{in}, since the dc to RF conversion efficiency is usually 7% or less.

In the case of Gunn diodes, T_{AR} is determined by using the change in low field resistance of the gallium arsenide active region with temperature. The low field (below threshold) diode resistance varies with temperature according to the following:

$$\frac{R_H}{R_C} = \left(\frac{T_{ARH}}{T_{ARC}}\right)^{\alpha} \quad (2)$$

where

R_H = diode low field resistance at active region temperature T_{ARH}, ^{o}K

R_C = diode low field resistance at active region temperature T_{ARC}, ^{o}K

The exponent α has been exponentially determined to lie between 1.00 and 1.25 for diodes from 12 gallium arsenide wafers. Diodes prepared from the same gallium arsenide wafer exhibit very little difference in α: however, larger variations were found between diodes from different wafers (see Table IX). In general, α was measured by applying 100 mV dc to a diode and recording the current as the temperature was raised from 30 to 175^{o}C by external heating. Plotting the data on log-log paper with temperature in degrees Kelvin, produced a straight line of slope α. Recently, only two current readings have been used, 30 and 150^{o}C.

The Gunn diode thermal resistance may be computed from measured values of the low field resistance taken at two temperatures. Combining Equations (1) and (2) yields

$$\theta = T_c \left[\left(\frac{R_H}{R_c}\right)^{1/\alpha} - 1 \right] / P_{in} \quad (3)$$

TABLE IX

A COMPARISON OF VALUES OF α FOR DIODES FROM THREE GALLIUM ARSENIDE WAFERS

Diode	Wafer 5155-2A	Wafer 6119-2B	Wafer 1016-2B
1	1.20	1.053	1.259
2	1.17	1.157	1.293
3	1.22	1.199	1.123
4	1.15	1.149	1.274
5	1.16	1.174	1.14
6	1.15	1.188	1.272
7			1.155
8			1.241
Average	1.175	1.153	1.220

Particularly in the case of a high input power diode, the case temperature during operation quickly rises above the case temperature when the diode is not operating. Equation (3) may be corrected for this change as follows:

$$\theta = \frac{T_{c1}}{V_{op} I_{op}} \left[\left(\frac{R_H}{R_c} \right)^{1/\alpha} - \frac{T_{c2}}{T_{c1}} \right] \tag{4}$$

where

T_{c1} = diode heat sink temperature with dc bias off

T_{c2} = diode heat sink temperature with dc bias on

R_c = diode low field resistance with dc bias off

R_H = diode low field resistance with dc bias on

α = a constant of value 1.0 to 1.25

V_{op} = applied dc bias voltage

I_{op} = dc operating current

Figure 8 shows the initial equipment arrangement used to measure R_H and R_c. Because θ is very sensitive to errors in measuring R_H and R_c, precautions have been taken to improve the basic accuracy obtainable by direct measurement from an oscilloscope face. R_H and R_c are measured at a specified prethreshold voltage using a 0.5 microsecond duration 1000 Hz repetition rate pulse voltage. The resulting pulse current is then measured with a current probe. In measuring R_H, the diode is operated at rated dc voltage and current and pulsed back to the same prethreshold voltage used to measure R_c. A small RF voltage at 10 to 20 MHz is injected along with the pulse signal at the diode anode. The exact amplitude of the sine wave voltage and current during the pulse is measured by matching amplitudes against a second RF voltage applied to the second channel of a dual trace oscilloscope. After matching, the second RF voltage is measured with an RF voltmeter.

Table X presents data for several Gunn diodes concerning the correlation of the thermal resistance measured using the technique just described with the results of die temperature measurement using a Barnes Engineering Model RM-2B Infrared Radiometer. The IR radiometer with 52X objective was used to measure the operating temperature within a 1 mil diameter spot on the back of the diode chip. In determining thermal resistance from this optical data, the temperatures at four equally spaced (if possible) points on the diode chip were used.

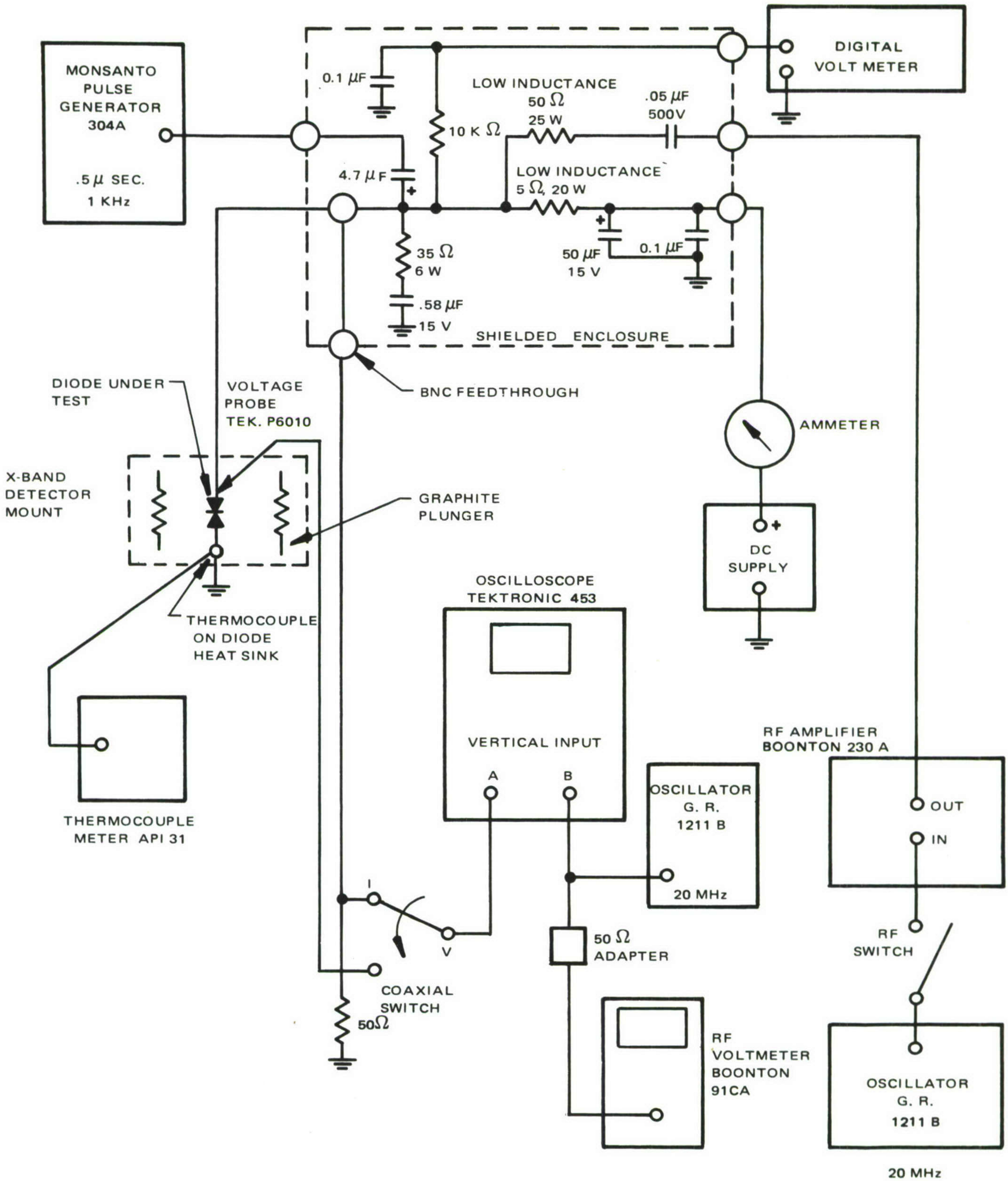

FIGURE 8 GUNN DIODE THERMAL RESISTANCE TEST SET

D-11500

TABLE X

A COMPARISON OF THERMAL RESISTANCE MEASURED USING THE IR RADIOMETER WITH THERMAL RESISTANCE MEASURING USING THE PULSE METHOD

Diode	θ (IR Radiometer) °C/W		θ (Pulse) °C/W
	Average	Maximum	
2102-1B-3	8.15	9.25	10.0
2103-10-10	8.0	8.0	9.62
2139-2B-2	10.2	11.7	12.3
2111-2B-3	8.84	10.4	9.56
6065-1A-3	8.62	9.22	9.72
6050-1A-5	8.56	11.25	9.52
6050-1A-6	8.44	10.05	7.89
2132-2A-1	7.68	9.14	9.05
2132-2A-2	8.8	11.0	9.65
2132-2A-3	9.54	10.7	9.28
2111-1D-2 (TCB Bonded)	16.5	18.3	14.9
6041-2-1	4.78	-	6.73
6041-2-2	5.2	-	6.47
6041-2-3	10.26	-	13.5
6041-2-4	4.87	-	9.84
6041-2-5	6.05	-	8.21

Note: PHS Diodes were used except where noted.

Unfortunately, when the data for Table X was collected, the value of α used in Equation (4) was taken as 1.0. Since α is, in general, larger than 1.0, the θ (pulse) values will generally be up to $2^{\circ}C/W$ lower than those shown in Table VIII. Nevertheless, the agreement, in most cases, is good enough to demonstrate the validity of the electrical measurement.

Although the thermal resistance measurement just described was demonstrated to be accurate, it was not suitable for large volume production testing because of the numerous complicated adjustment steps involved. A faster, more accurate method was required, which would not depend on operator judgement or skill, and could be adopted more readily to automated testing. Figure 9 presents a block diagram of an improved electrical method for Gunn diode thermal resistance measurement. A constant current is applied to the diode by the reference current generator. Normal operating voltage is then applied through the high speed switch. The comparator allows matching of the reference voltage supply with the voltage across the diode during the time (5 microseconds) that the bias is switched off. In this way, the diode low field resistance is determined with the diode self-heated to normal operating temperature. In general, the incremental resistance is usually determined by repeating the measurement for two closely spaced reference current levels, avoiding error, should the current versus voltage characteristic be non-linear at low fields. By repeating the measurement with the dc bias off, the cold resistance could also be determined.

A correlation study of PHS construction Gunn diode thermal resistance measured using the improved electrical method versus the IR radiometer was also carried out. The results appear in Figure 10.

The correlation shown is quite good and indicates the usefulness of the electrical method. Since repeatability accuracy of the improved electrical method is about 5%, the error evident in Figure 10 is attributable to the

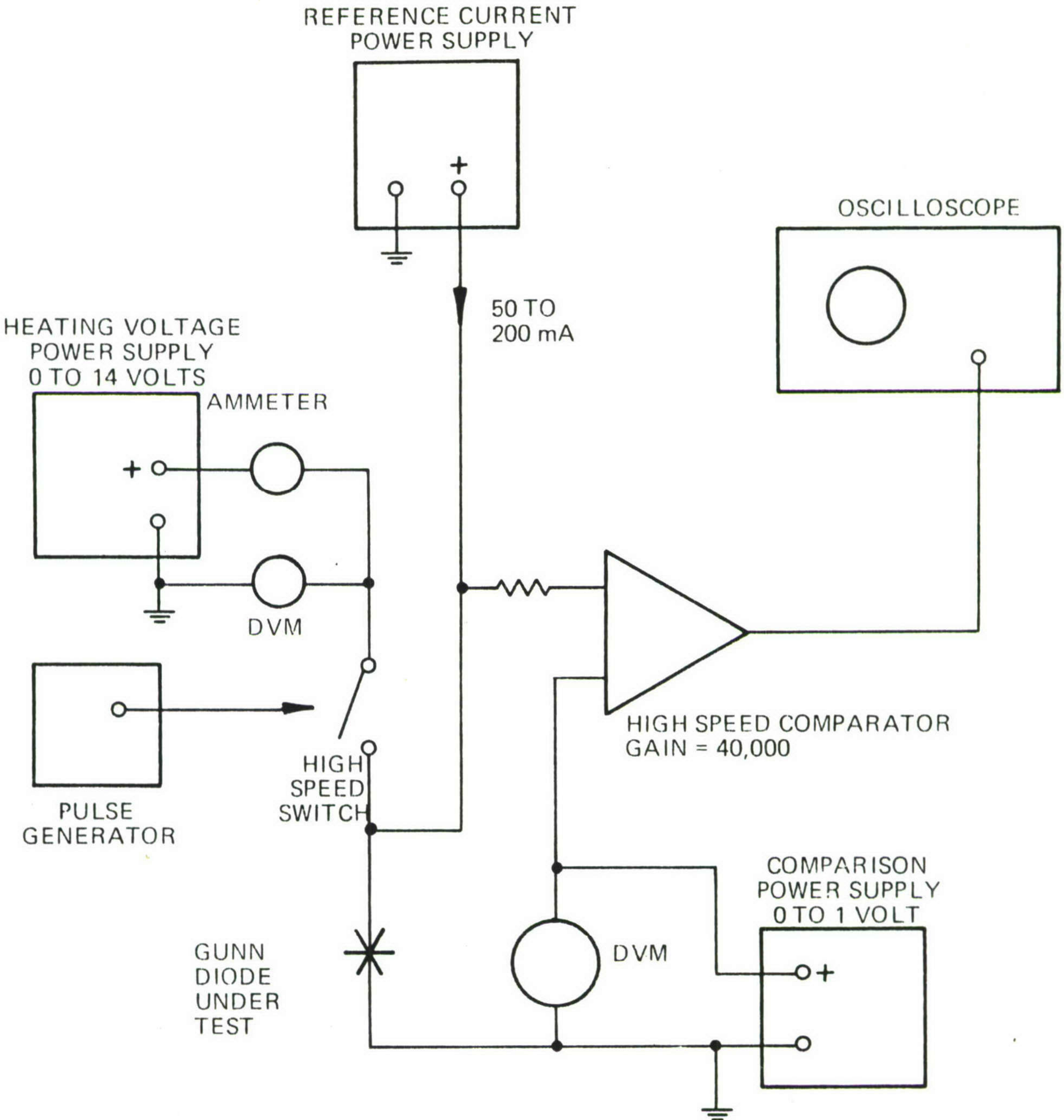

FIGURE 9 BLOCK DIAGRAM OF IMPROVED ELECTRICAL METHOD FOR GUNN DIODE THERMAL RESISTANCE MEASUREMENT

D 11694

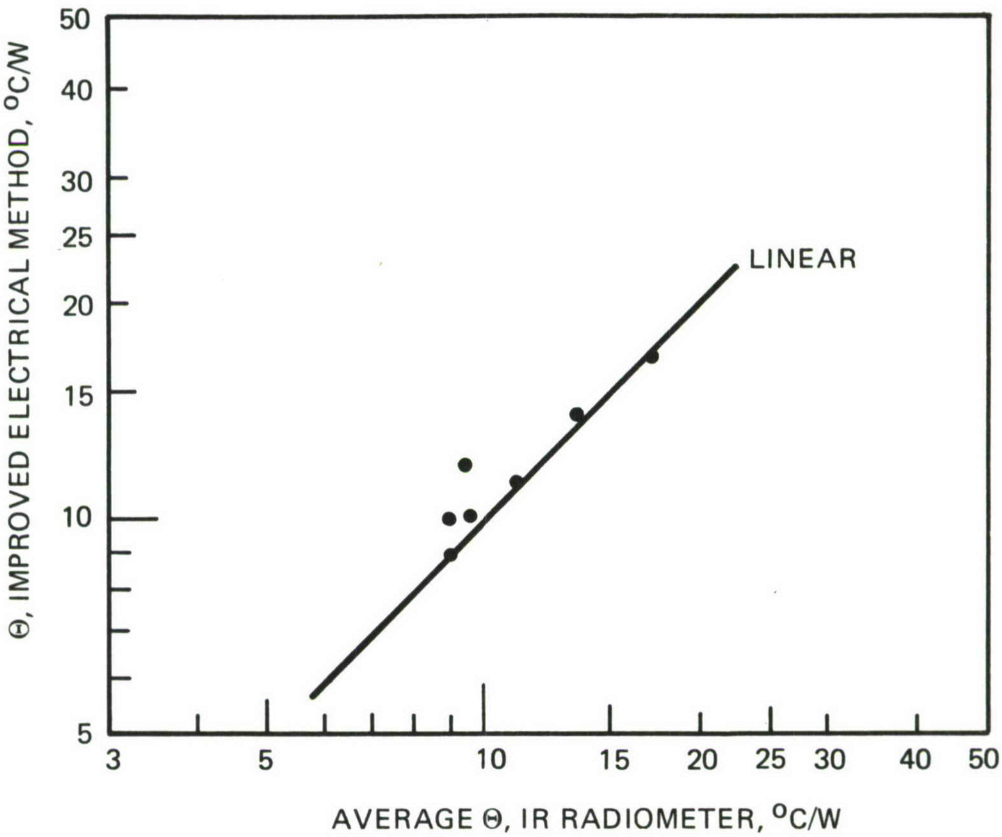

FIGURE 10 GUNN DIODE THERMAL RESISTANCE MEASURED USING THE IMPROVED ELECTRICAL METHOD VENSUS AVERAGE THERMAL RESISTANCE FROM IR MEASUREMENTS

D-12152

IR radiometer. Because a portion of the chip was necessarily obscured by the connecting straps, the IR radiometer data is probably in error by about $\pm 10\%$.

The Barnes Engineering Radiometer has also been used in an attempt to locate hot spots on the back of operating Gunn and gallium arsenide IMPATT chips. The apparatus of Figure 11 was used and a typical scan result appears in Figure 12. In this figure, E and S refer to the positions of the chip and strap edges. Although some indication of hot spotting is evident, it is possible that hotter regions under the contract straps or in an area not scanned were not detected. Also, hot spots of a diameter less than .001 inch would have appeared cooler than they actually were because the IR radiometer averages temperature in a .001 inch diameter spot.

A further source of error in IR radiometer temperature scan data concerns the necessity of determining the chip surface emissivity versus position while heating the chip to a known temperature (75°C). The target temperature is calculated as follows:

$$T = f\left[\frac{N_{BB}}{E_t}\right] + N_o \tag{5}$$

where

N_{BB} = measured target radiance

E_t = target emissivity

N_o = room temperature black body radiance

f = a function supplied in graphical form by Barnes Engineering

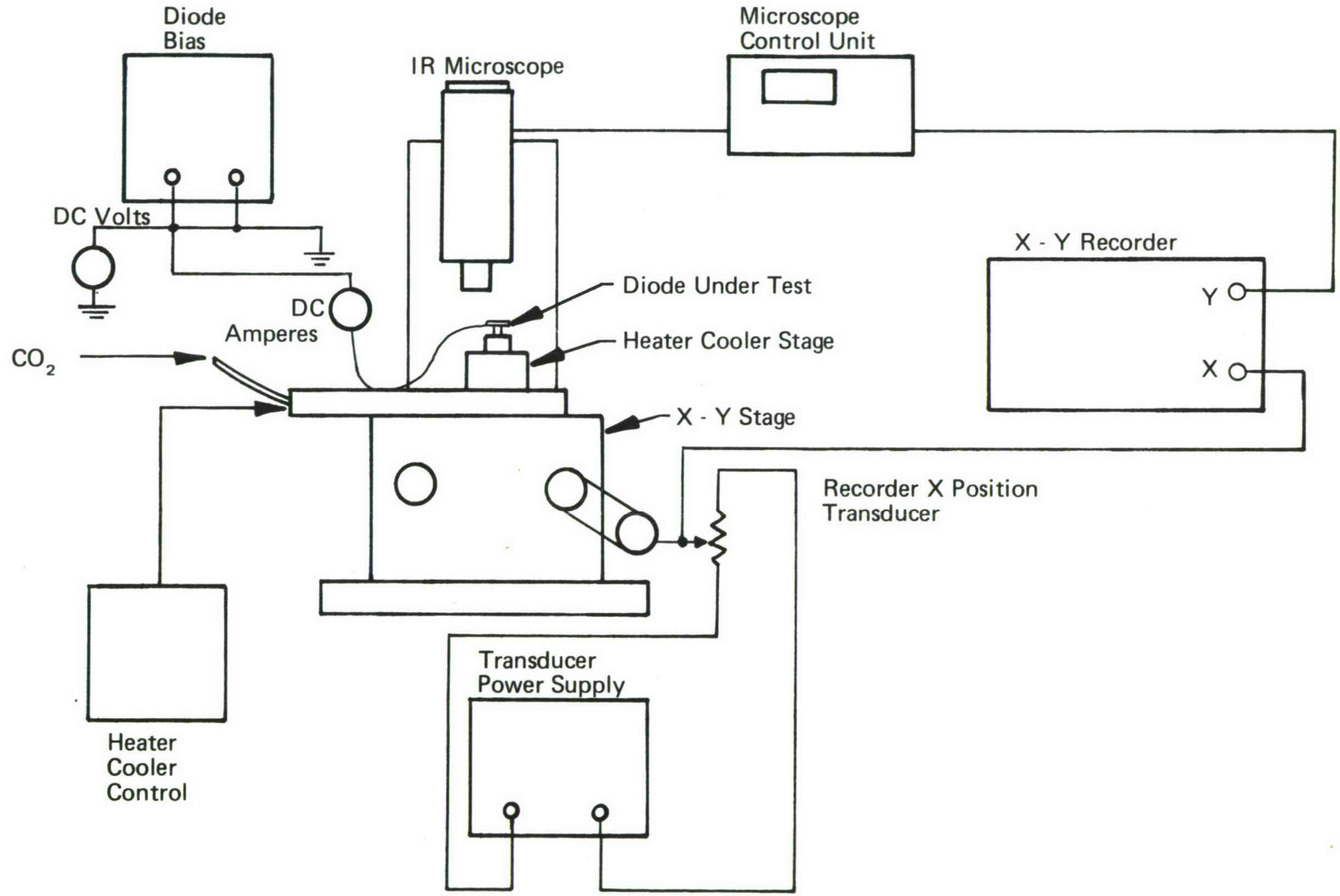

FIGURE 11 INFRARED MICROSCOPE AND RECORD - APPARATUS

D-11165

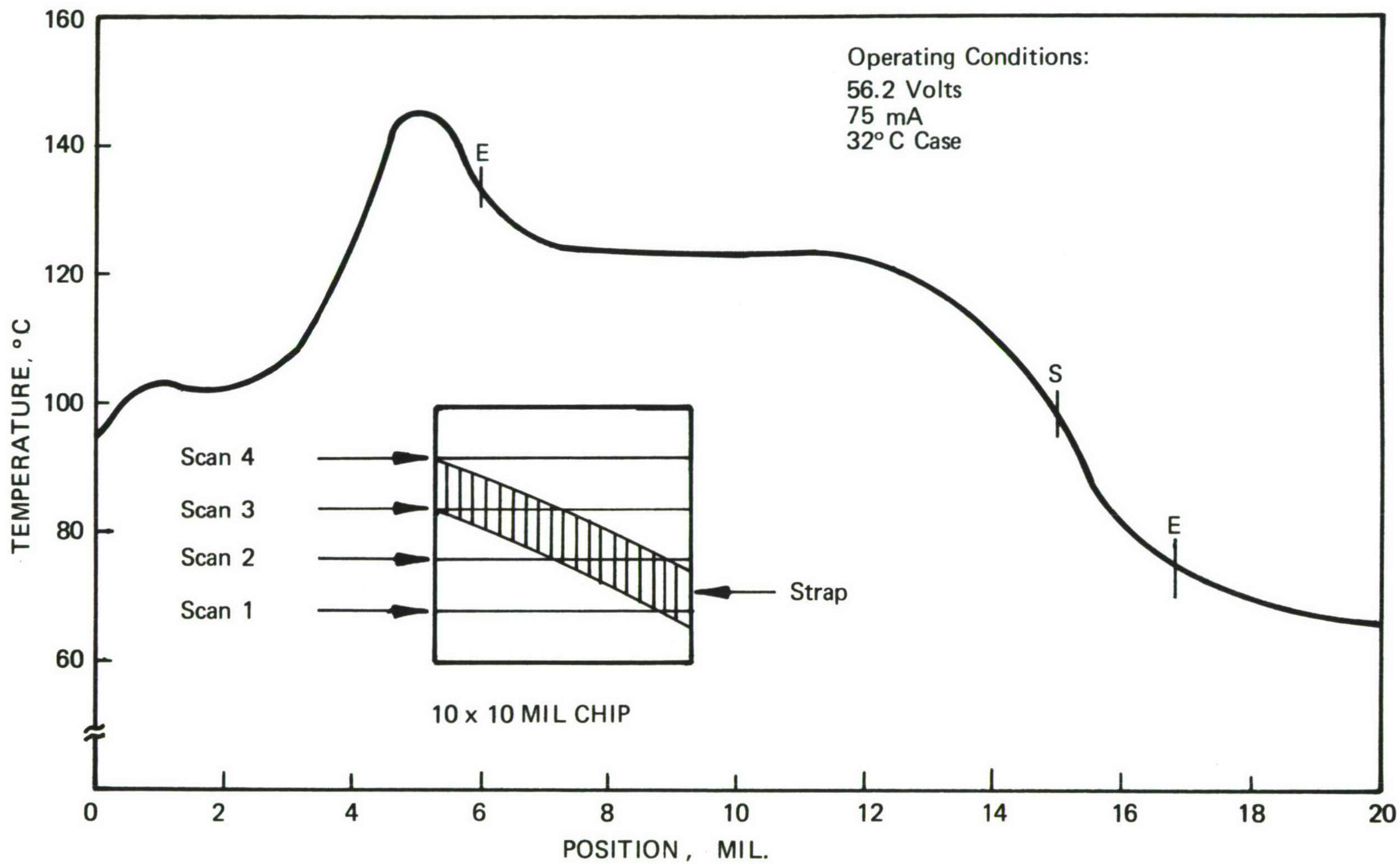

FIGURE 12 TEMPERATURE VERSUS POSITION Ga As IMPATT 5028-2 — SCAN #1

D-11154

The quantity actually measured on operating chips was the target radiance, N_{BB}. Any small position error between measurement of E_t and N_{BB} could have lead to significant temperature error. Therefore, the IR radiometer was judged to be of limited usefulness in hot spot location.

VI. GUNN DIODE STEP STRESS TESTING

The failure rate of electrical components plotted against hours of use from date of manufacture usually has the shape shown in Figure 13. High failure rates occur in two regions, early in life, and again much later in life. The early failure region is attributable to errors or defects in the manufacturing process, and can be eliminated by aging the units at the factory prior to shipment. In the middle region or useful life area, a small decreasing failure rate exists, and controls the diode MTBF, if infinite wear-out time is assumed. A second region of high failure rate occurs after many thousands of hours of operation and is attributed to component wear out. In order to investigate component performance in the wear out region, without requiring an unrealistically long period of time, some means of accelerating the aging is required. In semiconductor analysis, aging is usually accelerated by stressing the devices with an increase in operating temperature. When temperature is the stress, many physical processes are accelerated according to the Eyring-Arrhenius rate law [1, 2, 3]. The average time to wear out, t_m, at absolute temperature T is given by:

$$t_m = \exp \left\{ \left[\frac{\Delta H}{KT} + C \right] \right\} \text{ or} \tag{6}$$

$$\log t_m = \frac{\Delta H}{KT} + C \tag{7}$$

where

ΔH = the activation energy for the process
K = Boltzmann's constant
C = design constant factor
T = device active region temperature, $^{\circ}K$

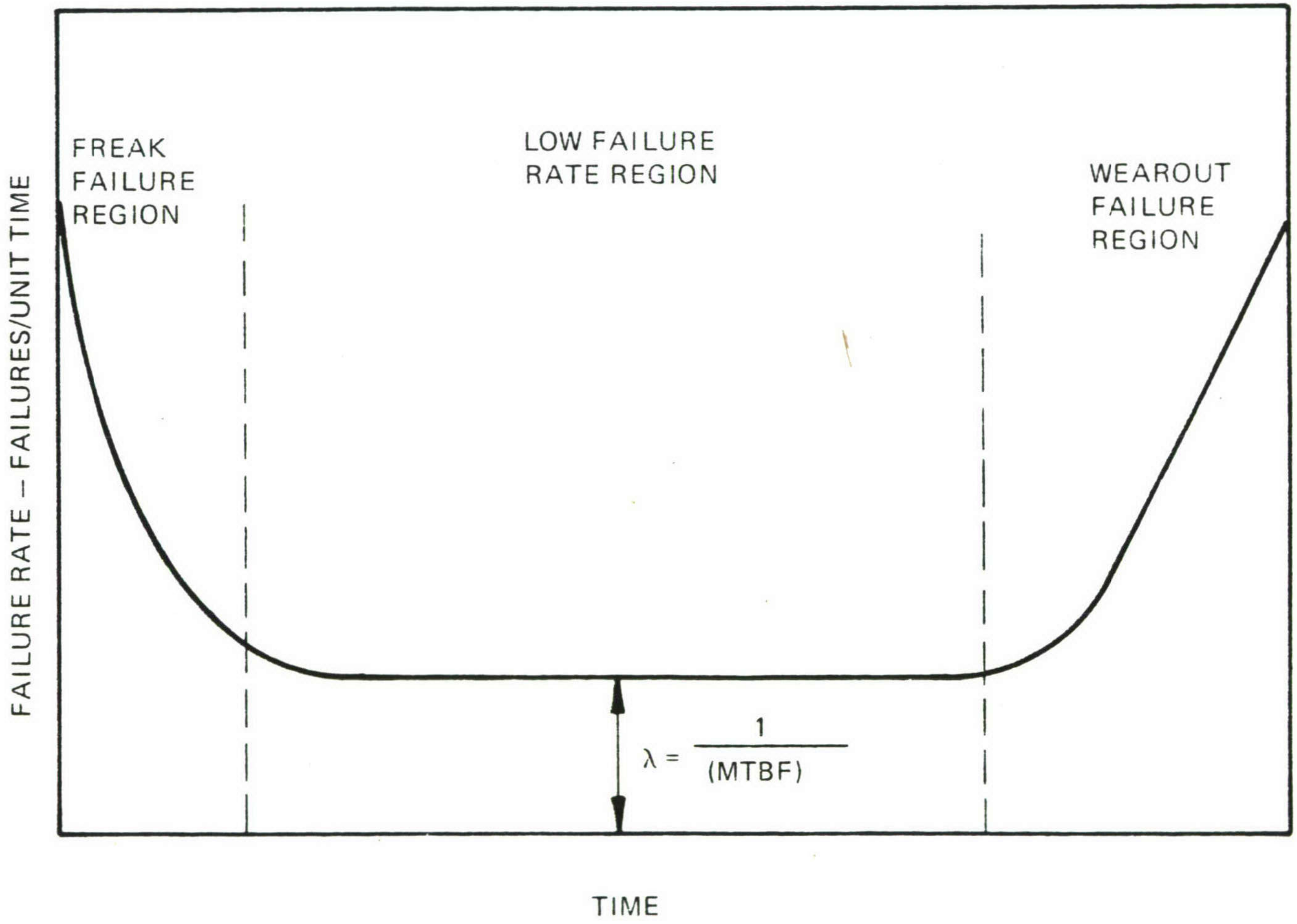

FIGURE 13 GENERALIZED FAILURE RATE VERSUS TIME

D-11501

Here, the factor C reflects variation from unit to unit in device manufacture or the effect of stress other than temperature. If, for a large number of units, temperature is held constant, and C is assumed to be normally distributed among units, then the time-to-failure is log normally distributed. Such a condition has been found to empirically describe most semiconductor failure distribution [4, 5]. Hence, the number of units failing per unit time is log normally distributed, and is given by:

$$N(t) = N_o\, p(t) = \frac{N_o}{\sigma\sqrt{2\pi\sigma}} \exp\left[\frac{(\log t - \log t_m)^2}{2\sigma^2}\right] \tag{8}$$

where

$N(t)$ = number of failures per unit time at time t
N_o = total number of units
$p(t)$ = probability of failure at time t
t_m = mean life time
σ = standard deviation

It can be shown that

$$\sigma = \log \frac{t_m}{t_{16}} \tag{9}$$

where t_{16} is the total time required for 16% of the units to fail. Once the validity of equation (8) has been established for a given process, the time-to-failure of any percentage of the population may be calculated from knowledge of σ and t_m. If t_m is determined for several different stress levels (temperatures), then using Equation (7), the activation energy, ΔH, may be determined, and t_m calculated for any given stress level. Convenient

nomographos are available for this purpose. Figure 14 is a graph of the failure rate acceleration predicted by the Arrhenius theory.

In order to determine the activation energy for a process, t_m must be determined experimentally for several different average active region temperatures. This technique is the so-called "constant stress" method, (see Figure 14), and involves operating a set of devices at a fixed temperature and recording the time-to-failure for each unit. The test must be repeated for at least two stress levels. Alternatively, the step stress method may be used where the devices are subjected to stress which is repeatedly increased in constant increments after a fixed time interval, until all devices fail. Here, the test is repeated using time intervals of at least two different lengths. All devices failing within a given time interval are considered to have failed at the end of the interval in question.

As shown in Figure 14, either the constant stress or step stress technique may be used to generate the Arrhenius accelerated failure curve.

Initially, the step stress method was chosen for Gunn diode accelerated ageing, because it was believed that the step stress method would yield results in a shorter time. Also, step stress testing allowed use of diodes with varying thermal resistances in the same test lot, while constant stress testing would have required sorting diodes on the basis of thermal resistance in order to stress all diodes in a lot to the same active region temperature.

The equipment used in Gunn diode step stress testing is shown in Figure 15. The diodes were mounted in 2-inch by 6-inch by 1/4-inch gold plated copper heat sink blocks which were in-turn placed on heater stages. Three blocks have been constructed, each holding 20 diodes. The stage temperature was then controlled by a temperature controller driven by a thermocouple mounted in the heat sink. The current monitoring circuit was designed so that ammeter switching did not momentarily interrupt diode

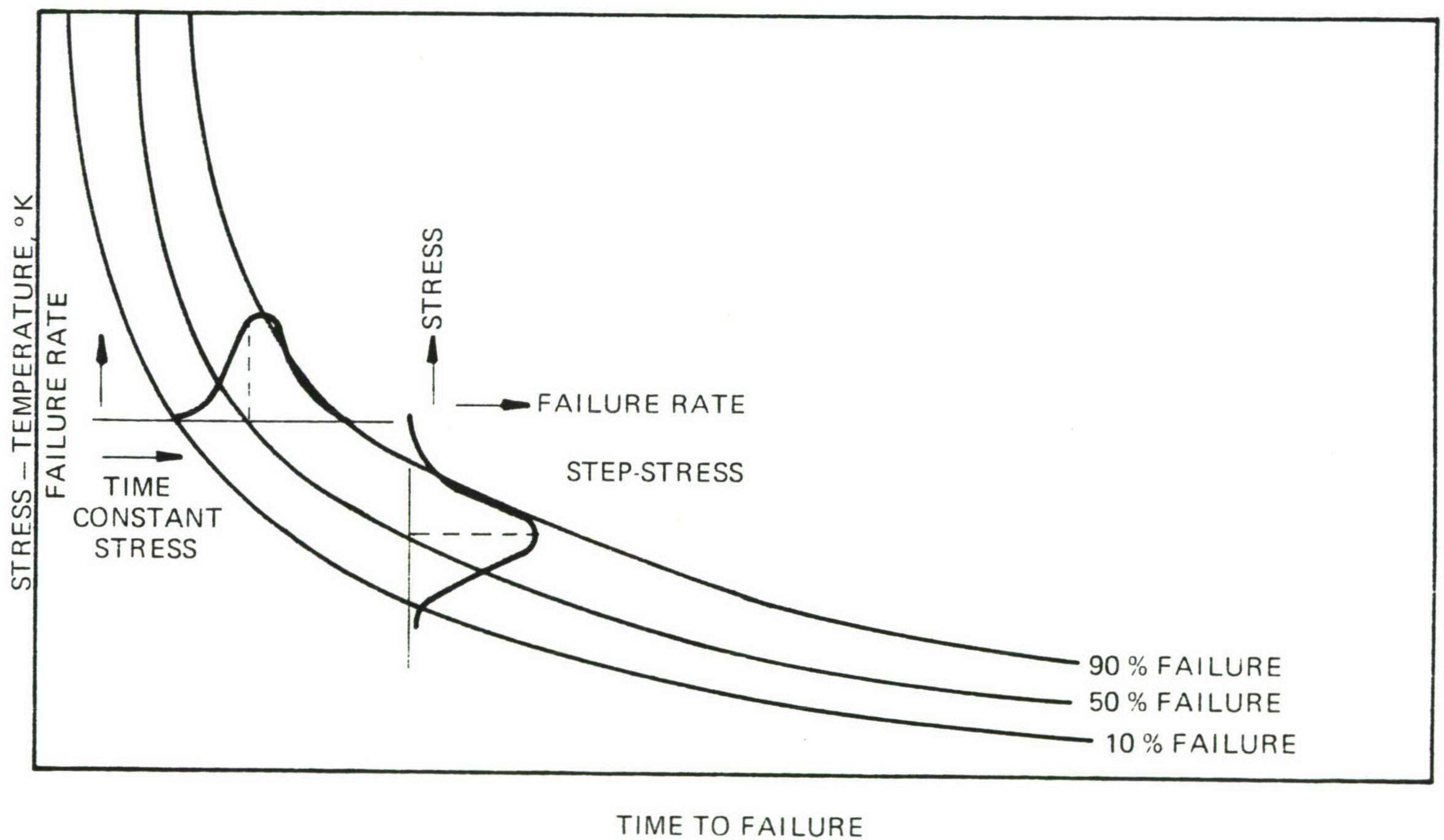

FIGURE 14 ACCELERATED FAILURE CURVE SHOWING STEP STRESS TEST AND CONSTANT STRESS TEST

D-11502

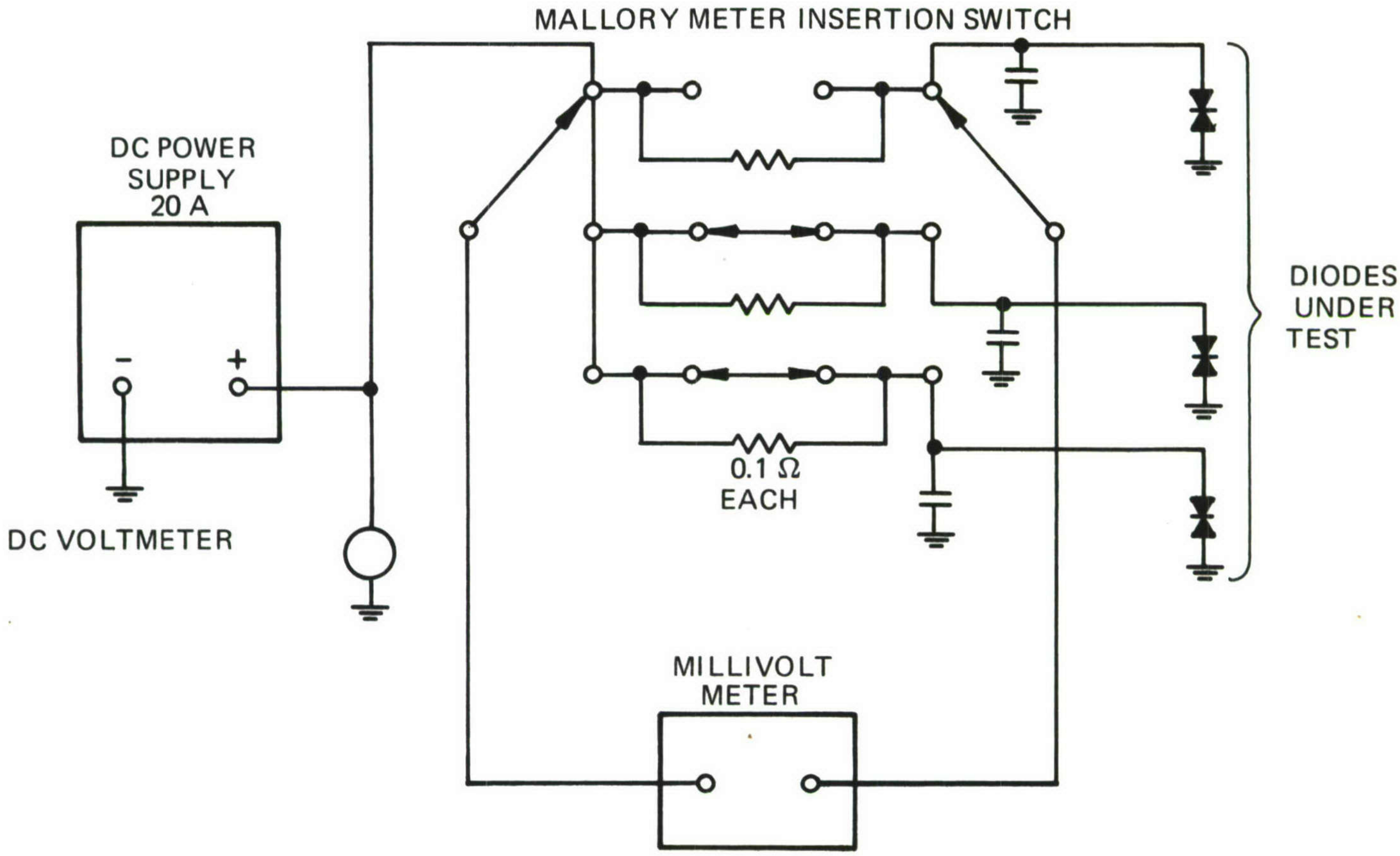

NOTE: Only three diodes are shown, but each meter insertion switch may be used to monitor up to 12 diodes.

FIGURE 15 CIRCUIT USED IN STEP STRESS TO FAILURE TESTING OF GUNN DIODES

D-11503

current, since such current interruption could initiate failure in units close to their wearout limit. Current was measured by connecting a digital millivoltmeter across a 0.1 ohm resistor permanently connected in series with each diode.

In computing the active region temperature of the Gunn diodes at failure, the thermal resistance measured prior to step stress testing was used. Thermal resistance was measured using the electrical method shown in Figure 9. However, a correction to the measured thermal resistance was required because the thermal conductivity of gallium arnsenide varies as C/T with absolute temperature. This correction, $\Delta\theta$, is computed as follows:

$$\Delta\theta = \frac{L}{2r^2 C\pi} (T_2 - T_1) \tag{10}$$

where

$\Delta\theta$ = change in thermal resistance if the temperature is changed from T_1 to T_2 $^{\circ}$K, $^{\circ}$C/W

L = thickness of active region, cm

r = mesa radius, cm

C = a constant (approximately 150), W/cm

In this derivation, cylindrical symmetry, one dimensional heat flow, and hemispherical spreading into a semi-infinite heat sink were assumed [6]. If failure occurs at about 300°C active region temperature, an increase in thermal resistance over the value measured at 30°C of 2°C/W for 9.5 micron thick 9 mil diameter units results.

In the first two step-stress runs, a second correction to the measured thermal resistance was required to account for the thermal drop between the diode stud and external heat sink. This drop was measured by

attaching a thermocouple to the stud of a diode and monitoring the temperature drop between the diode stud and the heat sink. In the case of the prong package, (ODS-30), a correction, θ_c, of 4 to 6°C/W thermal resistance was found. In later step-stress tests, the need for this correction was eliminated by soldering the diodes into the heat sink block.

In computing the failure temperature for each diode, the following formula was used:

$$T_F = V_{op} I_{op} \left[\theta + \Delta\theta + \theta_c \right] + T_{HS} \tag{11}$$

where

T_F = active region temperature at failure, °C

V_{op} = dc bias voltage

I_{op} = diode current at last reading before failure

θ = initial diode thermal resistance measured electrically

$\Delta\theta$ = increase in θ due to temperature dependence of the thermal conductivity of GaAs

θ_c = diode stud to heat sink thermal resistance (used only if diodes were not soldered in)

T_{HS} = heat sink temperature, °C, at the time failure occurred

All Gunn diode step-stress experiments were conducted at normal operating voltage for the diodes involved, (10 to 12 volts depending on active region thickness). The diodes used were burned-in 168 hours at 75°C heat sink temperature prior to installation in the step-stress apparatus. Only thermocompression diodes were used.

Eight complete Gunn diode step-stress experiments have been concluded thus far. Table XI summarizes the results obtained. The first two experiments involved 9 mil diameter, 9 micron thick active region, X-band, 100 mW output units stressed for 24-hour intervals. Figure 16 presents results obtained from these 17 units. The reciprocal failure temperature versus cumulative failure percentage is plotted on linear versus probability scale paper. The straight line obtained indicates that the reciprocal failure temperatures were normally distributed, as predicted by the Arrhenius equation (Equation (7)). If the number of units failing in time is log normally distributed, the number failing in reciprocal temperature is normally distributed. A mean failure temperature of 322°C was required to fail 50% of the diodes in a 24-hour period.

TABLE XI

SUMMARY OF GUNN DIODE STEP STRESS TESTING RESULTS

Run No.	Carrier Concentration $\times 10^{15}$ /cc	Active Region Thickness (μ)	Mesa Dia. (mil)	V_{op} (Volts)	Step Hours	No. Units	Average Active Region Failure Temperature
1 and 2	1.6	9.0	9	10	24	17	322°C
3	1.6	9.0	9	10	168	18	325°C
4	1.8	9.0	7	10	24	20	352°C
5	0.9	9.5	9	10	72	36	341°C
6	1.5	13.75	12	12	24	19	346°C
7	1.3	11	7	12	96	35	352°C
8	1.5	11	12	12	96	19	322°C

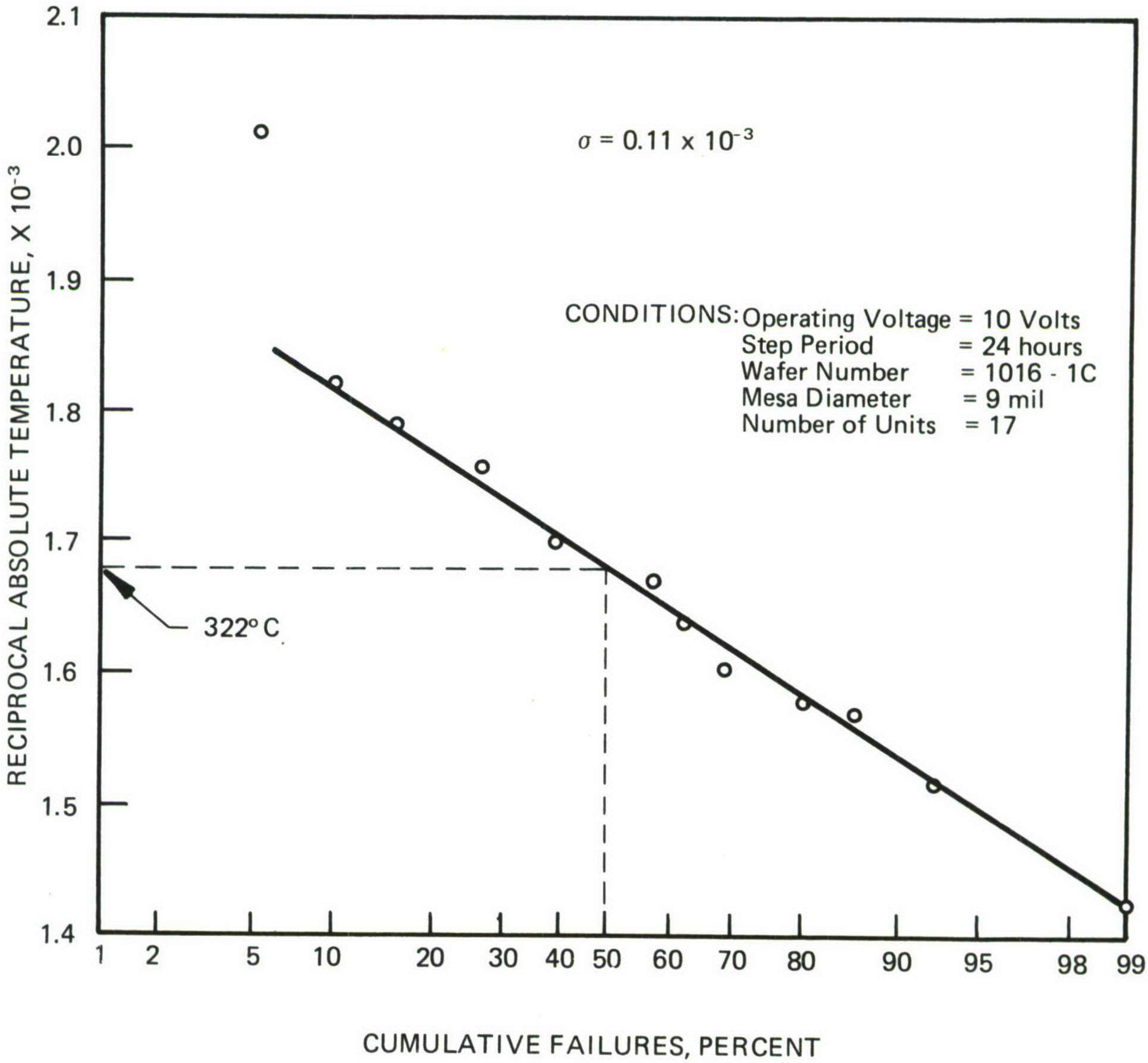

FIGURE 16 RECIPROCAL ABSOLUTE ACTIVE REGION FAILURE TEMPERATURE VERSUS CUMULATIVE PERCENT OF DIODES FAILING FOR GUNN DIODE STEP STRESS TESTS NUMBERS 1 AND 2.

In preparing Figure 16, a chart was constructed listing the number of diodes with active region temperature at failure falling in each $10^{\circ}C$ interval from 200 to $400^{\circ}C$. The temperature at the interval center was then used to characterize the group. A sample chart appears in Table XII. In plotting the data, one has been subtracted from the cumulative percentage in order to avoid losing the last data point, since the 100% point lies off scale on the probability paper.

In the third step-stress run, diodes from the same wafer as was used in Runs 1 and 2, were stressed for one-week periods, yielding the curve of Figure 17. Eighteen diodes were involved. As shown, a temperature of $325^{\circ}C$ was required to fail 50% of the units in a one-week period. The difference between this value and that obtained in the 24-hour test is insignificant (322° as compared to $325^{\circ}C$). In light of Equation (7), this result implies a zero activation energy. In other words, the failure temperature appears to be independent of operating time. Because the standard deviations of the failure temperature curves are different in the 24-hour and one-week tests, one could conclude that the diodes used in the two tests did not in reality come from the same populations.

In an attempt to resolve this problem, Run 5 was initiated, using diodes similar to those used in Runs 1, 2 and 3. Although not identical, these units were believed to duplicate the characteristics of the diodes used previously. In a 72-hour step-stress experiment, a mean active region failure temperature of $341^{\circ}C$ was obtained (see Figure 18). Again, this data does not fit the Arrhenius model when compared with the results of Runs 1, 2 and 3. A comparison may not be justified here, however, because several of the diodes used in Run 5 exhibited a new mode of failure. Instead of failing by becoming open or short circuited, above a certain active region temperature (about $340^{\circ}C$) the diode current began to drop with time, at constant heat sink temperature. Figure 19 is a graph of operating current

TABLE XII

SUMMARY OF STEP-STRESS DATA USED IN PREPARING FIGURE 16

Temperature Range, ^{o}C	No. Failures with T_A in Range	Cumulative Failures, %	Temperature Range Center, ^{o}C	Temperature Range Center, ^{o}K	$1/T_{center}$ $1/^{o}K \times 10^{-3}$
221-230	1	6.5	225	498	2.008
271-280	1	11.8	275	548	1.824
281-290	1	17.6	285	558	1.792
291-300	2	29.4	295	568	1.760
301-310	0		305	578	1.730
311-320	2	41.2	315	588	1.700
321-330	3	58.8	325	598	1.672
331-340	1	64.6	335	608	1.645
341-350	1	70.5	345	618	1.618
351-360	2	82.4	355	628	1.592
361-370	1	88	365	638	1.567
371-380	0		375	648	1.543
381-390	1	94	385	658	1.519
421-430	1	100	425	698	1.432

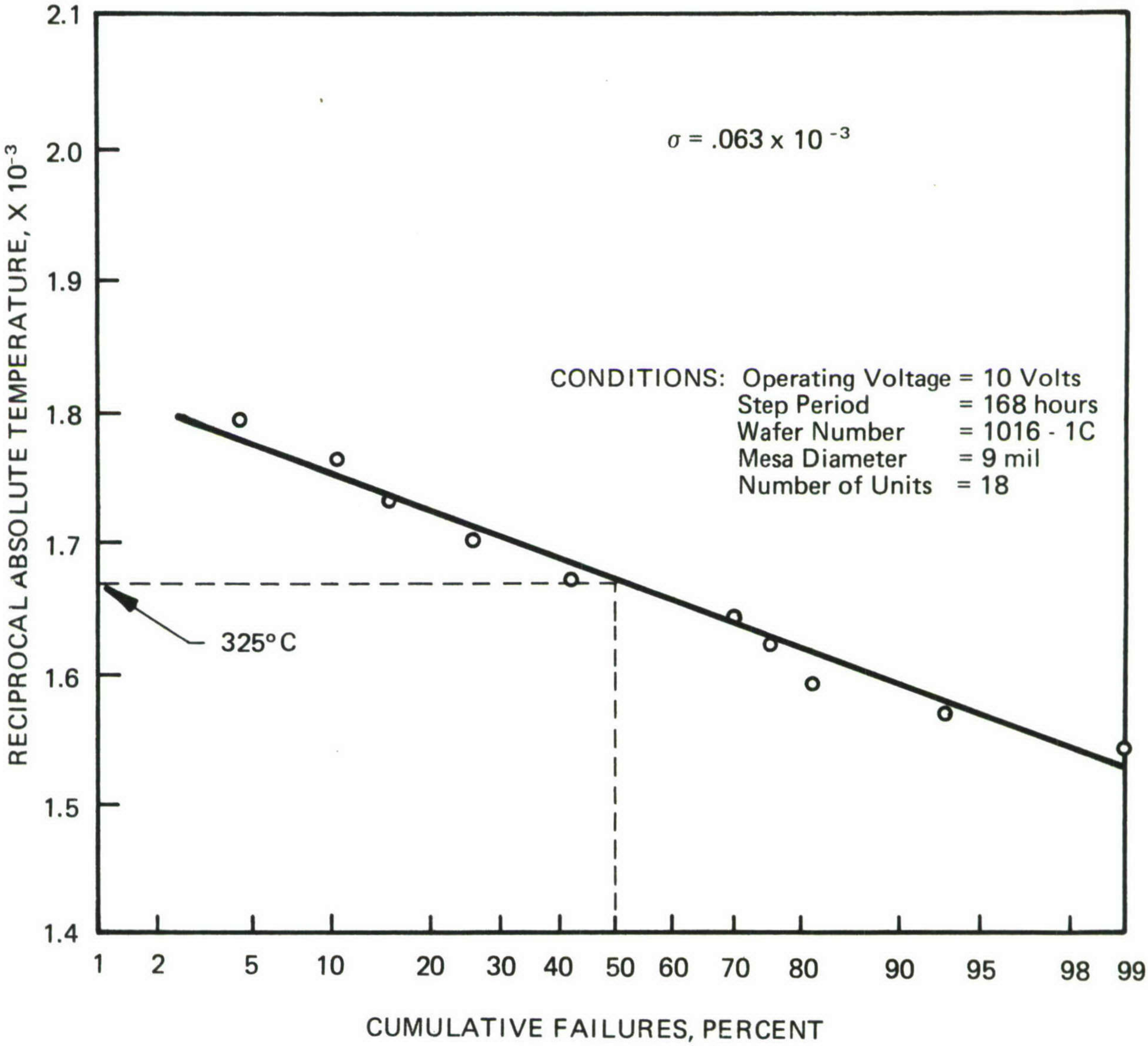

FIGURE 17 RECIPROCAL ABSOLUTE ACTIVE REGION FAILURE TEMPERATURE VERSUS CUMULATIVE PERCENT OF DIODES FAILING FOR GUNN DIODE STEP STRESS TEST NUMBER 3.

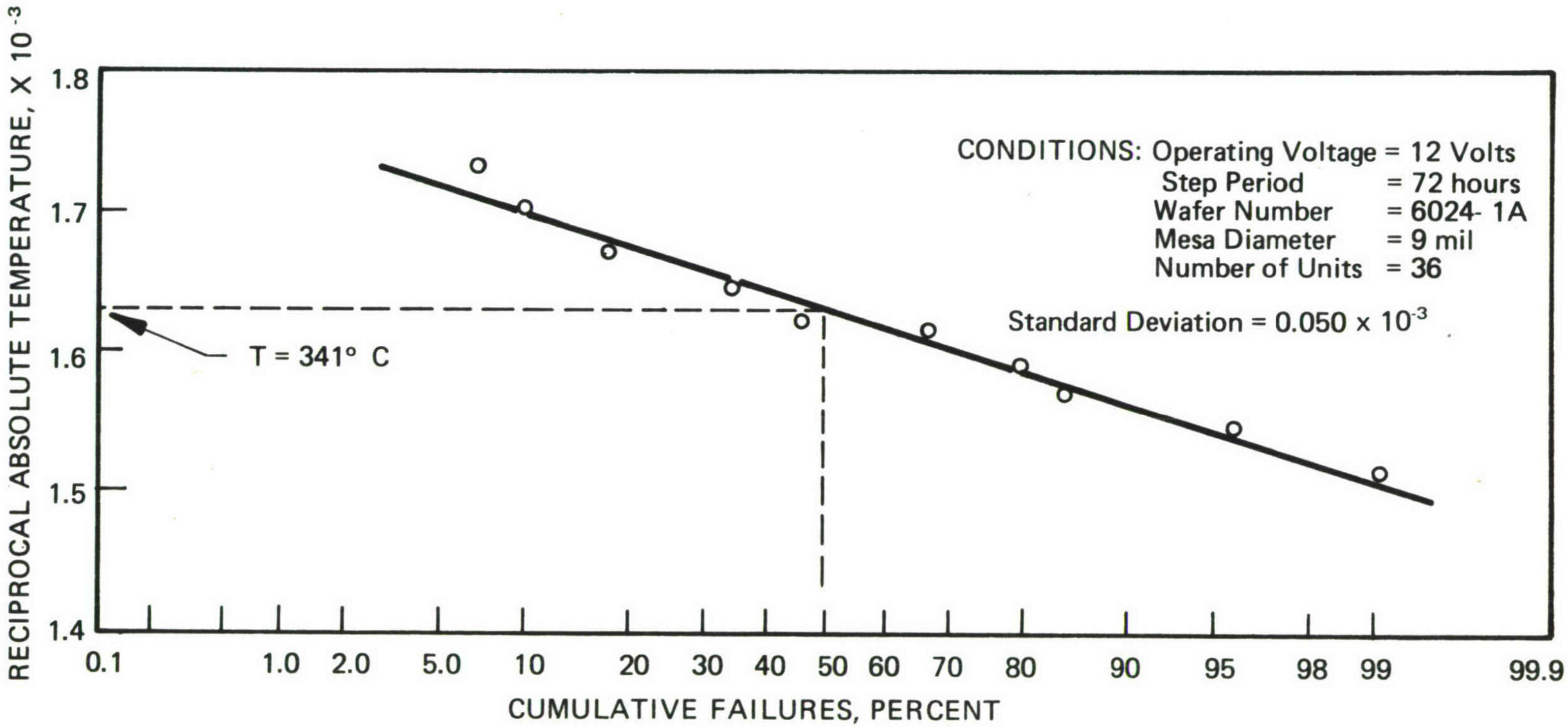

FIGURE 18 RECIPROCAL ABSOLUTE ACTIVE REGION FAILURE TEMPERATURE VERSUS CUMULATIVE PERCENT OF DIODES FAILING FOR GUNN DIODE STEP STRESS TEST NUMBER 5.

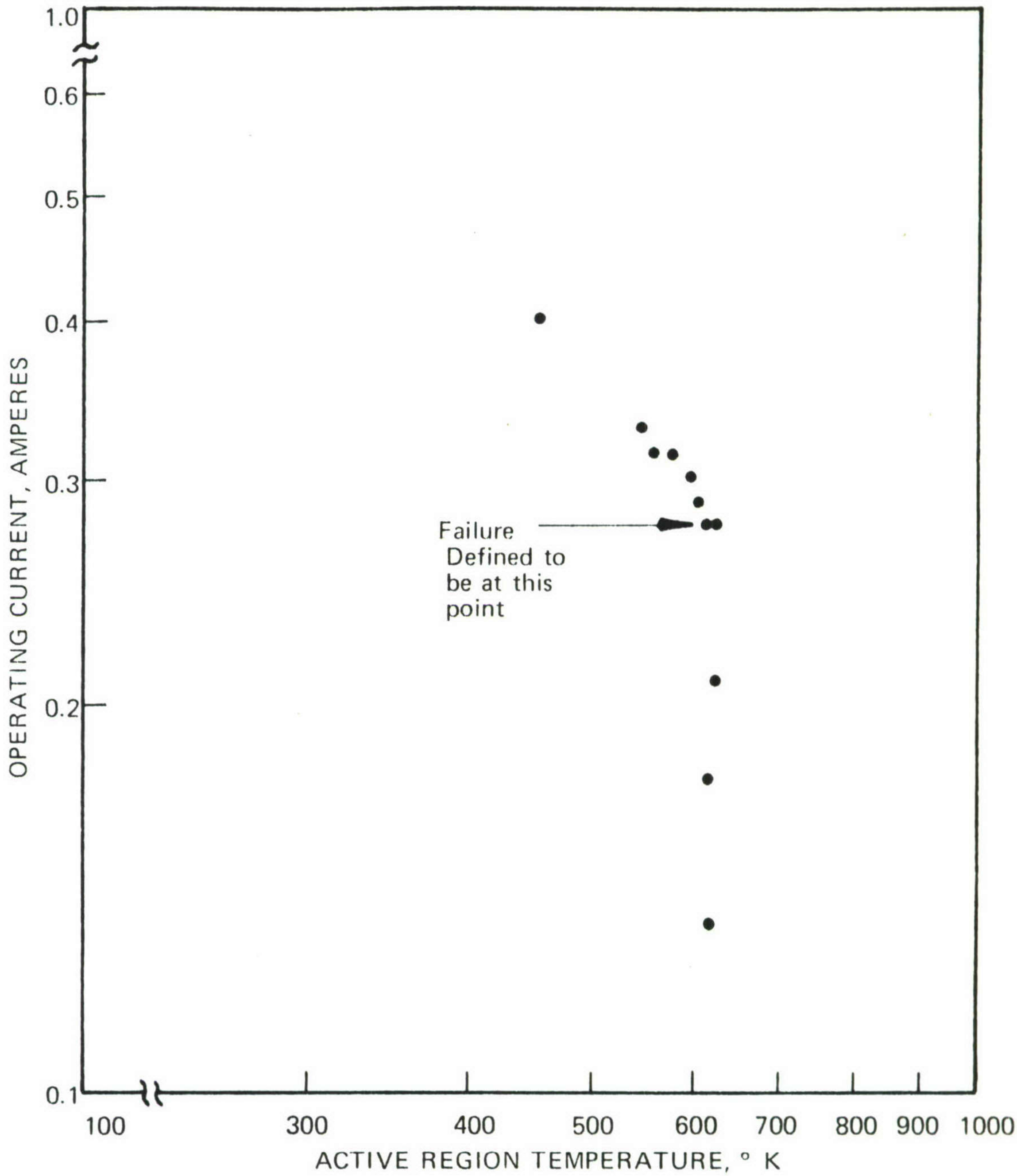

FIGURE 19 **OPERATING CURRENT VERSUS ACTIVE REGION TEMPERATURE FOR GUNN DIODE NUMBER 14. THE DATA WAS RECORDED DURING STEP STRESS TEST NUMBER 5.**

D - 11869

versus diode active region temperature for a typical unit exhibiting this type of failure. Failure was defined to have occurred at the highest active region temperature obtained before onset of this "current drop" phenomenon (see Figure 19). Of the 36 diodes involved in this run, 22 exhibited current drop. The current drop phenomenon was also observed in previous runs, but in only a small percentage of the diodes examined, (3 out of 20 diodes in Run 2, and 1 of 20 diodes in Run 3). Probably, current drop would have occurred in all diodes if failure had not occurred due to another mechanism at less than 340^{o}C.

At this point, a tentative explanation for this current drop behavior involving diffusion of the gold metallization into the gallium arsenide active region and subsequent resistivity increase due to acceptor formation was theorized. This hypothesis was investigated by a storage temperature experiment. After 27 days at 340^{o}C and zero bias, current drop had occurred in all but 1 of 16 diodes from the same wafer as was used in step-stress Run 5. The diodes were cooled to room temperature for daily current measurement. RF data being recorded after 5, 22 and 50 days and is presented in Table XIII. As shown, all diodes exhibited current drop accompanied by a reduction in RF output power following 50 days of high temperature storage. Some diodes, however, actually increased in efficiency (for example, #16). Another symptom of this mode of failure involved the disappearance of the threshold voltage (absence of current drop-back) accompanying severe current drop. Following 22 days of storage, diodes #8 and #15 exhibited no threshold voltage, and extreme degradation in RF power output.

Several diodes which exhibited current drop from step-stress run #5 and from the 340^{o}C storage temperature test were cross-sectioned and examined under high power magnification. Electron microprobe analysis was also carried out on one storage temperature diode with the kind of assistance of E.B. Hakim and Dr. J. Shappirio of ECOM, Fort Monmouth, New Jersey.

TABLE XIII

DEGRADATION OF GUNN DIODE RF PERFORMANCE DURING ELEVATED STORAGE TEMPERATURE TEST AT 340°C

Diode	Initial		Following 5 days		Following 22 days		Following 50 days	
	P_o (mW)	I_{op} (mA)	P_o (mW)	I_{op} (mA)	P_o (mW)	I_{op} (mA)	P_o (mW)	I_{op} (mA)
1	66	400	48	394	49	323	44	285
2	73	399	62	389	67	351	58	295
3	60	360	50	350	52	294	42	239
4	55	378	Open Circuit		--	---	--	---
5	50	368	30	342	27	262	10	241
6	67	401	39	385	65	369	50	292
7	57	388	Short Circuit		--	---	--	---
8	54	350	40	344	--	178	Open	
9	60	383	Open Circuit		--	---	--	---
10	65	390	47	380	49	337	Broken Pckg.	
11	57	393	41	384	52	353	Broken Pckg.	
12	38	280	Open Circuit		--	---	--	---
13	68	405	Short Circuit		--	---	--	---
14	68	400	50	395	65	356	60	314
15	66	419	50	412	3	190	Open	---
16	65	403	52	400	67	363	54	291

Conditions for RF Power Measurement: V_{op} = 10 volts

f_{op} = 9.1 GHz

Diodes cooled to room temperature for RF testing.

Figure 20 is a microscope photograph of diode #15 from the storage temperature test following cross-section, and for comparison, a diode which was not subjected to high temperature storage. Figures 21 and 22 present the same data for diodes #9 and #16 from step-stress run #5. Both diodes had exhibited current drop beginning at an active region temperature of $352^{o}C$. In both cases, the cross-section analysis revealed an apparent penetration of the gold metalization into the active region of the diode. The active region substrate interface is visible as a well-defined line in Figures 20, 21, and 22 due to the application of a stain etch. The hypothesis that a portion of the contact metalization had penetrated into the diode active region was substantiated by the electron microprobe analysis performed on one of the storage temperature diodes (#5). As shown in Figures 23 and 24, the X-ray image of gold indicates a high concentration in the area showing penetration in the optical microscope photograph. However, the micrograph of copper indicates no migration from the package pedestal. Two other somewhat surprising results of the microprobe analysis are evident in Figures 23 and 24. A large concentration of gallium is evident just above the package pedestal and a high nickel concentration region appears to exist in the penetration front as well as on top of the pedestal. No satisfactory explanation for these results can be offered at this time.

Because current drop and metalization penetration failure have occurred in a purely storage temperature situation, pure diffusion rather than ion migration is probably responsible for the change seen. If metalization diffusion begins only after a critical temperature is exceeded (perhaps the melting temperature of the metalization alloy), then the failure of step-stress testing to yield the average active region failure temperature could be understood.

Failure, due to contact metalization penetration, could be eliminated through the use of a higher melting temperature metalization scheme, or

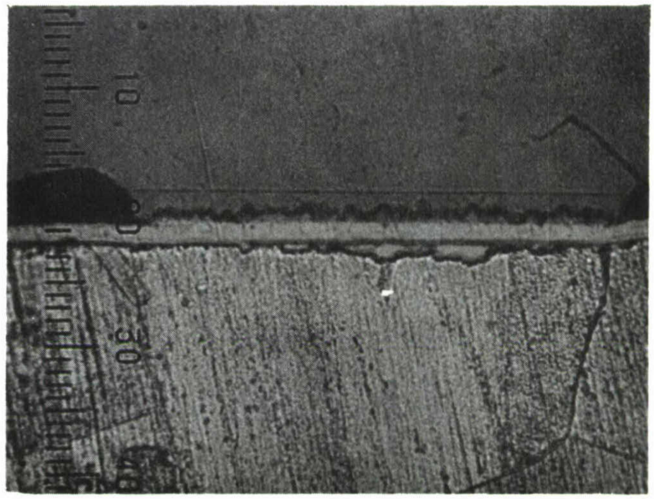

FIGURE 20 a MICROSCOPE PHOTOGRAPH OF A CROSS-SECTIONED GUNN DIODE FOLLOWING 1200 HOURS OF HIGH TEMPERATURE STORAGE AT 340°C. PENETRATION OF THE CONTACT METALLIZATION INTO THE ACTIVE REGION IS EVIDENT. EACH SCALE DIVISION IS 0.2 MIL.

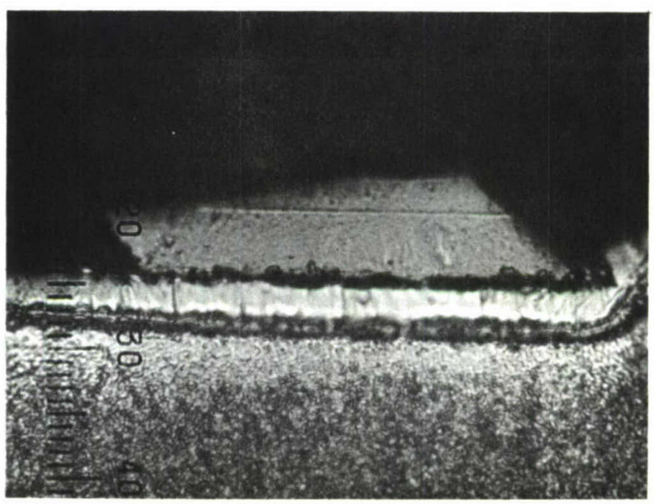

FIGURE 20 b MICROSCOPE PHOTOGRAPH OF A CROSS-SECTIONED GUNN DIODE FROM THE SAME WAFER AS THE DIODE SHOWN IN FIGURE 20 a. THIS DIODE WAS NOT SUBJECTED TO HIGH TEMPERATURE STORAGE. EACH SCALE DIVISION IS 0.1 MIL.

D-11941

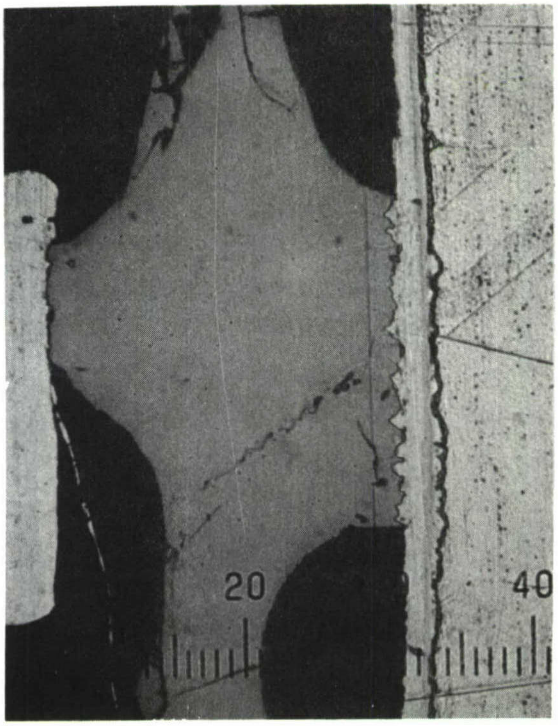

FIGURE 21 MICROSCOPE PHOTOGRAPH OF A CROSS-SECTIONED GUNN DIODE WHICH EXHIBITED CURRENT DROP FAILURE DURING STEP STRESS TESTING. PENETRATION OF THE CONTACT METALLIZATION INTO THE ACTIVE REGION IS EVIDENT. THE DIODE IS FROM STEP STRESS RUN 5, WATER 6024-1A, IDENTIFICATION NUMBER 9. EACH SCALE DIVISION IS 0.2 MIL.

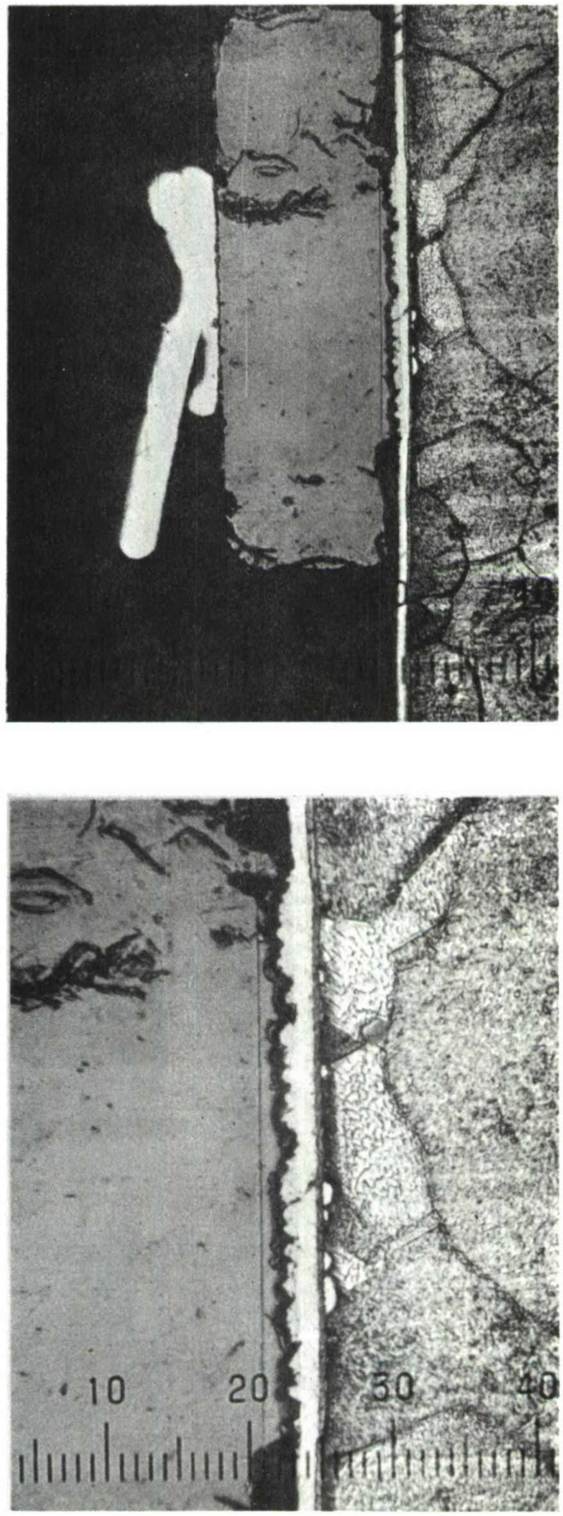

FIGURE 22 TWO MICROSCOPE PHOTOGRAPHS OF A CROSS-SECTIONED GUNN DIODE WHICH EXHIBITED CURRENT DROP DURING STEP STRESS TESTING. EACH SCALE DIVISION IS 0.4 MIL IN THE UPPER PHOTOGRAPH, 0.2 MIL IN THE LOWER. THE DIODE IS FROM STEP STRESS RUN 5, WAFER 6024-1A, IDENTIFICATION NUMBER 16.

D-11873

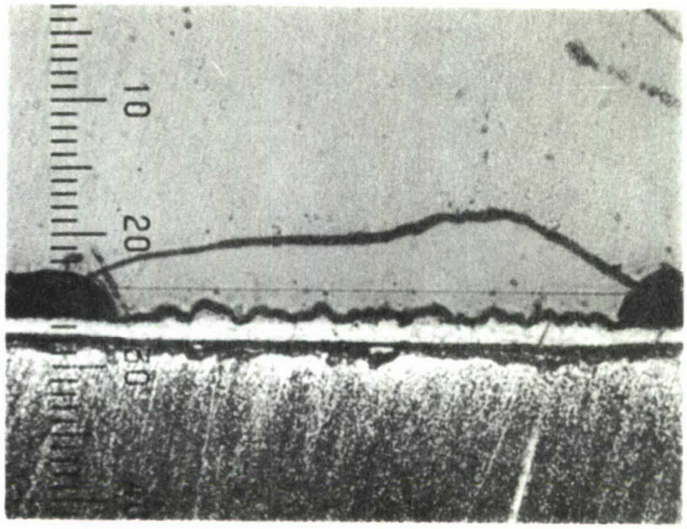

FIGURE 23 a MICROGRAPH OF INVERTED GUNN DIODE OBTAINED USING ELECTRON MICROPROBE ANALYSIS. THE DIODE EXHIBITED CURRENT DROP FOLLOWING 1200 HOURS OF STORAGE AT 340^{o}C.

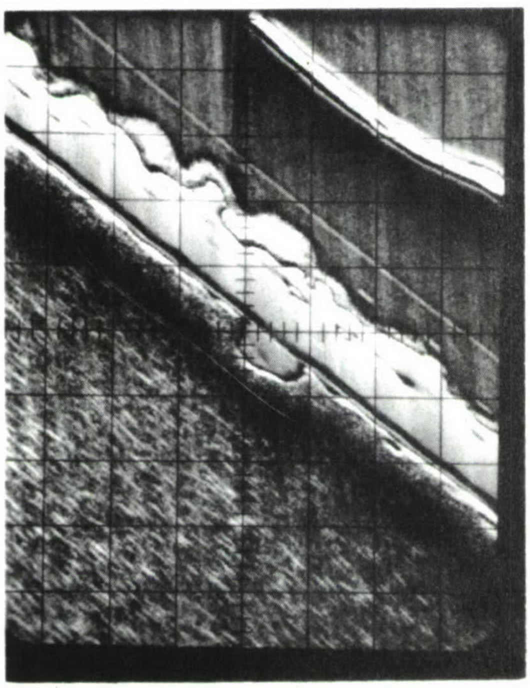

FIGURE 23 b SAMPLE CURRENT SCAN.

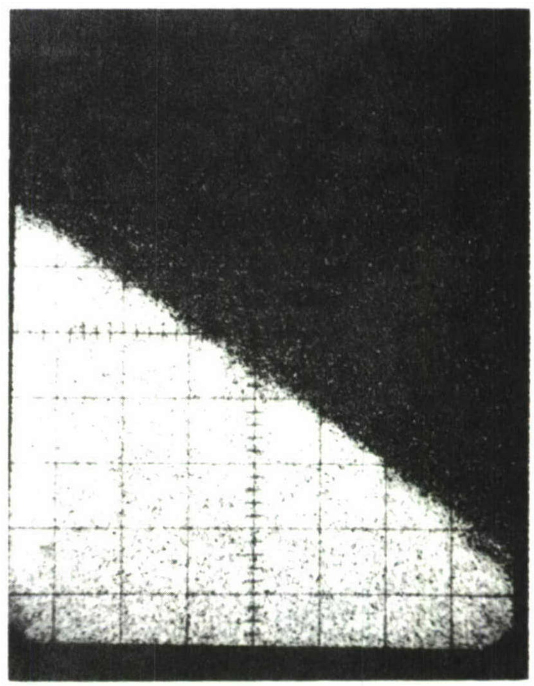

FIGURE 23 c X-RAY IMAGE OF COPPER.

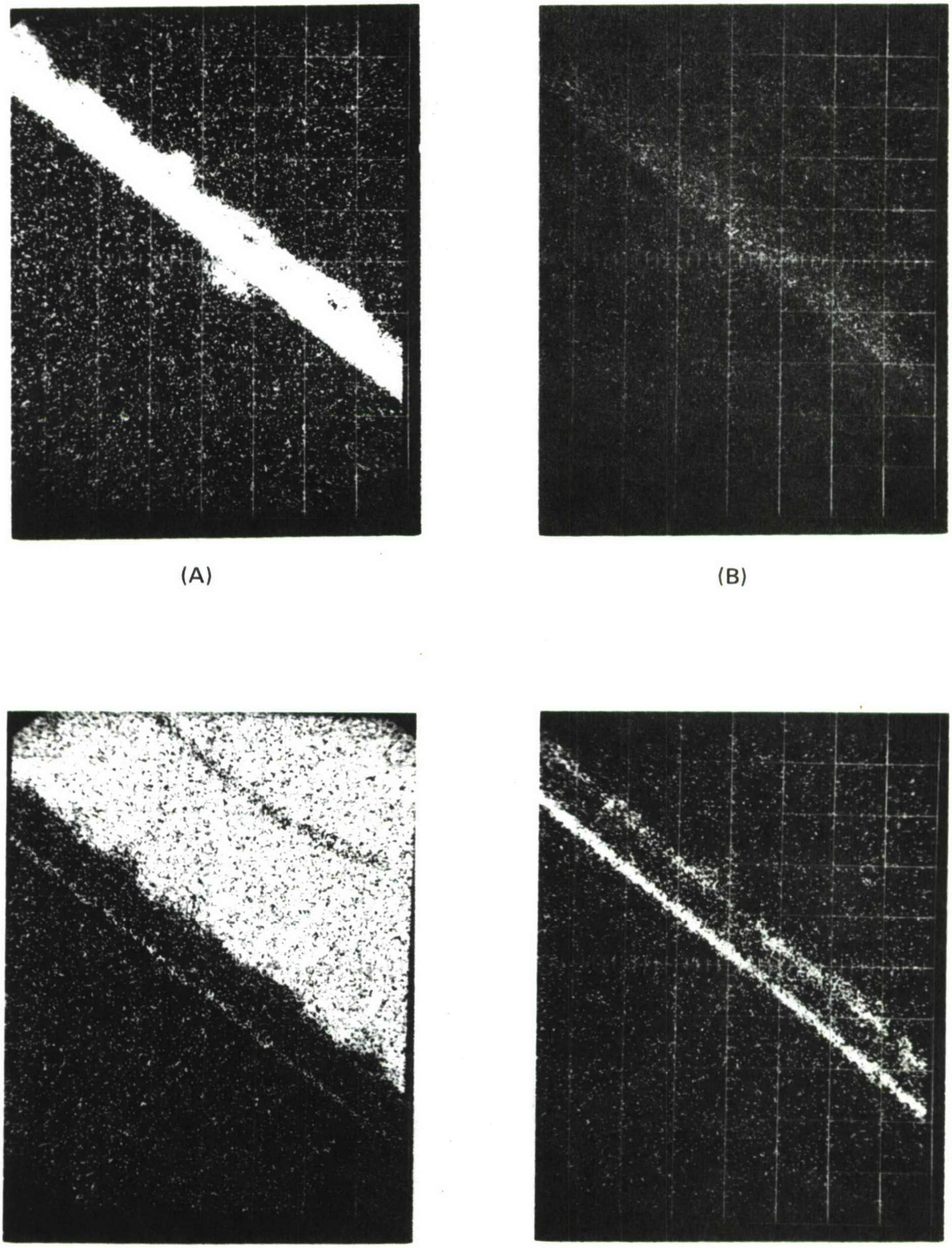

(A) (B)

(C) (D)

FIGURE 24 X-RAY IMAGES OF (A) GOLD: (B) GALLIUM: (C) GERMANIUM: AND (D) NICKEL, OBTAINED FOR THE DIODE OF FIGURE 23.

through the use of barrier layers of high melting point metals. K. Ohata and M. Ogawa [7] have recently demonstrated that a 400 Å film of platinum or nickel placed between a sintered gold germanium contact to n^+ gallium arsenide and the required plated gold layer used in bonding was beneficial in preventing the type of contact degradation seen here.

Additional Gunn diode step-stress testing has been completed. Figure 25 shows results of Run 4, a 24-hour step-stress test involving 7 mil diameter, 9 micron thick TCB construction Gunn diodes. In this case, an active region temperature of 352°C was required to fail 50% of the units in 24 hours. However, because a 7 mil diameter mesa diode would be expected to be bonded more uniformly than a 9 mil diode, these results cannot be combined with previous data in calculating an activation energy. Also, the 7 mil diode data is somewhat in doubt because the straight line fit is not exceptionally good at either the high or low failure percentage end of the curve.

Figure 26 presents the results of Run 6, a 24-hour step-stress test involving 12 mil mesa diameter thermo-compression-bonded Gunn diodes. Fifty percent of these higher power diodes failed at an average active region temperature of 340°C. The standard deviation of the failure temperature was larger for this group of diodes than for others tested (0.27×10^{-3} compared with an average of 0.090×10^{3} for other runs), indicating the existance of a comparably low failure temperature for some of these diodes. Also, at higher temperatures, Figure 26 shows significant deviation from the lower temperature "normal curve" characteristic.

Such behavior indicates the existence of a second failure mode, occurring at higher temperatures, resulting in the failure of all surviving units at active region temperatures above 400°C. None of the diodes involved in this run failed via the "current drop" mode.

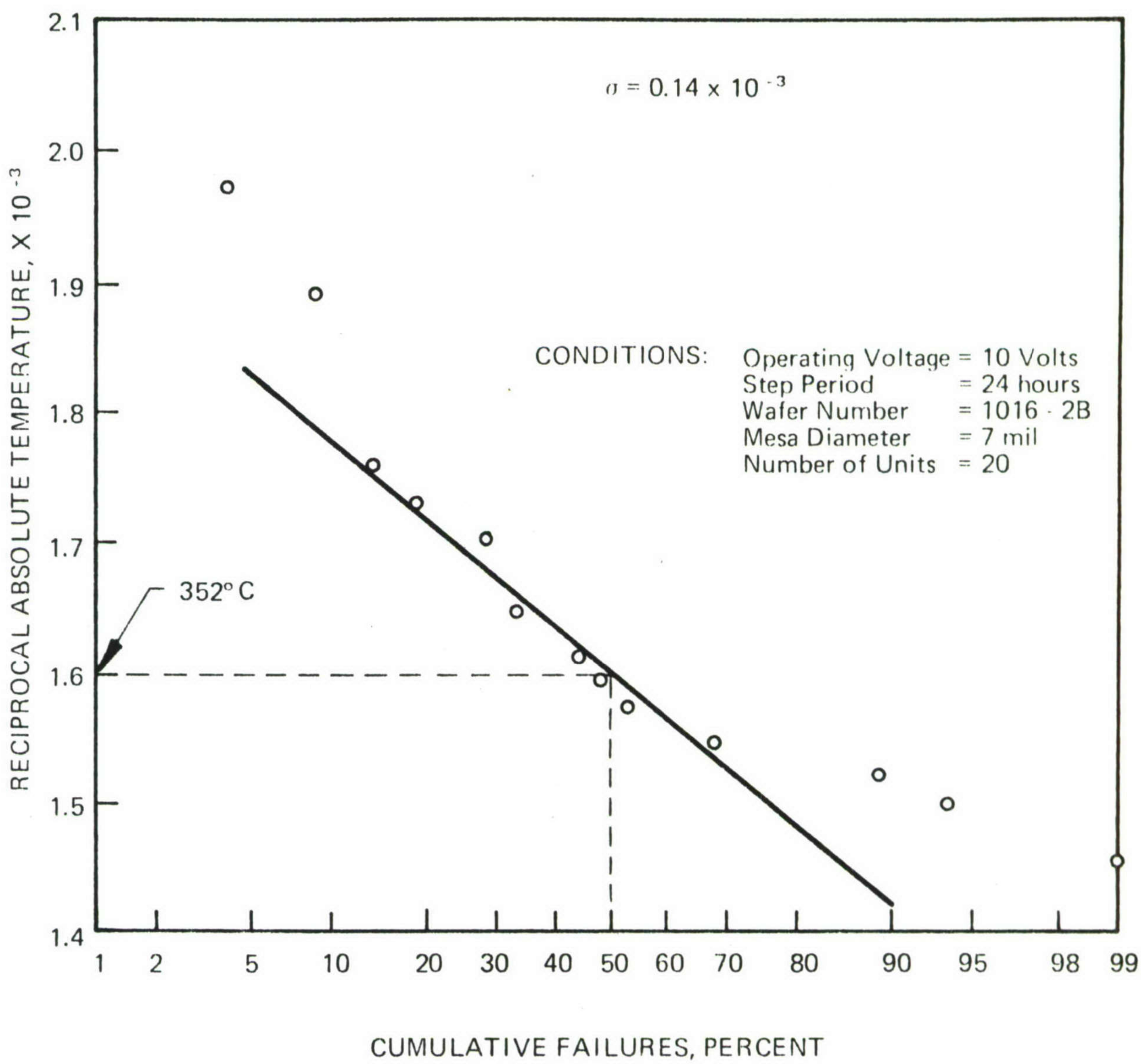

FIGURE 25 RECIPROCAL ABSOLUTE ACTIVE REGION FAILURE TEMPERATURE VERSUS CUMULATIVE PERCENT OF DIODES FAILING FOR GUNN DIODE STEP STRESS TEST NUMBER 4.

D-11697

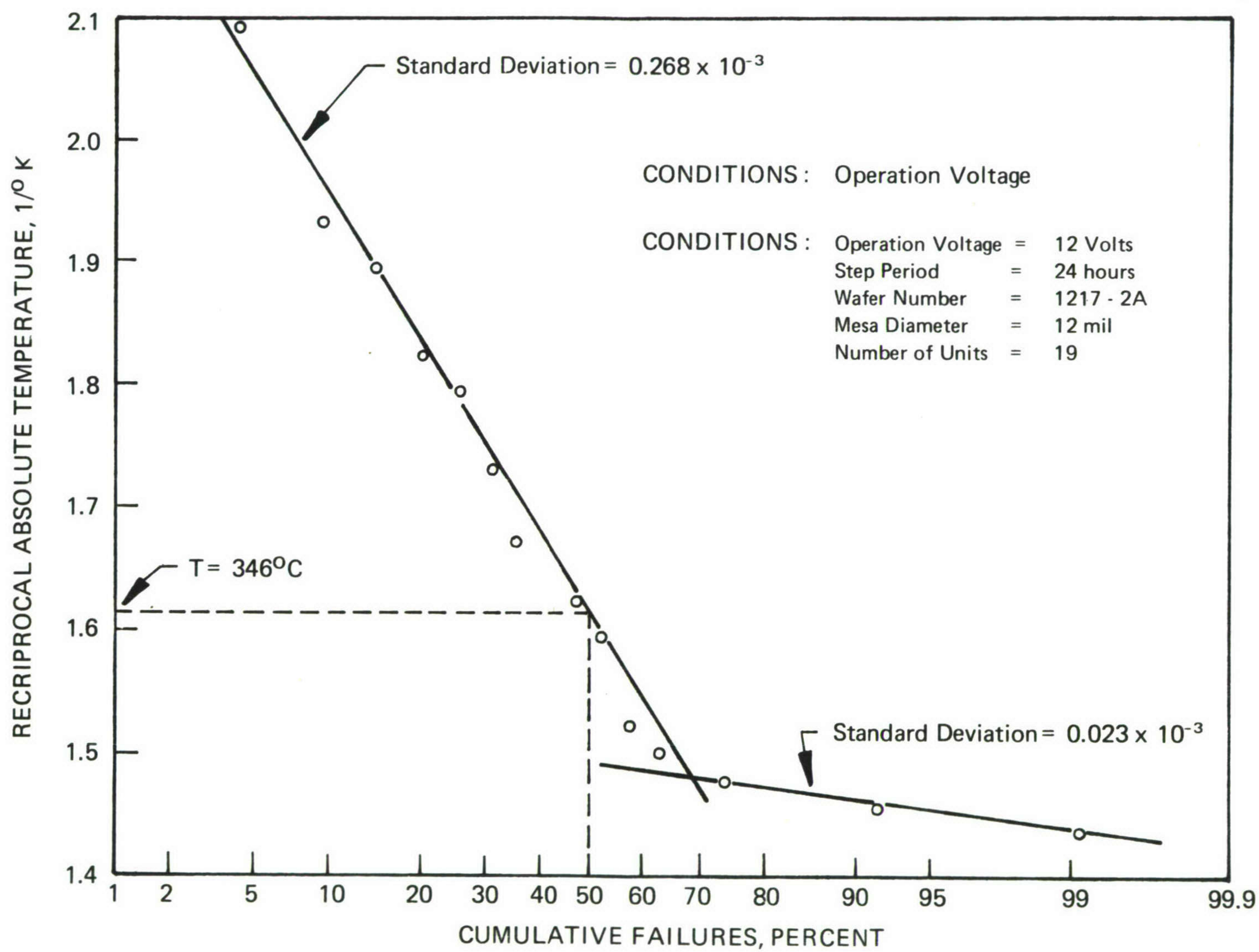

FIGURE 26 RECIPROCAL ABSOLUTE ACTIVE REGION FAILURE TEMPERATURE VERSUS CUMULATIVE PERCENT OF DIODES FAILING FOR GUNN DIODE STEP STRESS TEST NUMBER 6.

Two additional step-stress experiments (numbers 7 and 8) were conducted as shown in Table XI. Run 7, involving 7 mil diameter mesa diodes in 96-hour stress periods, resulted in a 352°C average active region failure temperature. Run 4, also involving 7 mil diodes, produced a 352°C average active region failure temperature, but in a 24-hour stress period. Again, no information concerning activation energy may be obtained from this data. Eleven of the 35 units involved failed via the current drop mode. The others became open or shorted, but would probably have exhibited current drop if catastrophic failure had not occurred first.

In the final step-stress run (#8), 12-mil diameter diodes were stressed for 92-hour periods and failed at an overage active region temperature of 322°C. This was to be compared with Run #6 where similar diodes had failed at 346°C in 24 hours. Although, for Run 8, the change in active region temperature is in the right direction with respect to hours of stress, in light of previous step-stress results, any activation energy calculated using this data would be suspect. Only four of the 19 diodes tested in Run #8 failed via the current drop mode.

Step-stress testing of Gunn diodes, to date, at Microwave Associates has not resulted in a determination of the activation energy for the dominant failure mechanism, chiefly because the mean failure temperature observed has been independent of the duration of the stress steps. In fact, similar diodes operated for longer step-stress periods (72 hours compared with 24 hours) have failed at higher average temperatures. Such behavior is in disagreement with the simple Eyring-Arrhenius failure rate acceleration law, and prevents determination of the activation energy of that failure mode responsible for long-term failure under actual operating conditions.

As shown in Figure 26, in many cases, the reciprocal absolute active region failure temperature versus cumulative percent of diode failing data may be approximated by two straight line segments. Such a construction

allows the sample of units tested to be divided into two parts, possibly involving two failure mechanisms. Of course, any estimate of device reliability involving only those diodes failing due to the supposed lower temperature mechanism is necessarily pessimistic because all superior units, which went on to fail via the high temperature mechanism, have been removed from the population. Nevertheless, if low temperature asymptotes to the data points are drawn for all the Gunn diode step-stress runs reported, and the 25% failure active region temperature established, the data of Table XIII is obtained.

Again, the data of Table XIII do not exhibit an acceleration of failure with increasing temperature as expected from the Arrhenius equation. In comparing tests involving mesas of the same diameter, in every case except Run 5, diodes stressed for longer step periods failed at a higher active region temperature.

The mechanism (or mechanisms) causing diode failure (other than current drop failure) during step-stress testing appears to be catastrophic in nature, occurring at or above a fixed active region temperature and not at all below that temperature. Such a mechanism could also involve the melting and subsequent alloying of the contact metalization into the diode active region resulting in complete shorting rather than current drop. Analysis of diodes which have failed has been hampered by the fact that except for the current drop mode, failure results in melting and sometimes complete vaporization of portions of the chips. Examples of such failures are shown in Figure 27.

TABLE XIV

SUMMARY OF GUNN DIODE STEP-STRESS TESTING RESULTS USING A LOW TEMPERATURE ASYMPTOTE TO ESTABLISH A 25% FAILURE ACTIVE REGION TEMPERATURE

Run No.	Carrier Conc. x 10^{15}/cc	Active Region Thickness μ	Mesa Dia., mil	V_{OP} Volts	Step, Hours	No. of Units	25% Active Region Failure Temp., ^{o}C
1 and 2	1.6	9.0	9	10	24	17	293
3	1.6	9.0	9	10	168	18	312
4	1.8	9.0	7	10	24	20	307
5	0.9	9.5	9	10	72	36	327
6	1.5	13.75	12	12	24	19	285
7	1.3	11.0	7	12	96	35	325
8	1.5	11.0	12	12	96	19	290

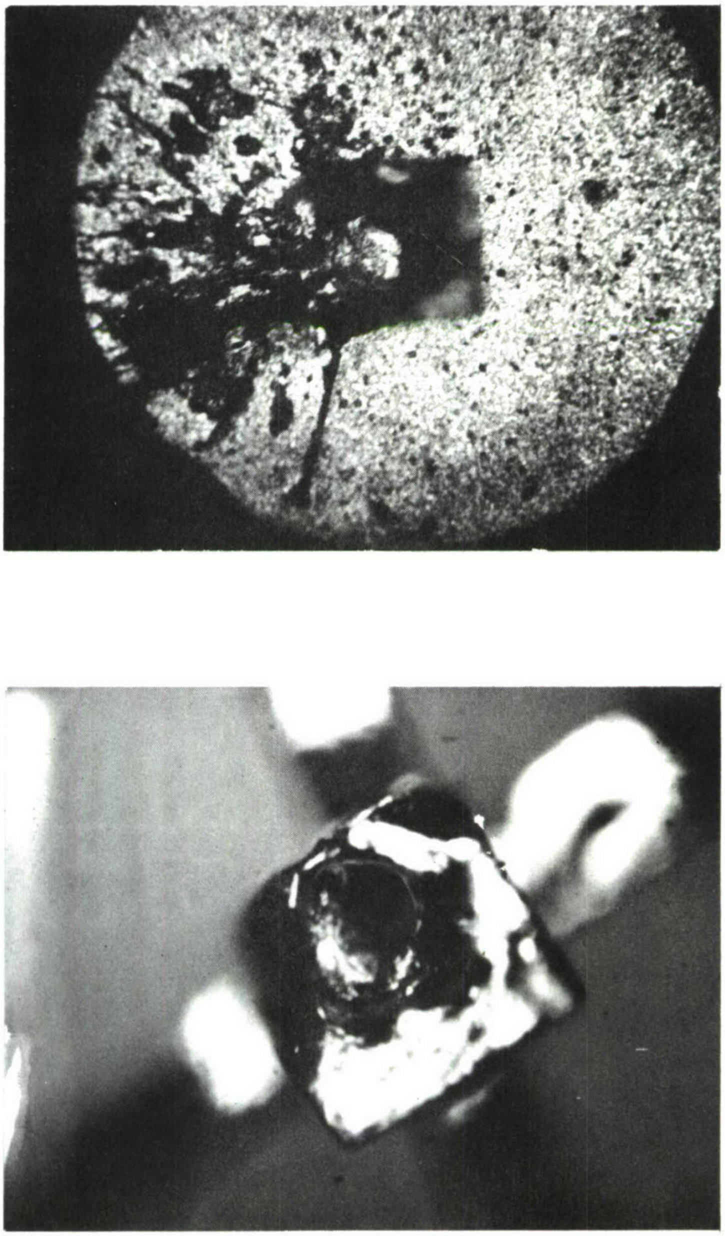

FIGURE 27 MICROSCOPE PHOTOGRAPHS OF TWO GUNN DIODES WHICH FAILED DURING STEP STRESS TESTING. EXTREME HEAT DAMAGE IS EVIDENT. THESE DIODES ARE FROM STEP STRESS RUN 4, WAFER 1016-2B.

VII. GUNN DIODE CONSTANT STRESS TESTING

Because of the failure of step-stress testing to yield the activation energy for Gunn diode accelerated aging, constant stress testing was initiated. Since the 50% failure point for all step-stress testing occurred at 325 to 350°C active region temperature, constant stress active region temperatures of 280°C and 300°C were chosen. Eight mil diameter, 9.4 micron active region thickness TCB construction diodes were chosen for use in the test. Seventy-seven diodes were screened as to thermal resistance, and 20 selected with thermal resistance between 16 and 17°C/watt. An average thermal resistance of 16.6°C/watt and average operating current of 525 mA at 10 volts and 40°C were obtained. Initially, these diodes were installed in the step-stress test apparatus, but operated at a constant heat sink temperature of 193°C, placing the average active region temperature at 280°C.

A similar set of 20 diodes was installed in a second test kit and a 300°C active region temperature maintained. Following 15 days, a power supply malfunction induced premature failure in 10 of the 300°C active region temperature diodes by applying a 3 volt over-voltage to the units during start-up following a power line failure. None of the 280°C diodes were affected.

The need for a more sophisticated test kit was apparent. A unit containing a delay circuit which would re-connect the diodes under test to the power supply only after the supply had stabilized following line voltage failure was constructed. In addition, an automatic running time meter with the capability of recording a failure due to either an open or shorted diode condition was incorporated. Appropriate current monitoring and switching systems allowed monitoring diode current without interrupting current flow. A schematic diagram of one section of the 20-position test kit is shown in Figure 28.

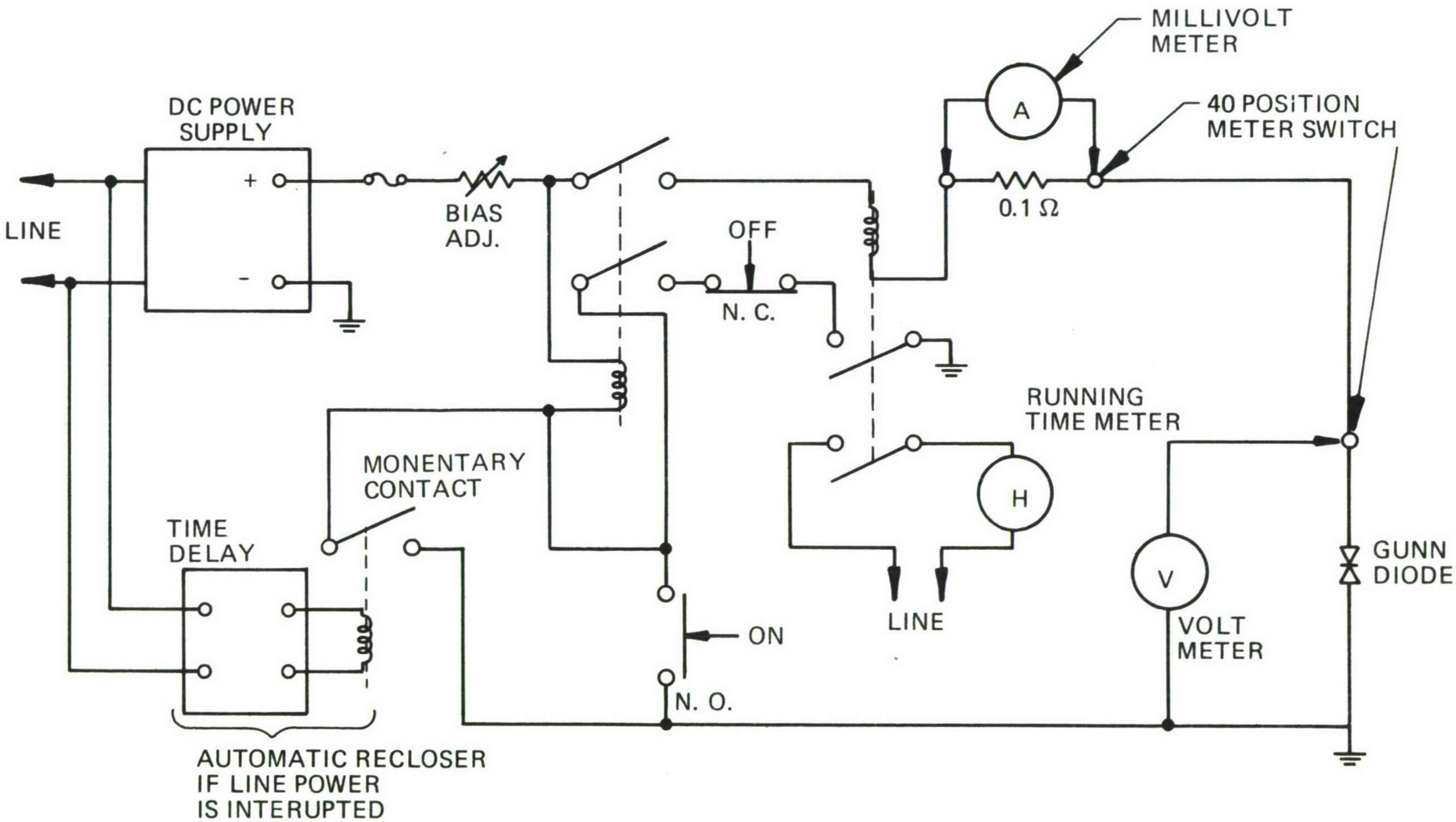

FIGURE 28 CIRCUIT DIAGRAM OF ONE SECTION OF 40 SECTION GUNN DIODE CONSTANT STRESS TEST KIT.

D-12335

Two complete kits were constructed, and placed in service on January 10, 1974. One kit was loaded with the diodes which had successfully survived 1,488 hours of operation at 280°C active region temperature on the old step-stress kit. The second kit was loaded with a fresh set of diodes to be stressed to 300°C active region temperature. Diodes of 7 mil diameter, 10 micron active region thickness were used and selected for thermal resistance of 24 to 26.5°C/watt. An average operating current of 499 mA was obtained at 10 volts and 40°C. These diodes are presently being operated at 10-volt bias and a heat sink temperature of 175°C, placing the active region temperature at 300°C. All diodes were soldered into the heat sink blocks.

At present, the diodes at 280°C active region temperature have accumulated 68,272 unit hours of operation at normal bias voltage without a failure. The 300°C active region temperature set have accumulated 42,924 unit hours with no failures. Because of the limited operating time, an estimate of the MTBF at 280°C or 300°C active region temperature is premature. These tests are being continued, and may require a year or more of additional operation to produce a sufficient number of failures to allow calculation of the activation energy.

VIII. ANALYSIS OF FAILURE MECHANISMS

In an attempt to analyze the cause of failure in TCB (thermo-compression bonded) and PHS (plated heat sink) Gunn diodes and gallium arsenide IMPATT diodes, several units were examined before and after failure (open or shorted condition) using both optical and scanning electron microscopes. Drawings of the two structures appear in Figures 29 and 30. Figure 31 is a photograph of a high power TCB construction Gunn diode before failure, and Figure 32 shows a similar diode following failure. The connecting strap has been completely vaporized and the back of the chip shows severe heat damage, with areas of evaporated crystalline material evident. This particular diode failed while being observed under the IR radiometer. A failure temperature of only 220°C was recorded. Evidently, the failure resulted from hot spot formation at a point other than where the temperature was being monitored. Such behavior could have been caused by a local doping fluctuation or damaged area on the chip surface. The hot spot may have lead to metallization atom migration into the chip, producing a high conductivity channel, and leading to a current runaway situation.

Figure 33 is a photograph of a PHS construction Gunn diode following failure. The only visual indication of failure is a small hole in the middle of the connecting strap. This hole evidently penetrated entirely through the gallium arsenide active region, shorting the diode. This failure appears to be a second example of hot spots leading to conductive channel formation. In this case, the hot spot could have been caused by damage to the chip during top bonding.

Figure 34 shows a gallium arsenide IMPATT diode before and after failure. This diode was observed to fail at only 200°C under the IR radiometer. Again, undetected hot spots must have existed, since the entire chip was ejected from the package leaving only the bond interface on the package pedestal.

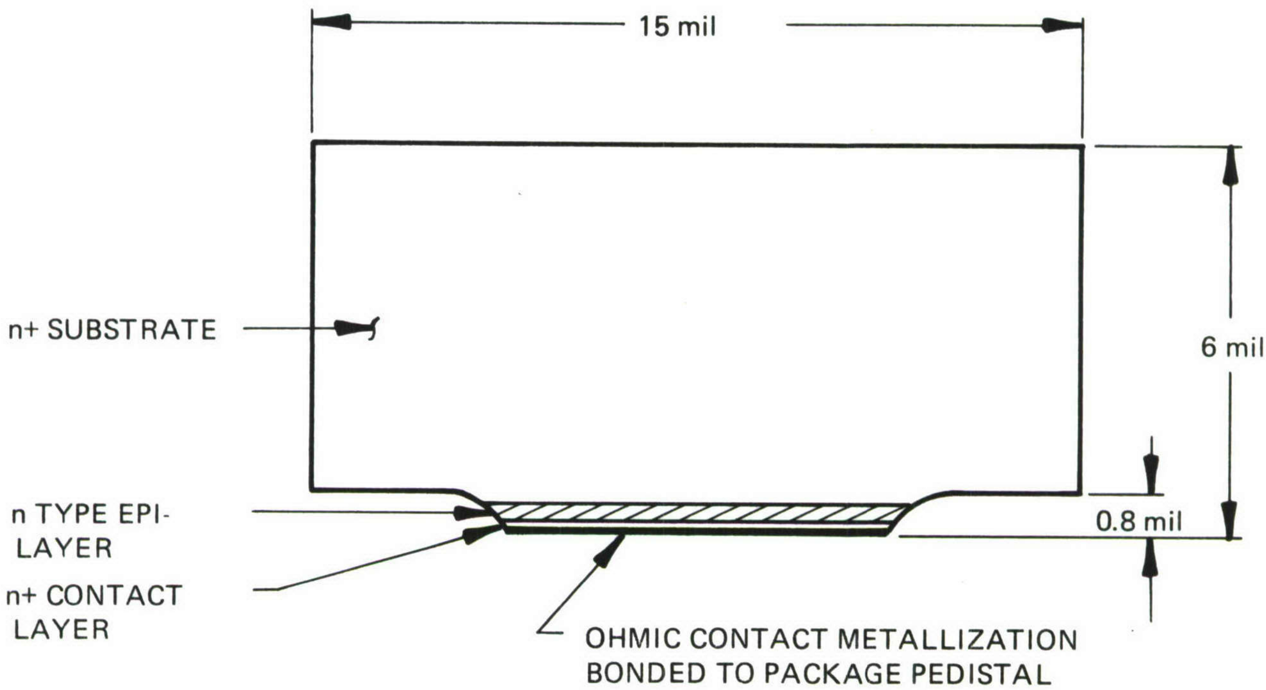

FIGURE 29 CROSS-SECTION OF A THERMO-COMPRESSION BONDED GUNN DIODE

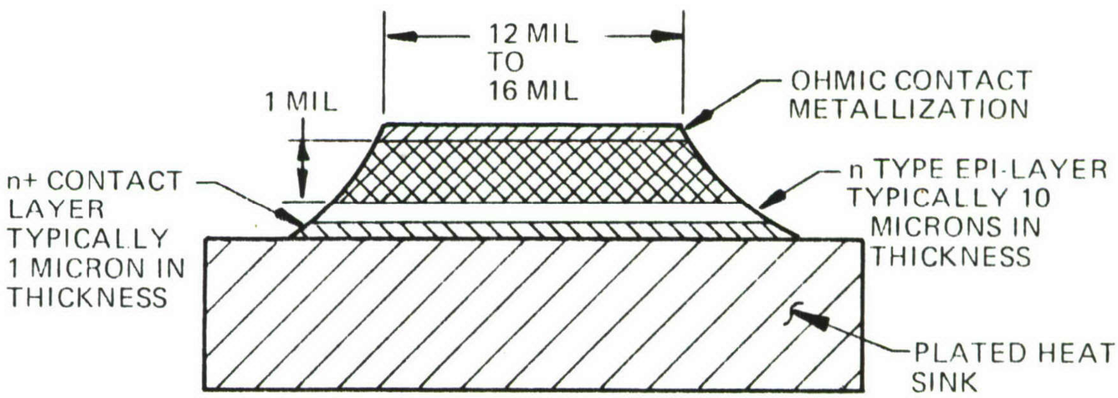

FIGURE 30 CROSS-SECTION OF A PLATED HEAT SINK GUNN DIODE

D 10215

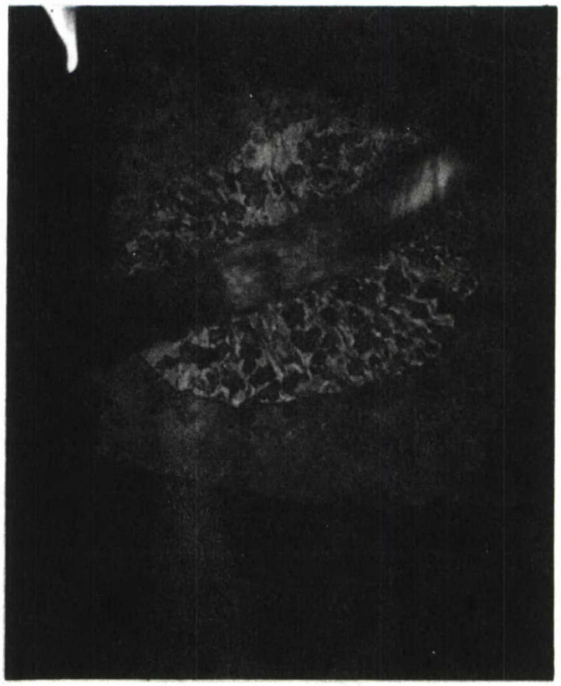

FIGURE 31 GUNN DIODE 2111-1D #2 BEFORE FAILURE. 15 x 15 MIL CHIP TCB BOND

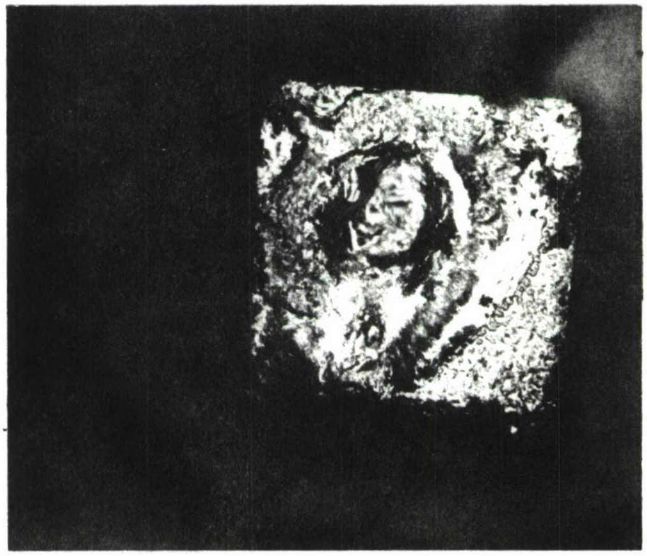

FIGURE 32 GUNN DIODE 2111-1D #1 FOLLOWING FAILURE. 15 x 15 MIL CHIP TCB BONDED.

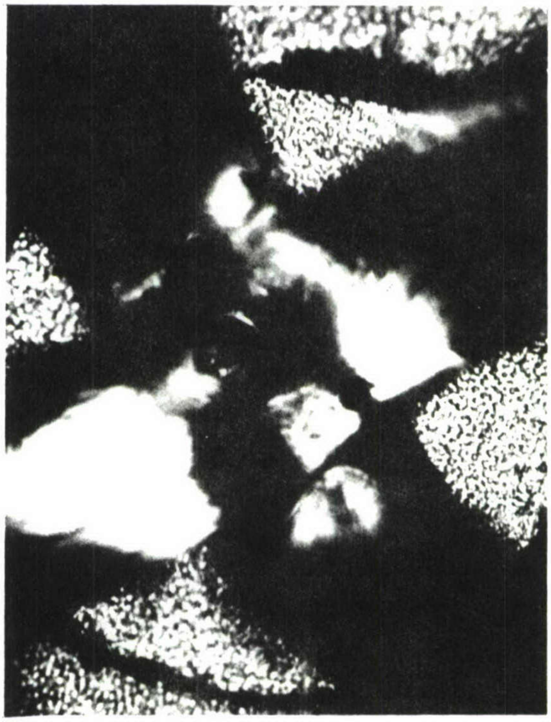

FIGURE 33 GUNN DIODE 2139 - 2B HS AFTER FAILURE – PLATED HEAT SINK CONSTRUCTION – 16 MIL DIAMETER MESA. THE ONLY VISUAL EVIDENCE OF FAILURE IS A SMALL HOLE THROUGH THE CENTER OF THE CONTACT STRAPS.

Ga As IMPATT DIODE 5028-2 12 x 12 MIL CHIP.
BEFORE FAILURE

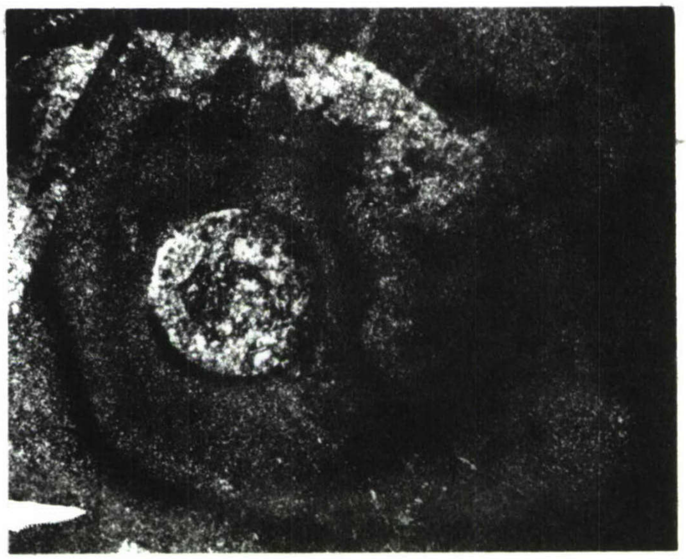

Ga As IMPATT DIODE 5028-2.
FOLLOWING FAILURE

FIGURE 34

D-11129

Additional evidence of hot spot formation is found in Figures 35 and 36 which show three electron microscope views of a PHS construction Gunn diode following failure. The depth and molten character of the failure area indicates the existence of an extremely hot spot. Some hot spot formation could be caused by cracking at the mesa edge due to flexure of the plated gold heat sink during separation of the chips. Such cracking is evident in Figure 35. The PHS diode shown in Figure 35 was constructed by plating the gold heat sink on the entire gallium arsenide wafer, etching the mesas, and then cutting the diodes apart. Such cutting necessarily resulted in some flexure of the heat sink pad. The process has now been improved, allowing plating of each heat sink pad individually, and avoiding the separation step and possible flexure damage.

Figure 37 shows another possible cause of hot spot formation. In this electron microscope photograph of a PHS Gunn diode, a crack is shown running directly under the point of attachment of one of the connecting straps. Such cracking appears to be due to excessive top bonding pressure. The possibility of such damage has now been reduced by using a thinner gold connecting strap, requiring less bonding pressure. The current carrying capacity of this strap is still well in excess of the maximum expected diode threshold current. Four 1/2 x 5 mil gold ribbons in parallel, as presently used on PHS construction diodes, were found to melt at a current of 25 amperes at a case temperature of 275°C. This data was determined from tests made using a strapped package without a diode chip.

Figure 38 shows similar damage to a TCB construction diode. Here, the top strap has been removed, revealing a fractured gallium arsenide region. Again, excessive top bonding pressure had damaged the gallium arsenide immediately below the top contact. Obviously, defects of this kind can be reduced in number by using less top bonding pressure, and a different thickness of top metallization.

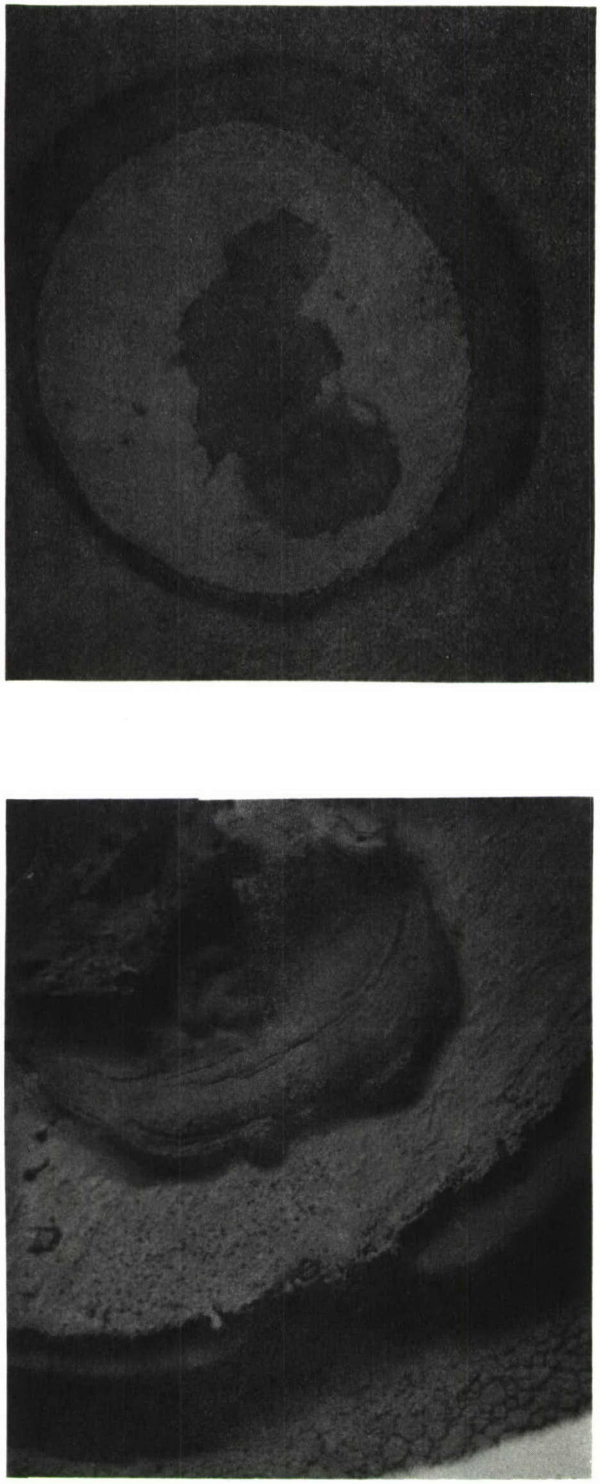

FIGURE 35 SCANNING ELECTRON MICROSCOPE PHOTOGRAPHS OF A PHS CONSTRUCTION GUNN DIODE FOLLOWING FAILURE. THE TOP STRAPS HAVE BEEN REMOVED, REVEALING THE FAILURE REGION. CRACKING AT THE EDGES POSSIBLY DUE TO STRESS FROM THE PLATED GOLD HEAT SINK IS SHOWN.

D-11288

FIGURE 36 ENLARGEMENT OF THE FAILURE REGION OF THE PHS CONSTRUCTION GUNN DIODE SHOWN IN FIGURE 35. THE DEPTH OF THE FAILURE REGION AND EFFECT OF EXTREME HEAT DAMAGE ARE VISIBLE.

D 11289

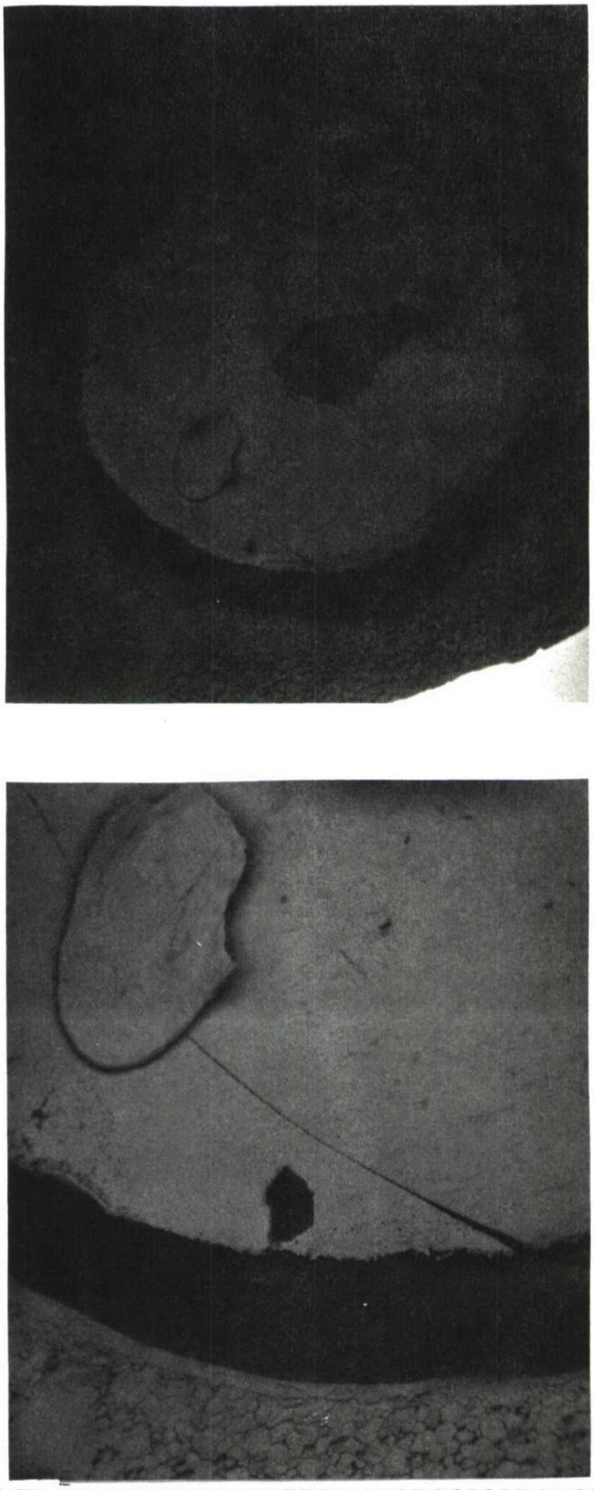

FIGURE 37 SCANNING ELECTRON MICROSCOPE PHOTOGRAPH OF A PHS CONSTRUCTION GUNN DIODE. A CRACK POSSIBLY CAUSED BY EXCESSIVE PRESSURE DURING TOP BONDING IS VISIBLE. A SLIGHT OVERHANG OF THE UPPER ELECTRODE IS ALSO SHOWN.

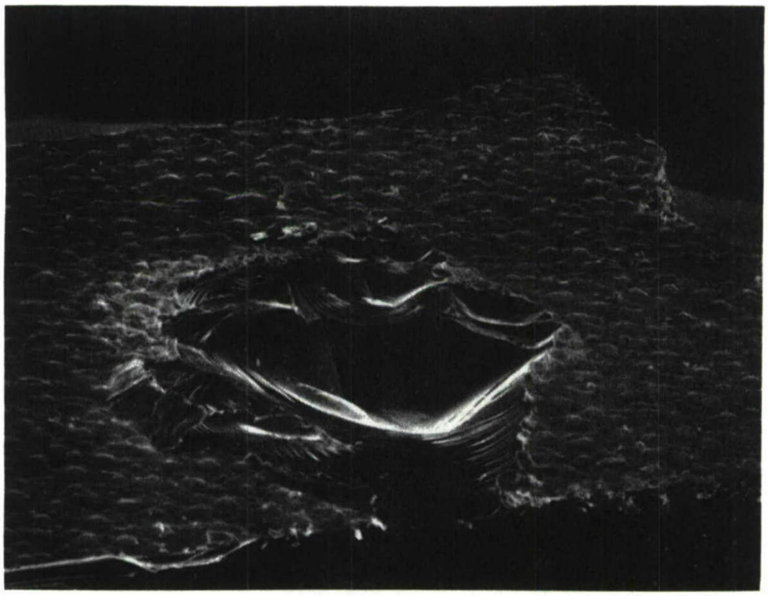

FIGURE 38 SCANNING ELECTRON MICROSCOPE PHOTOGRAPH OF THE BACK OF A TCB CONSTRUCTION GUNN DIODE CHIP. THE CONNECTING STRAPS HAVE BEEN PULLED OFF, FRACTURING THE GALLIUM ARSENIDE. THIS FRACTURING IS AN INDICATION THAT TOP BONDING MAY HAVE DAMAGED THE GALLIUM ARSENIDE SUBSTRATE. 500 X

D-11287

Another potential failure mechanism is shown in the electron microscope photographs of Figure 39. Here, squeeze out of the metallization during bonding of a TCB construction Gunn diode is evident. In Figure 39, the mesa profile is clearly seen. Sufficient metal has been squeezed-out to fill the substrate pedestal area near the mesa, probably shorting the diode. This type of possible failure has been minimized through use of a thinner gold metallization on the diode and less bonding pressure.

Figure 37 shows an additional potential failure mechanism. During mesa etching of this PHS Gunn diode, the top metallization was undercut, leaving a slight overhang. In an extreme case, such an overhang could bend down, shorting the diode. Any possible overhand is presently being removed by use of a double photolithographic process.

In light of the data presented here, the primary cause of Gunn diode failure appears to be hot spot formation. It is likely that hot spots form in the vicinity of damaged areas. Such damage could be caused by excessive thermo-compression bonding pressure, heat, and ultrasonic agitation. Also, excessive top bonding pressure could lead to this result, as could improper handling during processing. The recorded improvement in 24-hour burn-in yield is an indication that these problems have been for the most part solved.

Particularly in the case of large area Gunn diodes (12 mil or greater diameter) nonuniformity of the epitaxial active region across the diode diameter could lead to hot spot formation. Advances in gallium arsenide epitaxial layer growth will hopefully eliminate this problem. Recent experience with larger area (16 mil diameter) PHS diodes indicates that such nonuniformity hot spot formation is not a problem, since these units have survived one-week burn-in at $100^{\circ}C$ case temperature ($280^{\circ}C$ active region temperature).

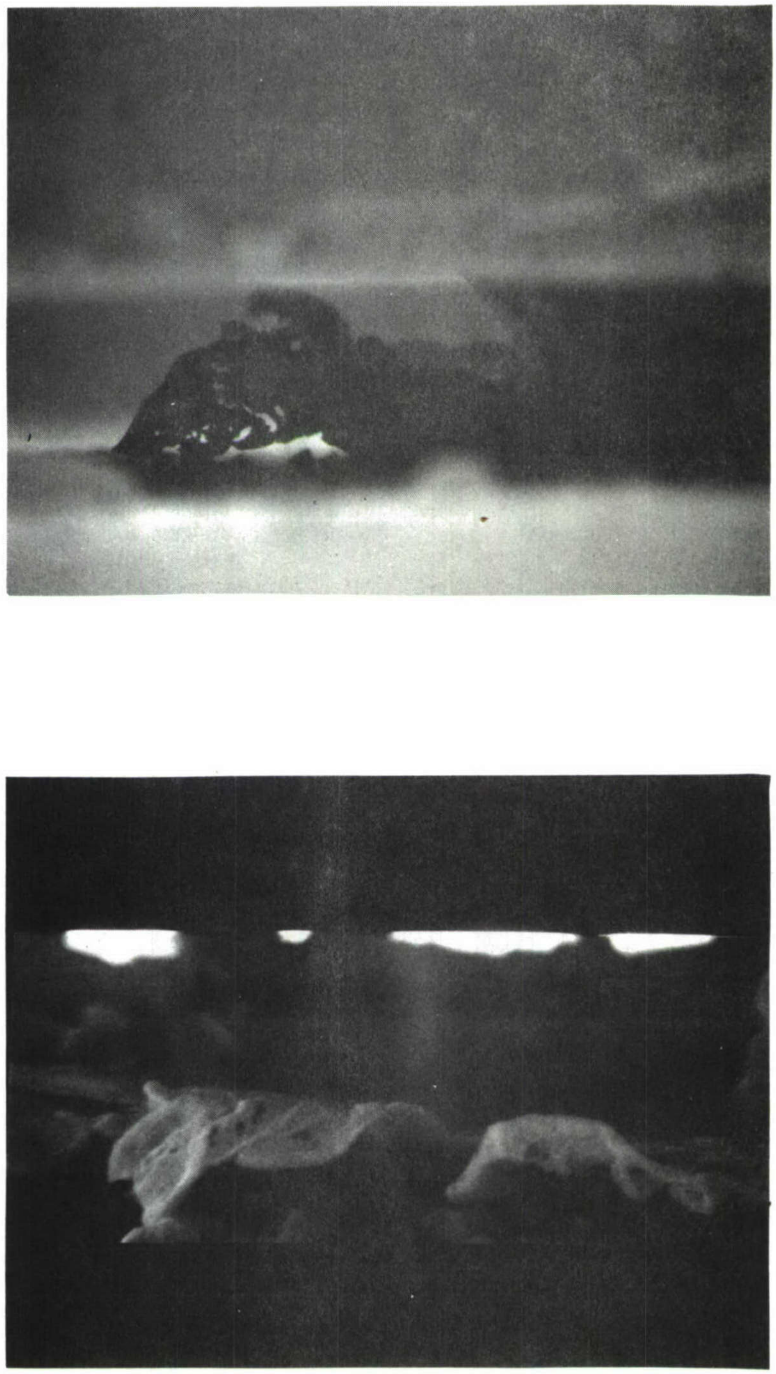

FIGURE 39 SCANNING ELECTRON MICROSCOPE PHOTOGRAPHS OF A TCB CONSTRUCTION GUNN DIODE SHOWING THE SQUEEZE-OUT OF THE METALLIZATION DURING BONDING. 4000 X

D-11286

IX. CONCLUSIONS AND SUMMARY

DC burn-in data on Gunn diodes has established that a minimum burn-in time of 24 hours at 80 to 100°C will reduce freak failures to a 3-1/2% level. A 48-hour burn-in has been shown to reduce the failure level to 1/2%. Diodes shipped to customers are burned in 24 hours at 80 to 100°C. Hence, the user has a 3-1/2% chance of receiving a unit that could fail, that is become open or shorted, if operated at 80 to 100°C case temperature. For high reliability applications, customers may specify extended dc burn-in.

Data has been collected on the change in Gunn diode dc and RF parameters during high temperature dc burn-in. Some trends were identified, namely, a decrease in prethreshold noise, power, and efficiency and an increase in pulse voltage threshold and pulse breakdown voltage. These trends are by no means clear cut. However, 24 hours of 80 to 100°C burn-in has produced a stabilization of Gunn diode RF parameters, on the average.

Special Gunn diode reliability tests including the switching transient experiment, the power and current monitor and the long-term dc burn-in experiment have demonstrated the Gunn diode's resistance to switching transient induced failure and long-term performance degradation. To date, six Gunn diodes have survived 139,320 on-off switchings without failure. After 15,620 hours of operation, the power output has increased 14% and the current dropped 0.6% in one Gunn diode oscillator being continuously monitored. In a long-term dc burn-in experiment, 15 diodes at 75°C stud temperature have accumulated 325,000 unit hours each. This data, combined with the previous long-term life test data, establishes a minimum MTBF of 154,000 hours.

The infrared radiometer has proved to be a very valuable tool in analyzing the effect of various processing changes on device performance. In particular, the failure temperature of Gunn and GaAs IMPATT diodes have

been observed to be 300 to 325°C and 270°C, respectively. It should be emphasized that only one unit had been observed to fail at that temperature. However, undetected hotter areas could have existed. The radiometer has proved to be valuable in perfecting the plated heat sink process for high power Gunn diodes and has aided in locating high thermal resistance regions in the heat flow path. In addition, an electrical technique for determination of Gunn diode thermal resistance has been demonstrated to be accurate by use of the radiometer.

A dc burn-in schedule has been tentatively established for gallium arsenide IMPATT diodes. Twenty-four hours of 50°C burn-in has resulted in a failure rate of 6%. Only 5% or less change in RF parameters occurred during this burn-in. Some question remains as to the ability of dc burn-in to eliminate units which would subsequently fail during RF testing. HTRB testing of gallium arsenide IMPATTs has proven to be unreliable for removal of inferior units.

Step-stress testing of Gunn diodes has been ineffective in determining the activation energy for the dominent long-term failure mode. A catastrophic failure mechanism occurring at active region temperatures above 325°C and not at all at lower temperatures prevented acceleration of the long-term failure mechanism. Accordingly, constant stress tests were initiated involving 40 diodes operated at normal bias voltage and an elevated heat sink temperature, placing the active region temperature at 280°C for one set of 20 diodes, and 300°C for the second. No failures have occurred following 68,272 unit hours for the 280°C active region temperature diodes, and 42,924 hours for the 300°C group.

Electron microscope photographs of both TCB and PHS construction Gunn diodes have revealed several potential failure mechanisms which have

been eliminated by changes in the manufacturing process. Revised metallization, bonding and etching techniques have alleviated problems involving chip cracking, metallization overhand, and pedestal metallization squeeze-out.

The improvement in Gunn diode reliability achieved as a result of changes in the manufacturing process and dc burn-in schedule is evident in the 12.6% improvement of Gunn diode dc burn-in yield from 72% to 84.6%.

REFERENCES

[1] Ross, J.M., "Reliability of Components for Communication Satellites", Bell Sys. Tech. J., 41, 1962

[2] Hunter, L.P., "Handbook of Semiconductor Electronics", pp. 19-42, McGraw-Hill, New York, 1970.

[3] Glasstone, S., Laidler, K., and Eyring, H., "The Theory of Rate Processes", Chapter 1, McGraw-Hill, New York, 1941.

[4] Dodson, G.A., and Howard, B.T., "High Stress Aging to Failure of Semiconductor Devices", Proceedings of the Seventh National Symposium on Reliability and Quality Control in Electronics, p. 262, Philadelphia, Pa., 1961.

[5] Goldwaite, L.R., "Failure Rate Study for the Lognormal Lifetime Model", Proc. Seventh National Symposium on Reliability and Quality Control in Electronics, Philadelphia, Pa., p. 208, 1961.

[6] Bravman, J.S., and Eastman, L.F., "Thermal Effects of the Operation of High Average Power Gunn Devices", IEEE Trans. E.D., ED-17, p. 744, 1970.

[7] Ohata, K., and Ogawa, M., "Degradation of Gold-Germanium Ohmic Contact to GaAs", presented at 1974 International Reliability Physics Symposium, Las Vegas, Nevada (to be published in Symposium Proceedings).

DISTRIBUTION LIST

101	Defense Documentation Center ATTN: DDC-TCA Cameron Station (Bldg. 5) Alexandria, Virginia 22314	12
107	Director National Security Agency ATTN: TDL Fort George G. Meade, Maryland 20755	1
108	Director, Defense Nuclear Agency ATTN: Technical Library Washington, D. C. 20305	1
200	Office of Naval Research Code 427 Arlington, Virginia 22217	1
203	Naval Ship Engineering Center ATTN: Code 6179B Prince Georges Center Bldg. Hyattsville, Maryland 20782	1
206	Commander Naval Electronics Lab Ctr ATTN: Library San Diego, California 92152	1
207	Commander U. S. Naval Ordnance Lab ATTN: Technical Library White Oak, Silver Spring, Maryland 20910	1
210	Commandant, Marine Corps Hq, U. S. Marine Corps ATTN: Code A04C Washington, D. C. 20380	1
212	Communications-Electronics Div. Development Center Marine Corps Develop & Educ Cmd Quantico, Virginia 22134	1

DISTRIBUTION LIST (Cont.)

217	Naval Air Systems Command Code: AIR-5336 Main Navy Building Washington, D. C. 20325	1
301	Rome Air Development Center ATTN: Documents Library (TDLD) Griffiss AFB, New York 13440	1
307	Hq ESD (TRI) L. G. Hanscom Field Bedford, Mass. 01730	1
309	Air Force Avionics Lab ATTN: AFAL/DOT, STINFO Wright-Patterson AFB, Ohio 45433	2
310	Recon Central/RSA AF Avionics Laboratory Wright-Patterson AFB, Ohio 45433	1
314	Hq, Air Force Systems Cmd ATTN: DLTE Andrews AFB Washington, D. C. 20331	1
315	Director Air University Library ATTN: AUL/LSE-64-285 Maxwell AFB, Alabama 36112	1
319	Air Force Weapons Laboratory ATTN: WLIL Kirtland AFB, New Mexico 87117	1
400	HQDA (DAMI-ZA) Washington, D. C. 20310	2
405	Ofc, Asst Sec of the Army (R&D) ATTN: Asst for Research Room 3-E-379, The Pentagon Washington, D. C. 20310	1
408	HQDA (DARD-ARP/Dr. R. B. Watson) Washington, D. C. 20310	1

409	Commanding General U. S. Army Materiel Command ATTN: AMCMA-EE 5001 Eisenhower Blvd. Alexandria, Virginia 22304	1
415	Commanding General U.S. Army Materiel Command ATTN: AMCRD-O 5001 Eisenhower Blvd. Alexandria, Virginia 22304	1
419	Commanding General U. S. Army Missile Command ATTN: AMSMI-RR (Dr. J. P. Hallowes) Redstone Arsenal, Alabama 35809	1
421	CG, U. S. Army Missile Command Redstone Scientific Info Ctr ATTN: Chief, Document Sect Redstone Arsenal, Alabama 35809	2
423	Commanding General U. S. Army Weapons Command ATTN: AMSWE-REF Rock Island, Illinois 61201	1
426	Commanding Officer Vint Hills Farm Station ATTN: Ch, Systems Engrg Div Opns Center Warrington, Virginia 22186	1
427	Commanding General USACDC Intel & Control Sys Gp Fort Belvoir, Virginia 22060	2
430	Commanding Officer USACDC Cbr Agency ATTN: CSGCB-ST, Mr. H. Whitten Fort McClellan, Alabama 36201	1
431	Commanding Officer USACDC Intelligence Agency Fort Huachuca, Arizona 85613	1

DISTRIBUTION LIST (Cont.)

432	Commanding Officer USACDC FAA Fort Sill, Oklahoma 73503	1
433	Hq, US Army Aviation Sys Cmd ATTN: AMSAV-C-AD P.O. Box 209 St. Louis, Missouri 63166	1
442	Commanding Officer Harry Diamond Laboratories ATTN: Library Washington, D. C. 20438	1
443	CO, USA Foreign Sci & Tech Ctr ATTN: AMXST-IS1 220 Seventh St, NE Charlottesville, Virginia 22901	2
444	CO, USA Foreign Science Div ATTN: AMXST CE Division 220 Seventh St, NE Charlottesville, Virginia 22901	1
448	Commanding Officer Picatinny Arsenal ATTN: SMUPA-TVI Dover, New Jersey 07801	1
449	Commanding Officer Frankford Arsenal ATTN: SMUPA-RT-S, Bldg. 59 Dover, New Jersey 07801	2
451	Commanding Officer Frankfrod Arsenal ATTN: L8400 (Dr. W. McNeill) Philadelphia, Pennsylvania 19137	1
462	Commanding Officer U. S. Army Materials and Mech Research Center ATTN: AMXMR-ATL, Tech Lib Br Watertown, Mass. 02172	1

DISTRIBUTION LIST (Cont.)

463	President US Army Artillery Board Fort Sill, Oklahoma 73503	1
464	Commanding Officer Aberdeen Proving Ground ATTN: Tech Library, Bldg 313 Aberdeen Proving Gr, Maryland 21005	2
465	Commanding Officer Aberdeen Proving Ground ATTN: STEAP-TL Aberdeen Proving Gr, Maryland 21005	1
480	Commanding Officer USASA Test and Evaluation Cen Fort Huachuca, Arizona 85613	1
483	US Army Research Office-Durham ATTN: CRDARD-IP Box CM, Duke Station Durham, North Carolina 27706	1
484	US Army Research Ofc-Durham ATTN: Dr. Robert J. Lontz Box CM, Duke Station Durham, North Carolina 27706	1
486	Commanding Officer USA Mobility Eqpt R&D Cen ATTN: Tech Doc Cen, Bldg. 315 Fort Belvoir, Virginia 22060	2
488	USA Security Agency ATTN: IARD Arlington Hall Sta, Bldg 420 Arlington, Virginia 22212	1
489	Commanding General US Army Tank-Automotive Command ATTN: AMSTA-RH-FL Warren, Michigan 48090	1
492	Commandant US Army Air Defense School ATTN: C&S Dept, MSL Sci Div Fort Bliss, Texas 79916	1

DISTRIBUTION LIST (Cont.)

493	Director USA Engr Waterways Exper Sta ATTN: Research Center Library Vicksburg, Mississippi 39180	2
495	CG, Deseret Test Center ATTN: STEPD-TT-ME(S) Met Div Bldg 103, Soldiers Circle Fort Douglas, Utah 84113	1
500	Commanding Officer Yuma Proving Ground ATTN: STEYP-AD (Tech Lib) Yuma, Arizona 85364	1
501	Commanding Officer US Army Arctic Test Center APO, Seattle 98733	2
502	CO, USA Tropic Test Center ATTN: STETC-MO-A (Tech Lib) Drawer 942 Fort Clayton, Canal Zone 09827	1
503	Director US Army Adv Matl Concepts Agcy ATTN: AMXAM Washington, D. C. 20315	1
504	Commanding General US Army Materiel Command ATTN: AMCRD-R 5001 Eisenhower Blvd Alexandria, Virginia 22304	1
508	Commanding Officer USACDC Infantry Agency ATTN: Central Files Fort Benning, Georgia 31905	1
509	Commanding Officer USACDC Maintenance Agency ATTN: CDCMA-D Aberdeen Proving Gr, Maryland 21005	1

DISTRIBUTION LIST (Cont.)

512	Commanding Officer USACDC Armor Agency Fort Knox, Kentucky 40121	1
516	Commandant US Army Field Artillery School ATTN: Target Acquisition Dept. Fort Sill, Oklahoma 73503	2
517	Commanding General US Army Missile Command ATTN: AMSMI-RFG (Mr. N. Bell) Redstone Arsenal, Alabama 35809	1
518	Commanding Officer Harry Diamond Laboratories ATTN: AMXDO-RCB (Mr. Nemarich) Washington, D. C. 20438	1
596	Commanding Officer USA Combat Developments Cmd Communications-Electronics Agcy Fort Monmouth, New Jersey 07703	1
598	Commanding Officer USA Satellite Comm. Agency ATTN: AMCPM-SC-3 Fort Monmouth, New Jersey 07703	1
599	Tri-Tac Office ATTN: CSS (Dr. Pritchard) Fort Monmouth, New Jersey 07703	1
604	US Army Liaison Office MIT, Bldg. 26, Rm. 131 77 Massachusetts Avenue Cambridge, Mass. 02139	1
605	US Army Liaison Office MIT-Lincoln Lab, Room A-210 P. O. Box 73 Lexington, Mass. 02173	1

DISTRIBUTION LIST (Cont.)

607	Commanding General USA Tank-Automotive Command ATTN: AMSTA-Z, Dr. J. Parks Warren, Michigan 48090	1
610	Director Night Vision Lab (USAECOM) ATTN: AMSEL-NV-OR (Mr. Segal) Fort Belvoir, Virginia 22060	1
614	Chief Missile Elec Warfare Tech Area EW Lab, USA Electronics Command White Sands Missile Range New Mexico 88002	1
616	CG, USA Electronics Command ATTN: AMSEL-PP/P-IED (Mr. C. Mogavero) 225 South 18th Street Philadelphia, Pa. 19103	1
617	Chief, Intell Matl Dev Office Electronic Warfare Lab, USAECOM Fort Holabird, Maryland 21219	1
680	Commanding General US Army Electronics Command ATTN: A15AAP Fort Monmouth, New Jersey 07703	1
	AMSEL-NV-D	1
	AMSEL-NL-D	1
	AMSEL-WL-D	1
	AMSEL-VL-D	1
	AMSEL-CT-D	3
	AMSEL-BL-D	1
	AMSEL-TL-DT	1
	AMSEL-TL-SS	3
	AMSEL-TL-IR	1
	AMSEL-TE	1
	AMSEL-MA-MP	1
	AMSEL-MS-TI	2
	AMSEL-GG-TD	1
	AMSEL-EN	1
	AMSEL-PA	2
	USMC-LNO	1

DISTRIBUTION LIST (Cont.)

	AMSEL-RD	1
	AMSEL-TL-D	1
701	Sylvania Elec Sys-Western Div ATTN: Tech Reports Library P. O. Box 205 Mountain View, California 94040	1
703	NASA Sci & Tech Info Facility ATTN: Acquisitions Br (S-AK/DL) P. O. Box 33 College Park, Maryland 20740	2
705	Advisory Gp on Electron Devices 201 Varick St. 9th Floor New York, New York 10014	2
706	Advisory Gp on Electron Devices ATTN: Secy, Sp Gr on Opt Masers 201 Varick Street New York, New York 10014	2
708	Ballistic Msl Radiation Anal Cen Univ of Mich., Willow Run Lab Institute of Science & Tech PO Box 618, Ann Arbor, Michigan 48107	1
711	Metals and Ceramics Inf Center Hughes Aircraft Company Centinela and Teale Streets Culver City, California 90230	1
715	Plastics Tech Eval Center Picatinny Arsenal, Bldg. 3401 Dover, New Jersey 07801	1
717	Reliability Analysis Center Rome Air Development Center ATTN: J. M. Schramp/RCRM Griffis AFB, New York 13440	1
718	Remove Area Confligt Info Ctr Batelle Memorial Institute 505 King Avenue Columbus, Ohio 43201	1

DISTRIBUTION LIST (Cont.)

719	Shock and Vibration Info Center Naval Research Lab (Code 6020) Washington, D. C. 20390	1
720	Thermophysical Properties Res Ctr Purdue Univ., Research Park 2595 Yeager Road Lafayette, Indiana 47906	1
721	Vela Seismic Info Center University of Michigan Box 618 Ann Arbor, Michigan 48107	3
	RCA Laboratories David Sarnoff Research Center Princeton, New Jersey 08540	1
	Communications Transistor Corp. 25 Route 22 Springfield, New Jersey 07081 ATTN: Mr. W. Ellenberger	1
	Teledyne Semiconductors 12515 Chadron Avenue Hawthorne, California 90250 ATTN: Mr. W. Waters	1
	TRW Semiconductor, Inc. 14520 Aviation Boulevard Laundale, California 90260 ATTN: Mr. Barns	1
	Com Sat Laboratories ATTN: R. Strauss Clarksburg, Maryland 20734	1
	Hewlett-Packard Company ATTN: D. Gross 1021 Eighth Avenue King Of Prussia, Pa.	1
	Raytheon Company ATTN: D. J. Gauthier 141 Spring Street Lexington, Mass. 02173	1

DISTRIBUTION LIST (Cont.)

Rensselaer Polytechnic Institute ATTN: Mgr., Gov't Contracts Troy, New York 12181	1
Commander, RADC ATTN: J. Carroll, RCRM Griffiss AFB, New York 13400	1
Mr. Harry Schaaft National Bureau of Standards Washington, D. C. 20334	1
Mr. D. Carley RCA Route 202 Somerville, New Jersey 08873	1
General Electric Company ATTN: Mr. T. F. Kendall Bldg. 7, Room 152 Electronic Park Syracuse, New York 13200	1
Motorola, Inc. 5005 East McDowell Road Attn: Dr. A. Lesk Phoenix, Arizona 85008	1
Texas Instruments, Inc. Semiconductor Components Division P. O. Box 5012 Dallas, Texas 75222 Attn: Semiconductor Library	1
Transitron Electronic Corporation 168-182 Albion Street Wakefield, Massachusetts Attn: Dr. D. Bakalar	1
Fairchild Semiconductor A Division of Fairchild Camera & Inst. Corp. 545 Whisman Road Mountain View, California 94303 Attn: Mr. M. Mahoney	1

DISTRIBUTION LIST (Cont.)

Autonetics 9150 E. Imperial Hwy. Downey, California Attn: Mr. W. Morris	1
Mr. Leon C. Hamiter National Aeronautics and Space Admin. George C. Marshall Space Flight Ctr. Attn: M-QUAL-QP Huntsville, Alabama 36555	1

UNCLASSIFIED

SECURITY CLASSIFICATION OF THIS PAGE (When Data Entered)

REPORT DOCUMENTATION PAGE		READ INSTRUCTIONS BEFORE COMPLETING FORM
1. REPORT NUMBER	2. GOVT ACCESSION NO.	3. RECIPIENT'S CATALOG NUMBER
4. TITLE (and Subtitle) RELIABILITY OF HIGH FIELD SEMICONDUCTOR DEVICES		5. TYPE OF REPORT & PERIOD COVERED Final Report July 1973 - January 1974
		6. PERFORMING ORG. REPORT NUMBER
7. AUTHOR(s) J.L.Heaton & T.B. Ramachandran		8. CONTRACT OR GRANT NUMBER(s) DAAB07-72-C-0101
9. PERFORMING ORGANIZATION NAME AND ADDRESS Microwave Associates, Inc. Burlington, Massachusetts		10. PROGRAM ELEMENT, PROJECT, TASK AREA & WORK UNIT NUMBERS
11. CONTROLLING OFFICE NAME AND ADDRESS United States Army Electronics Command Fort Monmouth, New Jersey 07703		12. REPORT DATE January 1974
		13. NUMBER OF PAGES 90
14. MONITORING AGENCY NAME & ADDRESS(if different from Controlling Office)		15. SECURITY CLASS. (of this report) UNclassified
		15a. DECLASSIFICATION/DOWNGRADING SCHEDULE

16. DISTRIBUTION STATEMENT (of this Report)

Approved for Public Release; Distribution Unlimited.

17. DISTRIBUTION STATEMENT (of the abstract entered in Block 20, if different from Report)

18. SUPPLEMENTARY NOTES

19. KEY WORDS (Continue on reverse side if necessary and identify by block number)

20. ABSTRACT (Continue on reverse side if necessary and identify by block number)

This report describes the results of a program of investigation concerning the reliability and failure modes of gallium arsenide Gunn and IMPATT diodes.

Data is presented concerning the burn-out distribution in time of Gunn diodes. Also, the changes in dc and RF parameters of 700 Gunn and 100 gallium arsenide IMPATT diodes resulting from 24 to 168 hours of dc high

temperature burn-in are present.

The results of long-term RF burn-in experiments on Gunn and gallium arsenide IMPATT diodes are reported, including calculation of the MTBF for a class of Gunn diodes. An improved thermal resistance measurement technique is described for Gunn diodes and results are compared with data obtained using an IR radiometer.

The results of three Gunn diode step stress experiments are presented. An abrupt failure mode occurring above approximately 325°C and not at all at lower temperatures has masked the long-term mode of failure and precluded determination of an activation energy using step-stress techniques.

Constant stress testing of Gunn diodes at a lower stress level was initiated in order to avoid this catastrophic failure mode. At present, these tests have not been completed.

Optical and electron microscope photographs are presented which are used in the analysis of the manufacturing defects leading to early failure in Gunn diodes. Correction of these defects has lead to an increased 24-hour burn-in yield.